UNIVERSITY OF MINNESOTA
ST. ANTHONY FALLS LABORATORY
Engineering, Environmental and Geophysical Fluid Dynamics

Project Report No. 430

Simulation of Lake Water Quality Using a One-Dimensional Model with Watershed Input: Model Description and Application to Lake Riley and Lake Elmo

by

Deborah E. West and Heinz G. Stefan

Prepared for

GRAZING LANDS RESEARCH LABORATORY
Agricultural Research Service, US Department of Agriculture
El Reno, Oklahoma

In cooperation with

MID-CONTINENT ECOLOGY DIVISION
US Environmental Protection Agency
Duluth, Minnesota

December 1998
Minneapolis, Minnesota

ACKNOWLEDGMENTS

The work reported herein was supported by the Agricultural Research Service, USDA, Grazing Lands Research Laboratory, El Reno, Oklahoma in cooperation with the Mid-Continent Ecology Division, US Environmental Protection Agency, Duluth, Minnesota. Robert Williams and Naomi Detenbeck were project officers.

TABLE OF CONTENTS

LIST OF TABLES

LIST OF FIGURES

LIST OF SYMBOLS

A	area (m^2)
BOD	biochemical oxygen demand (mg/L)
Chla	chlorophyll (mg/L)
$Chla_{min}$	minimum chlorophyll concentration for grazing to occur (mg/L)
$Chla_n$	chlorophyll concentration of a specific group (mg/L)
CN	curve number
DO	dissolved oxygen concentration (mg/L)
DO_{sat}	saturated oxygen concentration (mg/L)
d_s	depth of snow (cm)
f_{NH}	factor for dissolved oxygen limitation for nitrification
f(S)	Michalis-Menten growth limiting factor
f(T)	temperature function for growth
G_{max}	maximum growth rate (1/d)
Gr_{max}	grazing maximum (mg/ind/d)
HSC	half-saturation constant for grazing (mg/L)
HSCNH	half-saturation coefficient for preferential uptake of ammonium over nitrate (mg/L)
I	intensity of photosynthetically active radiation ($\mu E/m^2/h$)
K_1	light limitation coeffficient ($\mu E/m^2/h$)
K_2	light inhibition coefficient ($\mu E/m^2/h$)
K_{BOD}	organic decomposition rate (1/d)
k_e	surface oxygen gas exchange (transfer) coefficient (m/d)
K_m	mortality rate
K_N	half-saturation constant for nitrogen (mg/L)
K_{NH}	nitrification rate (d^{-1})
K_P	half-saturation constant for phosphorus (mg/L)
K_r	respiration rate
K_{rz}	zooplankton respiration rate

K_s	half-saturation constant for the nutrient (mg/L)
K_{Si}	half-saturation constant for silica (mg/L)
k_{so}	half-saturation value for the depence of SOD on DO (mg/L)
K_z	eddy diffusivity (m^2/d)
L_l	light limiting growth factor
M	snowmelt (mm)
M_f	degree-day melt factor (mm $^oC^{-1}$ d^{-1})
N	nitrogen concentration (mg/L)
NH_4	ammonium concentration (mg/L)
NO_3	nitrate concentration (mg/L)
NO_2	nitrite concentration (mg/L)
NO_3+NO_2	nitrate plus nitrite concentration (mg/L)
n	algal group
P	phosphorus concentration (mg/L)
P_e	depth of runoff (inches)
P_r	depth of precipitation (inches)
ρ_s	density of snow pack (kg/m^3)
ρ_{sn}	density of new snow (kg/m^3)
θ_{BOD}	temperature adjustment coefficient for detrital decomposition
θ_m	temperature adjustment coefficient for mortality
θ_N	temperature adjustment coefficient for nitrogen
θ_{NH}	temperature adjustment coefficient for ammonium
$\theta_{NH\Sigma}$	temperature adjustment coefficient for ammonia release from the sediment
θ_{NO}	temperature adjustment coefficient for nitrate-nitrite
$\theta_{NO\Sigma}$	temperature adjustment coefficient for nitrate-nitrite release from the sediment
θ_r	temperature adjustment coefficient for respiration
θ_{SOD}	temperature adjustment coefficient for sediment oxygen demand
θ_z	temperature adjustment coefficient for zooplankton grazing
θ_{zr}	temperature adustment coefficient for zooplankton respiration
S_b	rate of oxygen released at the water-sediment interface (g/m^2 d)

S_{NH}	rate of ammonia released at the water-sediment interface (g/m^2 d)
S_{NO}	rate of nitrate released at the water-sediment interface (g/m^2 d)
S_P	rate of phosphorus released at the water-sediment interface (g/m^2 d)
Si	silica concentration (mg/L)
SWE	snow water equivalent (mm)
t	time (d)
T	temperature (^oC)
T_a	air temperature (^oC)
T_b	base temperature (^oC)
TD	length of day light (h)
T_{max}	maximum temperature at which phytoplankton growth is reduced 90 percent
T_{min}	minimum temperature at which phytoplankton growth is reduced 90 percent
T_{opt}	optimal temperature at which maximum phytoplankton growth occurs
TP	total phosphorus (mg/L)
TSS	total suspended sediment (mg/L)
U_{10}	wind speed at 10 m height over the lake (m/s)
V	settling velocity
V_{iz}	volume of day depth (m^3)
V_r	volume day depth/layer ratio
Y_{CHO2}	mass yield ratio of chlorophyll to oxygen
Y_{NCHLA}	mass yield ratio of ammonium to chlorophyll
Y_{NHBOD}	mass yield ratio of ammonium to BOD
Y_{NHO2}	mass yield ratio of ammonium to oxygen
Y_{PBOD}	mass yield ratio of phosphorus to BOD
Y_{PCHLA}	mass yield ratio of phosphorus to chlorophyll
Y_{SCHLA}	mass yield ratio of silica to chlorophyll
z	depth (m)
ZP	zooplankton concentration ($\#/m^3$)

1. INTRODUCTION

This report covers development of a model called MINLAKE98, which combines Riley's (1988) lake water quality model with a year-round model of temperature and dissolved oxygen (Fang and Stefan, 1994). Once validated this combined model will be used to simulate the effect of runoff from two rural watersheds on the water quality of several ponds in the watershed.

For many lakes in the US, point source inputs (such as municipal and industrial effluents) have been monitored, modified, diverted, and modeled. Today, non-point sources are the concern. Current problems include changes in land use, runoff quantity and quality, and population density. The results are seen e.g. in Lake Sammamish, Washington: In 1968, wastewater effluent was diverted out of the lake decreasing the annual mean total phosphorus concentration by the late 1970's. However, since the early 1980's the total phosphorus concentration has begun to increase due to land use changes (Perkins, et al. 1997). An added dimension, is the effect of climate change has on runoff quality and the subsequent impact on lake water quality.

Lake water quality models which simulate year-round temperature and concentrations of phytoplankton, dissolved oxygen, and nutrients (phosphorus, nitrogen, and silica) can be used to study changes in trophic status of a lake. Examples include predicting changes resulting from global warming or different landuse management practices. For many lakes, noticable changes in the trophic state due to changes in management practices or changes due to global warming take more than a single open-water season to be observed. A model which includes simulation through the winter ice-cover period can provide a prediction of the following spring as opposed to an open-water model which requires re-initialization in the spring. Year-round simulation is also necessary for the prediction of long-term changes to a lake in response to changes in the watershed or due to climate change. Additionally, year-round models can predict anoxic periods during the winter which may be potential winter fish-kill events.

The model to be described herein is one of several models available for this purpose. It is a modified version of a previous model (MINLAKE) developed by Riley primarily for lake eutrophication studies and control strategies (Riley, 1988). Riley's model simulates several parameters including temperature, dissolved oxygen, phytoplankton, phosphorus, nitrogen, detritus, and suspended sediment as a function of depth in 1-day timesteps for the open water season. Hondzo and Stefan (1991) simulated only temperature with a modified version of Riley's model and found that the impact of climatic warming on lakes will most likely have serious implications for water resources and water quality. A later version developed by Fang and Stefan (1995) expanded the temperature and dissolved oxygen parameters as a function of depth in 1-day timesteps to the entire year including ice cover developed by Gu and Stefan (1990).

2. HISTORY OF MINLAKE

The Minnesota Lake Model (MINLAKE) has been developed over several years. The first version MINLAKE87 was developed by Riley (Riley and Stefan, 1988) based on RESQUAL II which was used for a study of Lake Chicot in Arkansas. RESQUAL was developed by Dhamotharan (Stefan et al., 1989) expanding a water temperature stratification and mixing model developed by Ford (Ford and Stefan, 1980).

MINLAKE was further expanded by Gu to simulate ice/snow cover growth and decay, as well as heat exchange between the sediment and water in the bottom layer (Gu and Stefan, 1990). Hondzo generalized the lake specific MINLAKE model to allow simulation of lakes in a region (Hondzo and Stefan, 1991). Fang expanded the heat exchange between sediment and water to all layers and included a year-round dissolved oxygen simulation (Fang and Stefan, 1996). Table 2.1 lists the chronological development of the various versions of the MINLAKE model and the parameters simulated.

2.1 Ford's Model

Ford and Stefan (1980) developed a one-dimensional unsteady water temperature stratification and mixing model for a daily timescale. In that model a surface-mixed layer is introduced The depth of the well-mixed layer is determined by the magnitude of the wind or convective mixing, or both, and its ability to transport heat absorbed at the water surface down into the lake. The effect of the heat input is to change the total potential energy of the thermal stratification by increasing or decreasing the internal energy of the lake. The major source of turbulent kinetic energy is assumed to be the wind shear stress. Mixing is determined by a stability criterion that compares the total kinetic energy available for mixing with the incremental potential energy of the temperature profile. Mixing is intermittent and occurs only when sufficient wind energy is available. The depth of the mixed layer is determined by the depth at which the available kinetic energy can no longer overcome the work required to entrain the mass of water in the layer below. To carry out the simulation the two layers are divided in to several horizontal layers of variable thickness and density. Mixing in the lower layers (metalimnion and hypolimnion) is included in the model by an eddy diffusion formulation.

2.2 Dhamotharan's Model

Dhamotharan made additions and changes in Ford's model to include density current inflow, outflow, and the effects of suspended sediment on the heat transfer processes (Stefan et al., 1989). This model is called RESQUAL I. The density of each

layer of water in the lake is determined by temperature, suspended solids content, and dissolved solids content. As the inflow moves into the lake/reservoir and towards its

Table 2.1. Development of MINLAKE and parameters simulated.

	Time, Space Constraints	Physical Parameters	Chemical Parameters	Biological Parameters
Ford, 1980	open water, lake specific	temperature	-	-
Dhamotharan , 1989	open water, lake specific	temperature, inflow, outflow, suspended solids	phosphorus	chlorophyll[1]
Riley, 1988	open water, lake specific	temperature, inflow, outflow, runoff, suspended solids	dissolved oxygen, phosphorus, nitrogen, silica, BOD	chlorophyll[2], zooplankton
Gu, 1990	year-round, lake specific	temperature, sediment heat flux[3]	-	-
Hondzo, 1991	year-round, general	temperature, sediment heat flux[3]	-	-
Fang, 1996	year-round, general	temperature, sediment heat flux[4]	dissolved oxygen	-

[1]empirical relationship.
[2]dynamically simulated.
[3]bottom layer only.
[4]all layers.

isopycnic layer, it entrains water from each layer through which it passes. The inflow will augment the volume of that layer and consequently the layers above it will be displaced upward. Outflow is simulated by withdrawing water from the layers in front of the outlet.

A water budget for the lake/reservoir includes surface inflow, outflow, precipitation, evaporation, and seepage to and from the surface layer. A water balance equation for each layer and between timesteps was developed. In summary RESQUAL I simulated lake stage, surface mixed layer depth, water temperature, and suspended solids.

For computation of suspended sediment concentration profiles, a one-dimensional, unsteady, convective-diffusive transport equation was formulated in finite differences and solved by a fully implicit hybrid scheme. The scheme had no restrictions with regard to Peclet number. In addition, a relationship between suspended solids (inorganic) and Secchi Depth as a measure of lake clarity was developed.

Dhamotharan further expanded RESQUAL I to simulate phytoplankton, available dissolved orthophosphorus, non-available particulate phosphorus, light attenuation coefficient and Secchi depth in a shallow stratified lake or reservoir (RESQUAL II). Phytoplankton concentrations were described by a suspended sediment equation except that fall velocities were smaller than for clay and terms for biological growth and loss kinetics were added. A relationship between growth rate, available light intensity and temperature was developed from available field measurements.

2.3 Riley's Model

Riley developed MINLAKE (Riley and Stefan, 1988) by expanding RESQUAL II to include additional biological components. MINLAKE was primarily designed for studying eutrophication and control strategies in small to medium size Minnesota lakes. The model simulates the continuous change of lake stratification and water quality in response to weather, inflow, outflow, exchange processes at the sediment interface and inlake processes. The latter include advective and diffusive transport, settling, chemical and biological kinetics. The water quality parameters modeled include temperature, up to three forms of algae (expressed as chlorophyll *a*), phosphorus and nitrogen, detritus, zooplankton, inorganic suspended sediment and dissolved oxygen. The model simulates each parameter as a function of depth in 1-day timesteps.

The biological-nutrient routines are the most complex part of the program. The complexity is due to the interrelationships among the many state variables. The biology is characterized by one to three phytoplankton groups and one zooplankton group. The growth of the phytoplankton in the model is potentially limited by phosphorus, nitrogen as either nitrate-nitrite or ammonium, or light. Phosphorus, nitrate-nitrite, and ammonium are state variables. Light penetration is computed based on incoming solar radiation and attenuation of light with depth. In addition, detritus is modeled as a pool of oxygen consuming, decaying organic matter (BOD) which is then linked to the dissolved oxygen concentration. Mineral releases during the decay process are also modeled.

A lake specific subroutine allows Riley's MINLAKE model to be configured to one particular lake by inserting equations for depth-area and depth-volume computations, fetch, and special features such as non-point inflows or groundwater flow. The subroutine also allows the modeler to modify or add source and sink terms to the biological-nutrient equations and to add submodels to simulate different treatment options.

2.4 Gu's Model

Gu and Stefan (1990) expanded the open water simulation of the hydrothermal processes in MINLAKE to include ice cover. To extend the simulation period of the MINLAKE model to a whole year, submodels to simulate the most significant hydrothermal features of the winter cover and the lake bottom were developed. Only thermal parameters are simulated in Gu's year-round version of the MINLAKE model.

The winter thermal structure of an ice-covered lake can be analyzed as a one-dimensional unsteady heat transfer problem in a four-layer medium consisting of snow, ice, water and sediment. Snow thickness is determined by snow precipitation, and compaction and melting due to longwave radiation or rainfall. Ice thickness is determined by growth and decay on the underside of the ice cover and melting on the top (after the snow cover has melted) due to longwave radiation or rainfall as well as internal melting due to absorption of solar radiation.

The heat transfer with the bottom sediments becomes an important external factor for the temperature structure of ice-covered lakes. The magnitude of this heat exchange is determined by the conductive heat transfer in the sediments of the bottom layer. The temperature of the sediments ten meters below the lake bottom is assumed to be constant year-round and close to the mean annual temperature of the hypolimnetic water.

2.5 Hondzo's Model

Hondzo and Stefan (1991) generalized the lake water temperature model which was originally developed for particular lakes and particular years to allow for simulation of a wide range of lake types and meteorological conditions within a region without calibration. Vertical turbulent diffusion coefficients were related to lake size and stratification stability. The generalized model is used for simulating past climate and future climate scenarios associated with doubling of atmospheric CO_2 in Minnesota.

2.6 Fang's Model

Fang and Stefan (1996) expanded the year-round regional hydrothermal MINLAKE model to include the simulation of dissolved oxygen. This version of MINLAKE is intended for year-round simulations to determine long term water temperature and dissolved oxygen behavior rather than short time behavior. In addition, the model has been modified in order to simulate temperature and dissolved oxygen structures in a set of regional lakes with out calibration for individual lakes.

Modifications included (a) computation of sediment heat flux for all layers from the water surface to the lake bottom (not only the bottom layer, (b) adaptation to the finite difference scheme by Pivovarov (1972) to determine the temperature distribution of water and ice/snow at the same time, and (c) simulation of dissolved oxygen based on fixed biological variables related to specific trophic levels instead of simulated variables. This allows the model to simulate a set of regional lakes without recalibration.

3. CURRENT MODEL DEVELOPMENT

MINLAKE98 (Figure 3.1) simulates a lake as a series of stacked layers of varying thickness. The layers include snow, ice, water, and sediment. Each of the water layers is considered well mixed. All of the water layers are in contact with the sediment of the lake. Only the surface layer is in contact with the atmosphere during the open water season. A schematic diagram of the water mass balance for the entire lake is presented in Appendix A Figure A.1. MINLAKE98 is intended for modeling climate change effects on lake water quality. A summary of the modifications is described in Section 3.2. A detailed description of modifications is given below.

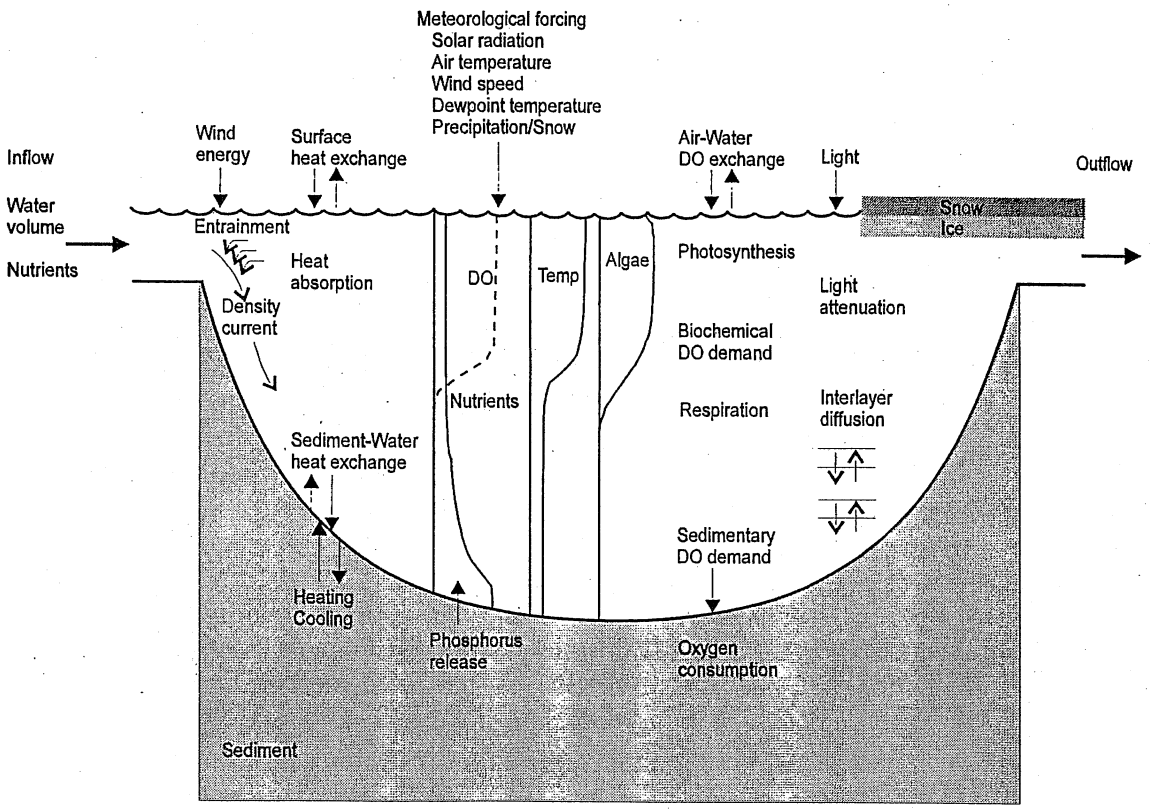

Figure 3.1. Schematic representation of processes in MINLAKE98.

3.1 Modifications and Additions

3.1.1 Phytoplankton (Chlorophyll *a*)

Chlorophyll *a* is used in MINLAKE as an indicator of phytoplankton standing crop (primary productivity) in a lake. Up to three algal groups can be simulated by the MINLAKE model (Riley and Stefan, 1988). A schematic diagram of the phytoplankton cycle is presented in Figure 3.2. This cycle is applicable to each algal group. Different coefficients and rates are used to represent a specific group.

Phytoplankton (chlorophyll) growth is simulated by external nutrient limitation using a Michaelis-Menten growth function. Light and phosphorus limitation are simulated. Nitrogen limitation for green algae as well as silica limitation for diatoms is also available. Respiration and mortality are combined in Riley's program but have been separated in MINLAKE98 to allow for differing rates. Respiration removes biomass (chlorophyll) and releases a proportional amount of nutrients directly to the water column. Nonpreditory mortality does not directly release nutrients to the water column but contributes to the detrital mass (BOD). Diffusion of chlorophyll occurs between layers at the same rate as heat (temperature). Loss of chlorophyll *a* due to grazing is treated separately as it is the result of the mobility of zooplankton. Settling results in the removal of chlorophyll from a layer and a contribution to the next layer (or the sediment).

The differential equation representing chlorophyll in the one-dimensional model is given as equation 3.1. The losses of phytoplankton (chlorophyll) due to nonpreditory mortality, zooplankton grazing, and respiration are calculated as first order sink terms. Growth is calculated as a zero order source term to maintain stability of the equation.

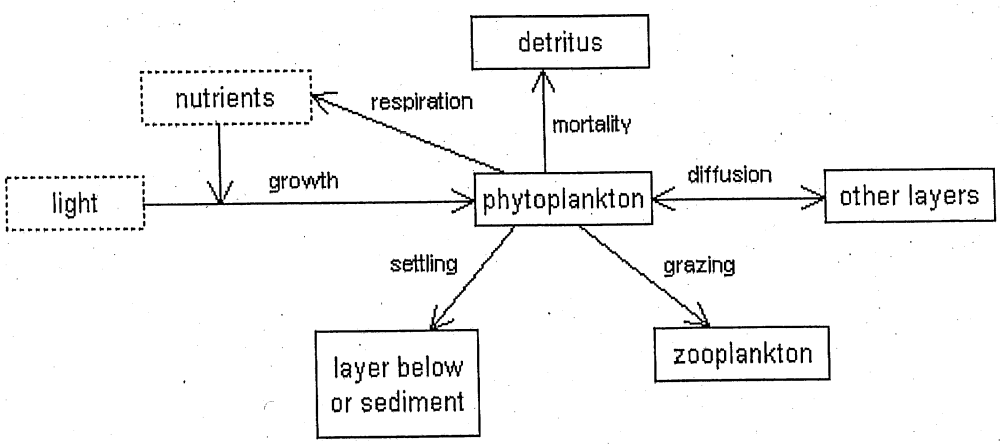

Figure 3.2. Illustration of the processes (arrows) and components (boxes) comprising the phytoplankton (chlorophyll) submodeled in MINLAKE98.

$$\frac{\partial Chla}{\partial t} - \underbrace{\frac{1}{A}\frac{\partial}{\partial z}\left(AK_z\frac{\partial Chla}{\partial z}\right)}_{diffusion} + \underbrace{\frac{V}{A}\frac{\partial(AChla)}{\partial z}}_{advection} + \underbrace{K_m\theta_m^{T-20}Chla}_{mortality} + \underbrace{K_r\theta_r^{T-20}Chla}_{respiration}$$

$$+\underbrace{Gr_{max}\frac{Chla - Chla_{min}}{Chla - Chla_{min} + HSC}\theta_z^{T-20}ZPV_r}_{\substack{zooplankton \\ grazing}}$$

$$\underbrace{-G_{max}f(T)\left[\frac{I\left(1+2\sqrt{K_1/K_2}\right)}{I+K_1+I^2/K_2}\cdot\frac{P}{K_P+P}\cdot\frac{N}{K_N+N}\cdot\frac{Si}{K_{Si}+Si}\right]_{min}}_{growth} Chla = 0 \qquad (3.1)$$

Individual parameters used in this equation are identified in the list of symbols.

Phytoplankton growth is dependent upon several factors:

- the maximum intrinsic growth rate of the algae ,
- the nutrient half-saturation coefficient,
- the water temperature,
- the solar irradiance,
- the external nutrient concentration, and
- the current chlorophyll concentration.

The **maximum growth rate** of algae varies between classes of algae and even at the species level. A range of values given by several researchers and summarized by EPA (1985) is presented in Table 3.1. Most of the maximum growth rates are between 0.9 /d and 2.0 /d. Calibration of the maximum growth rate coefficient, G_{max} , with chlorophyll field data is necessary.

MINLAKE98 is a 'fixed stoichiometry model' where the nutrient composition of the algal cells is assumed to remain constant. The growth of the algae is assumed to be a function of the **external nutrient concentration** using a Michaelis-Menten type relationship. The Michaelis-Menten growth limiting factor, f(S), for a nutrient S is

$$f(S) = \left(\frac{S}{K_S + S} \right) \tag{3.2}$$

where

S = concentration of the nutrient in the water (mg/L)

K_s = half-saturation constant for the nutrient (mg/L).

Growth limitation by phosphorus, nitrogen, and/or silica can be simulated by the MINLAKE98 model.

In the Michaelis-Menten growth limiting factor, both the concentration of the nutrient and the half-saturation constant for each nutrient are determining. Each species of phytoplankton has its own half-saturation constant for a given nutrient. Most of the half saturation values for phosphorus are between 0.001 mg/L and 0.02 mg/L with the lower values associated with diatoms. Most of the half saturation values for nitrogen are between 0.03 mg/L and 0.1 mg/L. The half saturation values for silica are between 0.03 mg/L and 0.1 mg/L (only diatoms require substantial amounts of silica).

Table 3.1. Phytoplankton Maximum Growth Rates and Half-Saturation Constants for Phosphorus, Nitrogen, and Silica. (EPA, 1985)

Algal Type	Maximum Growth Rate[1] (1/d)	Half Saturation Constant for P[1] (mg/L)	Half Saturation Constant for N[1] (mg/L)	Half Saturation Constant for Si[1](mg/L)
Total Phytoplankton	0.2 - 8.0	0.0005 - 0.08	0.0014 - 0.4	-
Green	0.7 - 9.2	0.002 - 0.475	0.001 - 1.236	-
Blue-green	0.2 - 11.0	0.0025 - 0.06	0.0 - 4.34	-
Diatoms	0.55 - 5.0	0.001 - 0.163	0.003 - 0.923	0.03 - 0.1

[1]Values are from experimental measurements reported in the literature and from documented models.

Water **temperature** affects the growth rate of the phytoplankton substantially. Lehman (1975) provided a function where the maximum yield occurs at an optimal temperature, T_{opt}; the growth rate coefficient decreases both above and below this temperature.

$$x = exp\left(-2.3 \left(\frac{T - T_{opt}}{T_{opt} - T_{min}} \right)^2 \right) \qquad for\ T < T_{opt}$$

$$x = exp\left(-2.3 \left(\frac{T - T_{opt}}{T_{max} - T_{opt}} \right)^2 \right) \qquad for\ T > T_{opt} \tag{3.3}$$

The "minimum temperature" T_{min} is the low temperature at which phytoplankton growth is reduced 90 percent. Riley's program assumed T_{min} = 0.0 °C. This is a good assumption for some phytoplankton species but not all. MINLAKE98 includes a variable for "minimum temperature" as part of the input to allow for more flexibility in simulating chlorophyll growth temperature limitations. Temperature limitations can vary with algae class as well as at the species level. Table 3.2 summarizes literature values reviewed in the CE-QUAL-R1 User's Manual (US Army Corps of Engineers, 1982). The "optimum temperature", T_{opt}, gives the range of temperatures for which growth is occurring near the maximum rate. The "maximum temperature", T_{max}, is the temperature at which growth is reduced 90 percent. The temperatures in Table 3.2 are from a literature review in CE-QUAL-R1.

Table 3.2. Optimum, Minimum, and Maximum Temperature Values for Phytoplankton. (U.S. Army Corps of Engineers, 1982)

Algal Type	Optimum Temperature[1] (°C)	Maximum Temperature[1] (°C)	Minimum Temperature[1] (°C)
Total Phytoplankton	10 - 40	15 - 42	0 - 18
Green	20 - 40	40 - 42	0 - 7
Blue-green	20 - 29	-	4
Diatoms	20 - 33	30 - 36	0 - 12

[1]Values are from CE-QUAL-R1 model documentation.

The values in Table 3.1 suggest that it is important to know the type of algae, at a class level at a minimum, to accurately simulate the chlorophyll growth, respiration, mortality, grazing by zooplankton, and effect of temperature.

In many eutrophic lakes **light** is the limiting growth factor. A Haldane equation (Megard et al., 1984) is used to calculate the light limitation coefficient, L_I. This function describes both light limitation and inhibition.

$$L_I = \frac{I\left(1+2\sqrt{K_1/K_2}\right)}{I+K_1+I^2/K_2} \tag{3.4}$$

In the MINLAKE96 model (Fang et al., 1996), the light limitation and inhibition coefficients, K_1 and K_2 respectively, are calculated using an empirical equation dependent upon the temperature of the water. The light limitation coefficient, K_1, is strongly dependent upon algal species. In MINLAKE98 phytoplanton classes are simulated, and

the light limitation and inhibition coefficients are specified by the user as in Riley's model.

Growth is usually limited by either light or phosphorus, depending upon which has the lowest limitation factor. When nitrogen and silica are also modeled the lowest growth limiting factor of light, phosphorus, nitrogen (greens only) and silica (diatoms only) is used to determine the phytoplankton growth rate. Carbon is considered to be available in excess on a daily timescale and is not modeled as a limiting nutrient.

Respiration rates do not appear to vary as greatly as settling rates. The range of respiration rates is presented in Table 3.3 (EPA, 1985). Most respiration rates are between 0.02 /d and 0.05 /d. Mortality rates are not as well known, and only values for total phytoplankton and for diatoms are presented in Table 3.3. MINLAKE98 differs from Riley's model in that respiration and nonpreditory mortality are treated separately. Respiration contributes immediately to the available phosphorus and dissolved oxygen concentration while mortality contributes with a timelag through detrital decay.

Table 3.3. Phytoplankton Settling Velocities, Respiration Rates, Non-Predatory Mortality Rates, and Zooplankton Grazing Rates. (EPA, 1985)

Algal Type	Settling Velocity[1] (m/d)	Respiration Rate[1] (1/d)	Non-Predatory Mortality Rate[1] (1/d)	Zooplankton Grazing Rate[1] (mg Chla/ind. day)
Total Phytoplankton	0.0 - 30.0	0.005 - 0.8	0.003 - 0.17	
Green	0.02 - 0.89	0.01 - 0.46	-	0.0015
Blue-green	0.0 - 0.2	0.03 - 0.92	-	0
Diatoms	0.02 - 17.1	0.03 - 0.59	0.03	

[1]Values are from experimental measurements reported in the literature and from documented models.

Zooplankton grazing rate depends upon the class of algae available. (Zooplankton grazing on phytoplankton is simulated only to represent the dynamics of the algae and not for studying zooplankton dynamics.) A single class of zooplankton is simulated with feeding preference on algae designated by grazing rates. Zooplankton are more likely to feed on green algae than blue-green algae.

Advection is used to describe the settling of the phytoplankton (chlorophyll *a*). The settling velocity for each algal class simulated is set by the user. The settling velocity of algae, varies between classes of algae, and even at the species level. A range of values by EPA (1985) is presented in Table 3.3. There is a wide range of values for each of the classes; however, in general the blue-greens exhibiting the lowest rates and the diatoms the highest rates. MINLAKE98 does not simulate the ability of some phytoplankton to float due to buoyancy (vacuoles), but this can be accounted for by

adjusting the settling rate. It is necessary to calibrate the settling velocity with available field data.

3.1.2 Phosphorus

Phosphorus is often the principal chemical affecting phytoplankton (chlorophyll *a*) concentration in lakes. The model simulates only the readily accessible phosphate composed of orthophosphate and polyphosphate ions referred to as soluble reactive phosphorus (SRP). A schematic diagram of the principal SRP flux components is presented in Figure 3.3. A schematic diagram of the SRP mass balance for the entire lake is presented in Appendix A Figure A.2. Phytoplankton growth removes SRP from the water at a mass yield ratio of approximately 1.1 mg phosphorus/mg chlorophyll *a*. Respiration releases phosphorus into the water column (Chapra, 1997). Mortality does not directly release phosphorus to the water column but contributes to the detrital mass (BOD); the phosphorus is released from the detrital mass through decay. The SRP is calculated for each layer. Diffusion of phosphorus occurs between layers but phosphorus is also transported indirectly between layers by phytoplankton and detritus settling. In MINLAKE98 there is no atmospheric deposition of phosphorus, as there is for models of Lake Superior (Chapra, 1977). Lake Superior has a considerable atmospheric input because of the large lake surface compared to the watershed area. For lakes modeled by MINLAKE98 the watershed area is usually much larger than the lake surface area. Adjustments for atmospheric input to the surface layer would be required for lakes with large surface areas. The differential equation representing phosphorus transport is presented as equation 3.5. The uptake of SRP due to phytoplankton (chlorophyll *a*) growth is calculated as a zero order sink term. Phosphorus release due to detrital decay and respiration is calculated as a zero order source term. The release of phosphorus from the lake sediment is calculated as a zero order source/sink term depending on the dissolved oxygen concentration in the overlying water.

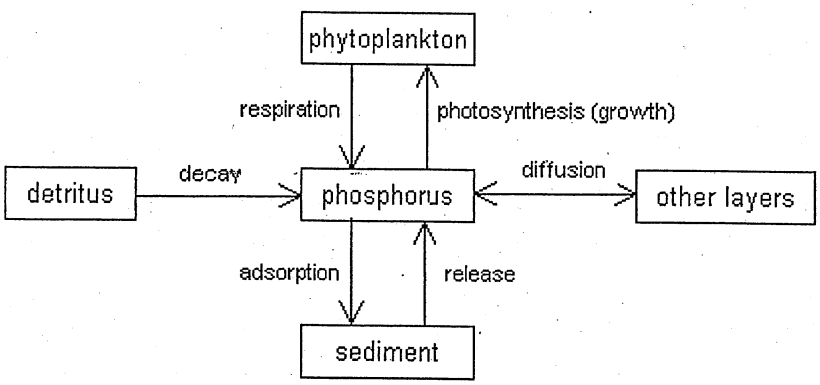

Figure 3.3. Illustration of the processes (arrows) and components (boxes) comprising the soluble reactive phosphorus submodel in MINLAKE98.

$$\frac{\partial P}{\partial t} \underbrace{- \frac{1}{A}\frac{\partial}{\partial z}\left(AK_z \frac{\partial P}{\partial z}\right)}_{diffusion}$$

$$\underbrace{+\sum_{n=1}^{3} G_{max} f(T)\left[\frac{I\left(1+2\sqrt{K_1/K_2}\right)}{I+K_1+I^2/K_2} \cdot \frac{P}{K_P+P} \cdot \frac{N}{K_N+N} \cdot \frac{Si}{K_{Si}+Si}\right]_{min} Y_{PCHLA} Chla_n}_{phytoplankton\ growth\ uptake}$$

$$\underbrace{-K_{BOD}\theta_{BOD}^{T-20} Y_{PBOD} BOD}_{detrital\ decay} \pm \underbrace{\frac{S_p}{A}\frac{\partial A}{\partial z}}_{sediment\ release} \underbrace{- \sum_{n=1}^{3} K_m \theta_m^{T-20} Chla_n Y_{PChla}}_{chlorophyll\ respiration} = 0 \qquad (3.5)$$

Individual parameters used in this equation are identified in the list of symbols.

MINLAKE98 differs from Riley's model in that the phosphorus uptake by algae is directly related to phytoplankton growth. Riley's model uses luxury uptake where more phosphorus is consumed than required for growth and saved for future use when phosphorus concentrations in the water are low. (See Section 3.1.1 for a more detailed discussion of the effect of phytoplankton photosynthesis on the uptake of phosphorus).

A phosphorus/chlorophyll *a* yield coefficient (Y_{PCHLA}) is used to determine the amount of phosphorus consumed during photosynthesis as well as the amount of phosphorus released during algal respiration. The value of Y_{PCHLA} is the mass yield coefficient of phosphorus to BOD (Y_{PBOD} = 0.0091 mg P/mg BOD) divided by the mass yield coefficient of chlorophyll to BOD (Y_{CBOD} = 0.0083 mg Chla/mg BOD) [$Y_{PBOD}/Y_{CBOD} = Y_{PCHLA}$]. This value of Y_{PCHLA} = 1.1 mg P/mg Chla is close to that presented by Thomann and Mueller (1987) of 1.0 µg P/µg Chla. (The Y_{PCHLA} was originally in Riley's program but later removed as it is not needed for luxury uptake simulation.) Riley's value was developed from a ratio of carbon to phosphorus [Stumm and Morgan, 1981] and a fixed chlorophyll/carbon ratio.

Point source inputs (such as municipal and industrial effluents) to many lakes in the US have been modified or diverted. This has eliminated large sources of input of phosphorus to the lakes. For many lakes with a history of progressive eutrophication the lake sediments have now become the primary source of phosphorus to the water. If the sediment-water interface is anoxic, phosphate ions go to the water at an increased rate, dependent upon the concentration difference between porewaters and the overlying water (Horne and Goldman, 1994). In many eutrophic lakes the dissolved oxygen concentration in the hypolimnion falls below 1 mg/L during both the summer and late

winter (during ice cover). When this happens phosphorus, as well as other ions, are released from the sediment.

Riley uses a constant phosphorus release rate from the sediments, independent of dissolved oxygen concentration. This phosphate flux rate must be calibrated to the hypolimnetic phosphorus profile under anoxic conditions. MINLAKE98 uses a function of dissolved oxygen (DO) concentrations to specify phosphorus release from the sediments instead of a constant release rate. This is based on field data from three lakes in Minnesota were retrieved from EPA's STORET database. The data cover a wide range of years: the Square Lake data and Fish Lake data are from 1972 to 1996 and the Lake Riley data from 1980 to 1995. In all 790 pairs of dissolved oxygen and total phosphorus (TP) points were retrieved. The relationship between these two variables is presented in Figures 3.4a, 3.4b, and 3.4c. As can be seen in Figure 3.4a the concentration of total phosphorus remains fairly constant for dissolved oxygen concentrations from 2 to 14 mg/L. Although this is not a comparison of just interstitial waters, it confirms that dissolved oxygen levels below 2 mg/L appear to trigger a release of phosphorus from the sediment. Total phosphorus was plotted instead of SRP because of the limited number of SRP data points available. On average 50 percent of the total phosphorus is SRP. Monthly profiles of total phosphorus and SRP versus depth for several lakes show that total phosphorus and SRP show the same trends (Jensen, 1998). Ishikawa and Nishimura (1989) reviewed phosphate sediment flux rates. They found aerobic rates from -0.006 g/m^2d (sink) to 0.259 g/m^2d (source) and anaerobic rates from 0.060 g/m^2d (source) to 0.336 g/m^2d (source).

In MINLAKE98, dissolved oxygen concentrations of 0.2 mg/L and 1.0 mg/L are used to trigger a change in the sediment dissolved phosphorus release rate. The sediment phosphorus release rate below 0.2 mg/L DO is set by the user. The SRP release rate at DO concentrations between 0.2 mg/L and 1.0 mg/L is set to one half the release rate at DO concentrations less than 0.2 mg/L DO. The release rate for dissolved oxygen concentrations greater than 1.0 m/L is set to 0.0. Because the range in values found by various researchers is very wide, the sediment phosphorus release rate should be calibrated for each lake. The phosphorus release rate is also dependent upon temperature (CE-QUAL-R1). During ice cover the phosphorus release rate is reduced to 50%. This value needs to be calibrated to the winter hypolimnetic phosphorus profile.

Most available data of phosphorus in lakes give total phosphorus (TP). MINLAKE98 simulates the change in SRP which is the bioavailable form. To compare simulated SRP results with TP field data, total simulated phosphorus is estimated as the sum of the dissolved phosphorus, P, the BOD concentration times the phosphorus/BOD yield coefficient, and the chlorophyll concentration times the phosphorus/chlorophyll *a* yield coefficient.

$$TP = P + BOD \times Y_{PBOD} + Chla \times Y_{PCHLA} \tag{3.6}$$

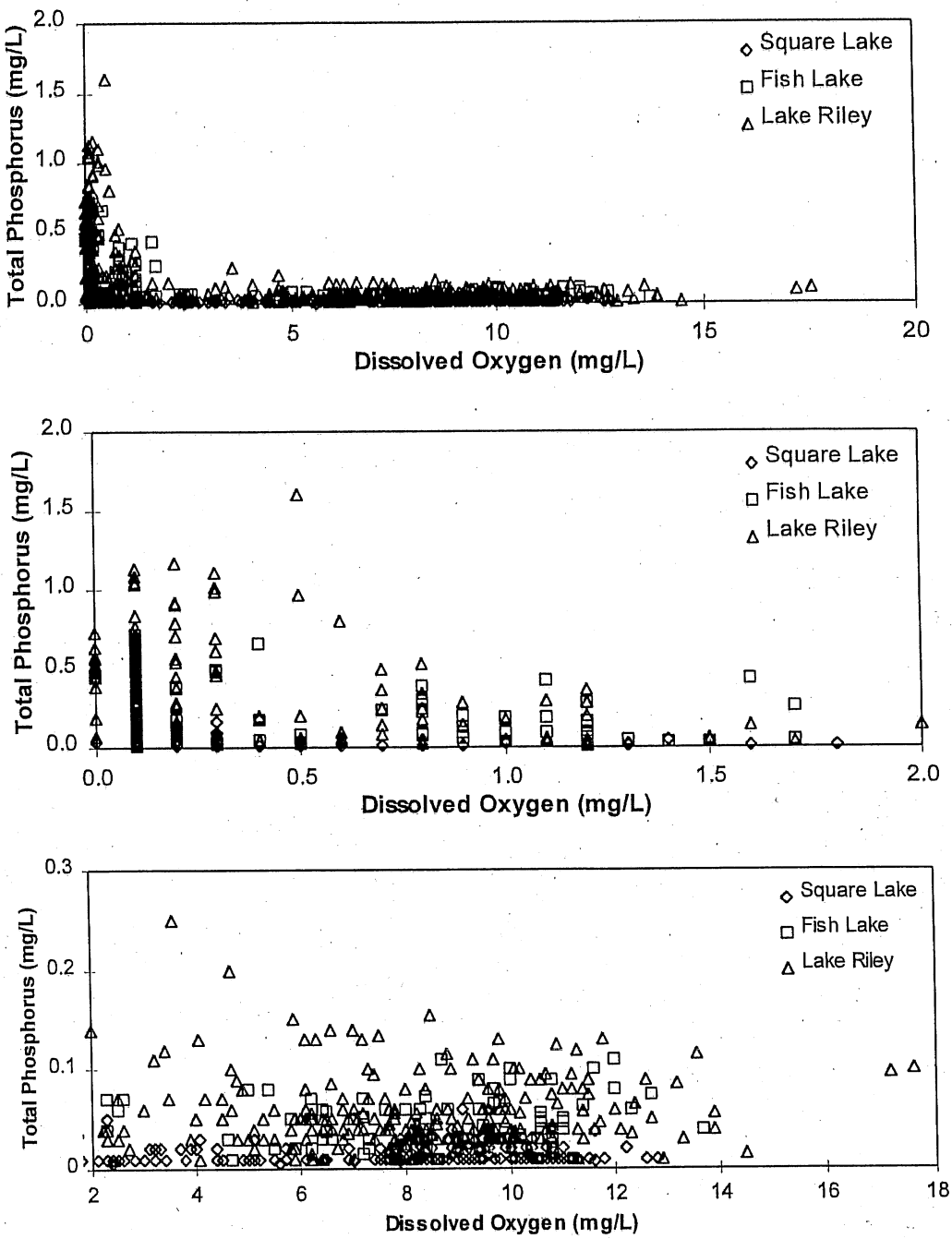

Figure 3.4. Total phosphorus versus dissolved oxygen in three lakes in Minnesota (a) for the entire range of dissolved oxygen concentrations, (b) for dissolved oxygen less than 2.0 mg/L, and(c) for dissolved oxygen larger than 2.0 mg/L.

3.1.3 Nitrogen

In most northern lakes nitrogen is not the limiting nutrient; however, when phosphorus is in excess, nitrogen can become the limiting nutrient for algae growth. Nitrogen is in two biologically available forms (nitrate+nitrite and ammonium) with a preference in the uptake of ammonium over the uptake of nitrate (nitrate+nitrite). Nitrate must first be reduced before it is utilized by the algae (Horne and Goldman, 1994). MINLAKE98 models both nitrate+nitrite and ammonia separately. A schematic diagram of the ammonia submodel presented in Figure 3.5 and the nitrate submodel in Figure 3.6. A schematic diagram of the ammonia mass balance and the nitrate+nitrite mass balance for the entire lake is presented in Appendix A Figures A.4 and A.5 respectively. Respiration releases ammonia but not nitrate. Mortality does not directly release ammonia or nitrate to the water but contributes to the detrital mass (BOD). Ammonia is released through decay of the detrital mass. The ammonia budget and the nitrate budget are calculated for each layer. Diffusion of ammonia and nitrate occurs between layers. Ammonia is also transported indirectly between layers by phytoplankton and detritus settling. Nitrification oxidizes ammonia to nitrate. In this model there is no atmospheric deposition of ammonia or nitrate. Denitrification (the reduction of nitrate to nitrogen gas, N_2) is not simulated. The differential equation representing the ammonia transport is presented as equation 3.7; equation 3.8 is for nitrate transport. The uptake of ammonia or nitrate due to phytoplankton (chlorophyll) growth is calculated as a zero order sink term. Ammonia release due to detrital decay and respiration is calculated as a zero order source term. The sediment release of ammonia or nitrate is calculated as a zero order source/sink term depending on the dissolved oxygen concentration of the overlying water. Nitrification is calculated as a first order sink term for ammonia and a zero order source term for nitrate+nitrite.

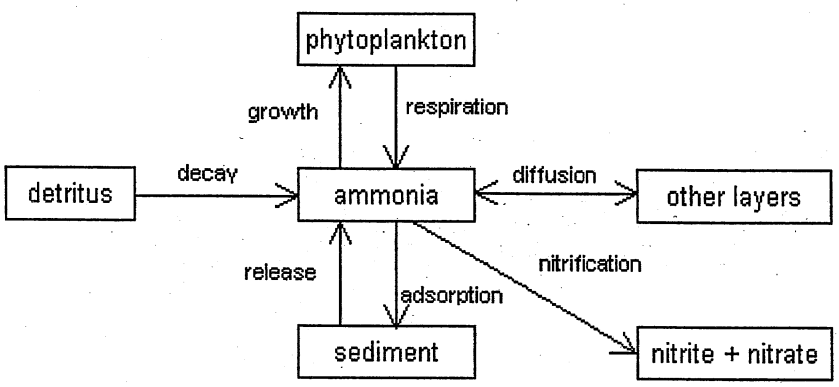

Figure 3.5. Illustration of the processes (arrows) and components (boxes) comprising the ammonia submodel in MINLAKE98.

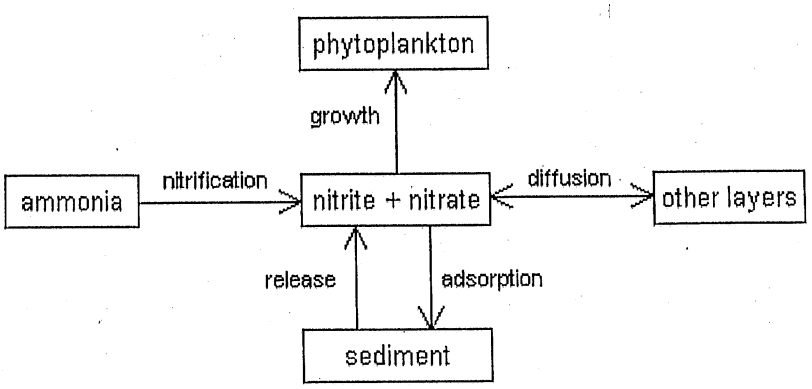

Figure 3.6. Illustration of the processes (arrows) and components (boxes) comprising the nitrate+nitrite submodel as treated in MINLAKE98.

$$\underbrace{\frac{\partial(NH_4)}{\partial t} - \frac{1}{A}\frac{\partial}{\partial z}\left(AK_z\frac{\partial(NH_4)}{\partial z}\right)}_{diffusion} - \underbrace{K_N\theta_N^{T-20}(NH_4)}_{nitrification}$$

$$\underbrace{+\sum_{n=1}^{3} G_{max}f(T)\left[\frac{I\left(1+2\sqrt{K_1/K_2}\right)}{I+K_1+I^2/K_2}\cdot\frac{P}{K_P+P}\cdot\frac{N}{K_N+N}\cdot\right]_{min}}_{phytoplankton\ growth\ uptake}$$

$$\underbrace{*\left(\frac{NH_4}{HSCNH_n+NH_4}\right)\left(\frac{NH_4+NO_3+NO_2}{HSCNH_n+NH_4+NO_3+NO_2}\right)Y_{NCHLA_n}Chla_n}_{phytoplankton\ growth\ uptake\ (cont.)}$$

$$\underbrace{-K_{NH}\theta_{NH}Y_{NHBOD}BOD}_{detrital\ decay} \pm \underbrace{\frac{S_{NH}}{A}\frac{\partial A}{\partial z}\theta_{NHS}^{T-20}}_{sediment\ release} - \underbrace{\sum_{n=1}^{3}K_{rn}\theta_{rn}^{T-20}Chla_nY_{NHChla}}_{phytoplankton\ respiration} = 0 \qquad (3.7)$$

Individual parameters used in this equation are identified in the list of symbols.

$N = NH_4 + NO_3 + NO_2$.

$$\frac{\partial(NO_3+NO_2)}{\partial t} - \underbrace{\frac{1}{A}\frac{\partial}{\partial z}\left(AK_z\frac{\partial(NO_3+NO_2)}{\partial z}\right)}_{diffusion} - \underbrace{K_N\theta_N^{T-20}(NH_4)}_{nitrification}$$

$$\underbrace{+\sum_{n=1}^{3} G_{max} f(T)\left[\frac{I\left(1+2\sqrt{K_1/K_2}\right)}{I+K_1+I^2/K_2}:\frac{P}{K_P+P}:\frac{N}{K_N+N}:\right]_{min}}_{phytoplankton\ growth\ uptake}$$

$$\underbrace{*\left[1-\left(\frac{NH_4}{HSCNH_n+NH_4}\right)\right]\left(\frac{NH_4+NO_3+NO_2}{HSCNH_n+NH_4+NO_3+NO_2}\right)Y_{NCHLA_n}Chla_n}_{phytoplankton\ growth\ uptake\ (cont.)}$$

$$\underbrace{\pm\frac{S_{NO}}{A}\frac{\partial A}{\partial z}\theta_{NOS}^{T-20}}_{\substack{sediment\\ release}} = 0 \qquad (3.8)$$

Individual parameters used in this equation are identified in the list of symbols.

$N = NH_4 + NO_3 + NO_2$.

MINLAKE98 differs from Riley's model in that the ammonia and nitrate consumption by algae is directly related to growth. In MINLAKE98 phytoplankton growth is simulated by external nutrient limitation and does not allow for nitrogen fixation (storage of excess nitrogen to be used later). Riley's model uses luxury uptake where more ammonia or nitrogen is consumed than required for growth and saved for future use when nitrogen concentrations in the water column are low. In addition, mortality releases excess ammonia directly to the water; MINLAKE98 simulates the release of ammonia from dead algae indirectly through detrital decay. (See the chlorophyll section for a more detailed discussion on the productivity of phytoplankton and its effect on the uptake of nitrogen.

3.1.4 Silica

Diatoms require large quantities of silica for their cell walls called frustules. Silica can become a limiting nutrient for diatom growth because 25 to 60 percent of the dry weight of diatoms is silica (Horne and Goldman, 1994). The model simulates silicic acid (H_2SiO_4) which is the only form of silica that can be used by algae. A schematic diagram of the silica flux is presented in Figure 3.7. A schematic diagram of the silica mass balance for the entire lake is presented in Appendix A Figure A.3. Phytoplankton

(diatom) growth removes silica from the water at a mass ratio of approximately 45 mg silica/mg chlorophyll *a*. Respiration and mortality do not contribute to the available silica. The silica budget is calculated for each layer. Diffusion of silica occurs between lakewater layers. Silica is also transported indirectly between layers by diatom and detritus settling. The differential equation representing the silica transport is presented as equation 3.9. The uptake of silica by phytoplankton (chlorophyll *a*) growth is calculated as a zero order sink term.

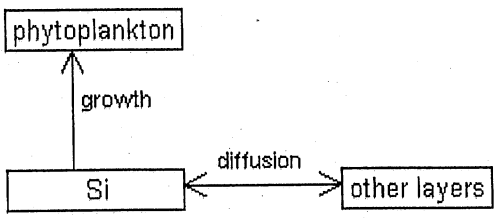

Figure 3.7. Illustration of the processes (arrows) and components (boxes) comprising the silica submodel treated in MINLAKE98.

$$\frac{\partial Si}{\partial t} - \underbrace{\frac{1}{A}\frac{\partial}{\partial z}\left(AK_z\frac{\partial Si}{\partial z}\right)}_{\text{diffusion}}$$

$$\underbrace{+\sum_{n=1}^{3} G_{max} f(T)\left[\frac{I\left(1+2\sqrt{K_1/K_2}\right)}{I+K_1+I^2/K_2}\cdot\frac{P}{K_P+P}\cdot\frac{N}{K_N+N}\cdot\frac{Si}{K_{Si}+Si}\right]_{min}}_{\textit{diatom growth uptake}} Y_{SCHLA}Chla_n = 0 \quad (3.9)$$

Individual parameters used in this equation are identified in the list of symbols.

MINLAKE98 differs from Riley's model in that the silica flux is one-directional only. Silica is consumed by algae but not released through respiration or detrital decay. The only source of silica is from stormwater runoff or inflow. This one-directional silica cycle is similar to the silica cycle presented by Horne and Goldman (1994) and in CE-QUAL-R1 (US Army Corps of Engineers, 1982).

3.1.5 Dissolved Oxygen

A schematic diagram of dissolved oxygen (DO) fluxes in a lake is presented in Figure 3.8. A schematic diagram of the dissolved oxygen mass balance for the entire lake is presented in Appendix A Figure A.6. During the open water season reaeration is a significant source of dissolved oxygen. It is possible for the phytoplankton (chlorophyll *a*) to add dissolved oxygen to the water layer through photosynthesis to the point where water is supersaturated with dissolved oxygen. In this case the dissolved oxygen is released into the atmosphere. These dynamic processes can have time scales of less than one day - the timestep of the simulation. Therefor the simulated dissolved oxygen profiles are an average over the day and not "snapshots" like observed profiles Dissolved oxygen removal from the water layer through respiration is simulated to occur at a constant rate throughout the day while photosynthesis occurs only during day light hours. The sediment oxygen demand is applied to all layers in proportion to the sediment surface area in contact with the water layer. Calibration of the sediment oxygen demand is especially important for simulating DO in the hypolimnion. Diffusion of dissolved oxygen occurs between layers of the hypolimnion. Zooplankton respiration is simulated to occur at the day depth only. Even though the zooplankton migrate during the simulated day to graze on phytoplankton, respiration in other layers is not simulated. The zooplankton spend the largest amount of their time in the day depth layer. Biochemical oxygen demand (BOD) removes oxygen from the water layer through the decay of detrital material. Nitrification removes oxygen from the water layer through the conversion of ammonia or organic nitrogen to nitrate. Nitrification is only simulated if nitrogen is simulated. The differential equation representing the dissolved oxygen transport is presented in equation 3.10. Reaeration or release of oxygen at the surface layer is calculated as both a first order source/sink term. Respiration, photosynthesis, zooplankton respiration, sediment oxygen demand, BOD, and nitrification are calculated as a zero order (with regard to oxygen) source/sink terms.

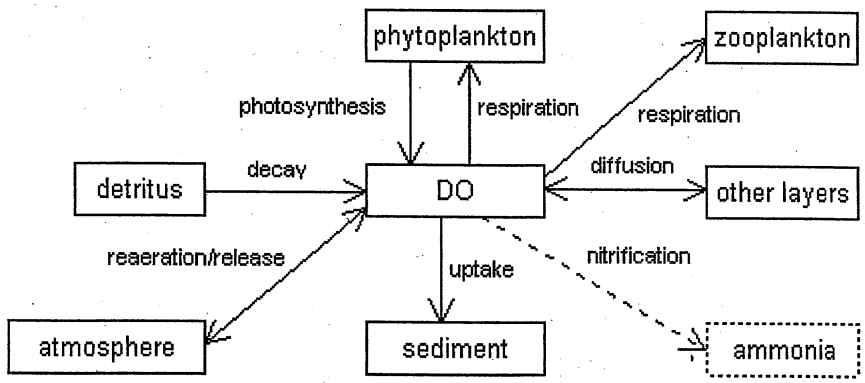

Figure 3.8. Illustration of the processes (arrows) and components (boxes) comprising the dissolved oxygen submodel in MINLAKE98. Nitrificiation is simulated only if nitrogen is simulated.

$$\frac{\partial DO}{\partial t} \underbrace{- \frac{1}{A}\frac{\partial}{\partial z}\left(AK_z \frac{\partial DO}{\partial z}\right)}_{diffusion}$$

$$+ \underbrace{\frac{1}{YCHO2}\sum_{n=1}^{3}\left(K_{rn}\theta_{rn}^{T-20} - G_{max}f(T)\left[\frac{I\left(1+2\sqrt{K_1/K_2}\right)}{I+K_1+I^2/K_2} \cdot \frac{P}{K_P+P} \cdot \frac{N}{K_N+N} \cdot \frac{Si}{K_{Si}+Si}\right]_{min}\right)}_{respiration\ and\ photosynthesis} Chla_n$$

$$+ \underbrace{K_{BOD}\theta_{BOD}^{T-20}BOD}_{\substack{detrital \\ decay}} + \underbrace{\frac{S_b}{A}\frac{\partial A}{\partial z}\theta_{SOD}^{T-20}}_{\substack{sediment \\ oxygen \\ demand}} + \underbrace{\frac{1}{YNHO2}K_{NH}\theta_{NH}^{T-20}NH}_{nitrification} - \underbrace{k\left(DO_{sat} - DO\right)_{surface}}_{\substack{reaeration \\ (surface\ only)}}$$

$$\underbrace{+0.04167TD \cdot K_{zr}\theta_{zr}^{T-20}ZP\frac{0.001}{V_{iz}}}_{\substack{zooplankton\ respiration \\ (day\ depth\ only)}} = 0 \qquad (3.7)$$

Individual parameters used in this equation are identified in the list of symbols.

Diffusion of dissolved oxygen between layers occurs similarly to heat. However, the maximum epilimnetic diffusion coefficient is different from that used for heat and is a function of the wind speed (Walters, 1978). The hypolimnetic diffusion coefficient is a function of the density and the surface area of the lake.

Fang increased the sensitivity of the model to light intensity when calculating **photosynthesis**. Riley computed the light distribution over the photoperiod in 8 subsections. The distribution is assumed to be symmetrical about a midday maximum. Fang computes the light distribution over the photoperiod in hourly subsections. The distribution is assumed to be a sine function starting from sunrise.

Fang's model differs from Riley's in that it does not simulate chlorophyll *a*. Instead a seasonal cycle is imposed on a given mean annual chlorophyll concentration. The mean annual value is selected dependent on the trophic state of a lake. Fang simulates photosynthetic oxygen production directly without calculating chlorophyll production. MINLAKE98 simulates both chlorophyll *a* and nutrients. The light intensity is used to calculate the light limitation component of photosynthetic growth (production). DO production is calculated from the biomass (chlorophyll *a*) production using a ratio of

mg chlorophyll/mg oxygen released in photosynthesis. The productivity is also used to calculate the uptake of nutrients.

Respiration rates are simulated separately for each algae class (respiration rates are presented Section 3.1.1). The respiration rates are also dependent upon temperature. Temperature adjustment coefficients are presented in Table 3.4. MINLAKE98 uses a step-wise function to reduce the respiration rate with decreasing DO concentration. The user defined rate is reduced to half of its value for DO concentrations less than 1.0 mg/L and set to zero for DO concentrations less than 0.2 mg/L.

For the DO simulations in a lake during the winter ice cover period oxygen consumption by plant respiration is assumed to be very small and is not represented as a separate sink term. The reasons are that phytoplankton concentrations are small and water temperatures are low.

Table 3.4. Temperature Adjustment Coefficients for Dissolved Oxygen Sources and Sinks.

Source or Sink	Range[1]	MINLAKE98
Phytoplankton respiration	1.08[2]	1.08
BOD	1.02 - 1.15[3]	1.047
SOD	1.02 - 1.13[3]	1.065
Nitrification	1.0548 - 1.0997[2]	1.08
Zooplankton respiration	-	1.06

[1]Values are from experimental measurements reported in the literature and from documented models.
[2]Ethomann and Mueller, 1987.
[3]EPA, 1985.

Detritus (dead biomass) consumes oxygen as it decays. This is simulated as **biochemical oxygen demand (BOD).** The BOD decay rate, K_{BOD}, is also dependent upon temperature. A range of values is presented in Table 3.5 (EPA. 1985). For MINLAKE98, a value of 0.05 d^{-1} is recommended for the open water season. The BOD decay rate is dependent upon the DO concentration the user defined rate is reduced to half of its value for DO concentrations less than 1.0 mg/L and set to zero for DO concentrations less than 0.2 mg/L. During ice cover a value of 0.03 d^{-1} which is independent of temperature is used. The value of 0.03 d^{-1} during ice cover was used successfully by Fang for several studies (Fang 1984b, Fang and Stefan, 1984a, Fang and Stefan 1996.

Table 3.5. Rate Coefficients for Dissolved Oxygen Sources and Sinks. (EPA, 1985)

Source or Sink	Range[1]	MINLAKE98
BOD	0.02 - 3.4 d^{-1}	0.05 d^{-1}
SOD	1.04 - 1.13 g $m^{-2}d^{-1}$	0.5 - 2.0 g $m^{-2}d^{-1}$
Nitrification	0.10 - 9.0 d^{-1}	0.25 d^{-1}
Zooplankton respiration	0.001 - 0.772 d^{-1}	0.002 d^{-1}

[1]Values are from experimental measurements reported in the literature and from documented models.

In MINLAKE98 the temperature adjustment coefficient, θ_{BOD}, is assumed constant. The widely used temperature adjustment coefficient value of 1.047 is used. A range of values given by several researchers and summarized by EPA (1985) is presented in Table 3.4. Some researchers have found that this value is only valid for temperatures between 20°C and 30°C and suggest higher values for lower temperatures (Fair *et al.*, 1968). As the BOD concentration in a lake is frequently not measured and simulation can only be grossly calibrated, the temperature adjustment coefficient will be held constant.

Sedimentary oxygen demand is treated as a sink term for each layer, since each layer is in contact with sediments. The sediment oxygen demand (SOD) is dependent upon temperature. Temperature adjustment coefficients at temperatures ranging from 10°C to 30°C given by Thomann and Mueller (1987) are presented in Table 3.4. A value of 1.065 which is used by several other researchers is also used in MINLAKE98. During ice cover the SOD rate is specified according to trophic state of a lake as well as the presence of a euphotic zone (see Table 3.6). The SOD values in Table 3.6 are based on field studies summarized by Barica and Mathias (1979) in ice covered temperate zone lakes in Canada. The user also has the option of making the SOD rate dependent upon the presence of the euphotic zone by a user defined coefficient. (A default value of 1.0 is used by MINLAKE98 - i.e. the presence or absence of the euphotic zone does not affect the SOD rate.)

MINLAKE98 uses a step-wise function to reduce the SOD rate with DO concentration similar to that used for the BOD rate. The user defined rate is reduced to half of its value for DO concentrations less than 1.0 mg/L and set to zero for DO concentrations less than 0.2 mg/L.

Table 3.6. Sediment Oxygen Demand Rates during Ice Cover.

	Eutrophic	Mesotrophic	Oligotrophic
Secchi depth (m)	$z_s < 1.8$ m	1.8 m $< z_s <$ 4.5 m	>4.5
Euphotic zone (g/m^2 d)	0.23	0.16	0.08
Below euphotic zone (g/m^2 d)	0.30	0.23	0.16

z_s = Secchi depth (m)

The consumption of oxygen through **nitrification** is simulated when nitrogen concentrations are modeled. Nitrification removes oxygen from the water layer through the conversion of ammonia or organic nitrogen to nitrate. MINLAKE98 utilizes an overall oxidation rate of the organic plus ammonia nitrogen instead of individual kinetic reactions. A range of values for the nitrification rate, K_{NH}, determined by several researchers is presented in Table 3.5 (EPA, 1985). MINLAKE98 uses a values of 0.25 d^{-1}. The nitrification rate is dependent upon the DO concentration, the user defined rate is reduced to half of its value for DO concentrations less than 1.0 mg/L and set to zero for DO concentrations less than 0.2 mg/L.

Nitrification is also affected by temperature. A range of values given by several researchers and summarized by EPA (1985) is presented in Table 3.4. A value of 1.08 is used by MINLAKE98.

The transfer of oxygen between the atmosphere and the surface layer depends upon the saturation value and the actual value of the water. If the water is undersaturated oxygen is transferred from the atmosphere to the water surface layer (**reaeration**). If the water is supersaturated then the oxygen transfers from the water to the atmosphere (**release**). For freshwater dissolved oxygen saturation concentration is dependent upon the temperature and the lake elevation and given by APHA (1985). The oxygen exchange coefficient determined by Wanninkhof et.al. (1990) in the field is used in MINLAKE98. The oxygen exchange coefficient can be written as (Fang and Stefan, 1994b).

$$k_e = 0.02256 \left[0.10656\, e^{(-0.0627T)} + 0.00495\right]^{-0.5} U_{10}^{1.64} \qquad (3.11)$$

Individual parameters used in this equation are identified in the list of symbols.

The oxygen gas transfer coefficient is affected by both surface water temperature and wind speed. This equation developed by Fang (1994b) is a change from Riley's which is only dependent upon wind speed and not temperature.

For the DO simulations in a lake during the winter ice cover period, Fang made modifications to account for the presence of an ice cover and low temperatures. Reaeration is set to zero because the lake ice cover prevents any significant gas exchange between the atmosphere and the water body.

Zooplankton respiration is simulated for the number of hours of daylight at the day depth only. The day depth identifies the layer in which the zooplankton are seeking refuge during the day as they are responding to predation pressure. The zooplankton tend to remain in the lowest layer of a lake where there is at least 0.5 mg/L of dissolved oxygen. No zooplankton respiration is simulated during non-daylight hours assuming that while migrating the zooplankton do not remain in one layer for enough time to significantly impact the dissolved oxygen concentration in the other layers.

3.1.6 Runoff

MINLAKE98 simulates two kinds of runoff: (1) storm-water runoff and (2) snowmelt runoff. The significance of snowmelt runoff depends on location of the watershed and the amount of snowfall. The percentage of snowmelt runoff of the total runoff can vary significantly from year to year. In central Alberta, Canada, snowmelt runoff accounted for 86 to 100% of the watershed runoff in 1993 and 1994 but for only 29% in 1995 (Harms and Chanasyk, 1998).

Riley (1988) included direct storm water runoff in the program as part of the lake specific subroutine. Fang (1994a) removed the lake specific subroutine and modeled only direct precipitation and evaporation with no other inflows or outflows in the year-round regional model. MINLAKE98 includes stormwater runoff and snowmelt runoff as part of the inflow subroutine.

Rain water runoff is calculated using the Soil Conservation Service (SCS) method (Chow *et al.*, 1988). Direct runoff from a storm is given by equation 3.12, where P_e is the depth of runoff in inches, P_r is the amount of precipitation in inches, and S is calculated from the curve number, CN, as shown in equation 3.13.

$$P_e = \frac{(P_r - 0.2S)^2}{P_r + 0.8S} \tag{3.12}$$

$$S = \frac{1000}{CN} - 10 \tag{3.13}$$

When simulating runoff in a watershed, a curve number depending on the type of landuse and hydrologic soil group surrounding the lake needs to be calculated. For simplicity, an antecedent moisture condition of II is assumed. Tables of runoff curve numbers for selected agricultural, suburban, and urban land uses can be found in Chow *et al.* (1988).

Literature values for concentration of nutrients, BOD, and suspended solids in stormwater runoff are listed in Table 3.7. Actual values vary greatly and are dependent upon land use, soil type, and conservation practices. The temperature of the stormwater runoff is assumed to be the same as the surface water layer of the lake and the dissolved oxygen concentration is assumed to be the saturation value at that temperature.

Table 3.7. Input Parameters for Stormwater Runoff.

Parameter	Units	Value (Range)
BOD	mg/L	19 (2 - 84)[1]
TSS	mg/L	610[1]
Silica	mg/L	-
Phosphorus	mg/L	0.5[1]
Nitrogen	mg/L	2.3[1]
Temperature	°C	surface water temperature[2]
DO	mg/L	saturated[2]

[1]Thomann and Mueller, 1987.
[2]Assumed.

Riley's MINLAKE program simulated the open water season and therefore did not include snowmelt runoff. MINLAKE98 simulates snowmelt runoff using a temperature-index approach presented by Maidment (1993). This method relates snowmelt, M, to average daily air temperature, T_a.

$$M = M_f(T_a - T_b) \tag{3.14}$$

MINLAKE98 uses the mean air temperature, T_a, a base temperature, T_b, of -1°C [U.S. Army Corps of Engineers, 1956], and a degree-day melt factor, M_f, determined from the density of the snow, ρ_s. A snow density of 300 kg/m^3, as used by Fang in calculating precipitation to the lake surface, is applied in the model.

$$M_f = 0.011\rho_s \tag{3.15}$$

The snow cover on the watershed is converted to snow water equivalent (SWE) using equation (3.16) from Maidment (1993). A density of 100 kg/m^3 for new snow is used.

$$SWE = 0.01 d_s \rho_{ns} \tag{3.16}$$

Literature values for concentration of nutrients, BOD, and suspended solids in snowmelt runoff are listed in Table 3.8. Actual values vary greatly and are dependent upon land use and current snowpack depth. The values for BOD, TSS, phosphorus, and nitrogen used for stormwater runoff are also used for snowmelt; they need to be validated. The temperature of the snowmelt runoff is assumed to be just above freezing and the dissolved oxygen concentration is assumed to be the saturation value at that temperature.

Currently, the parameters for runoff (phosphorus, nitrogen, BOD, DO, temperature, and suspended solids loading, watershed area and curve number) for both stormwater runoff and snowmelt are coded directly into the MINLAKE98 program. In the future, the user will be able to specify these values as part of the input file.

Table 3.8. Input Parameters for Snowmelt Runoff.

Parameter	Units	Value (Range)
BOD	mg/L	19 (2 - 84)[1]
TSS	mg/L	610[1]
Silica	mg/L	-
Phosphorus	mg/L	0.5[1]
Nitrogen	mg/L	2.3[1]
Temperature	°C	0.01[2]
DO	mg/L	saturated[2]

[1]Thomann and Mueller, 1987.

[2]Assumed.

3.1.7 Outflow

Outflow from a lake is simulated as surface outflow. Water withdrawal is from "selective" layers. Only the layers in direct contact with the outflow channel contribute to the outflow. In Figure 3.9 only the first three layers (1, 2, & 3) would contribute to the outflow. The volume of water removed from a layer by outflow is proportional to the thickness of the layer. In Figure 3.9 the volume of water removed from layer 1 would be $(\Delta z_1/h) \times Q_{out} \times 1$ day. Outflow calculations assume a rectangular cross-section for the outflow channel. Currently the model does not calculate concentrations of the water quality parameters in the outflow.

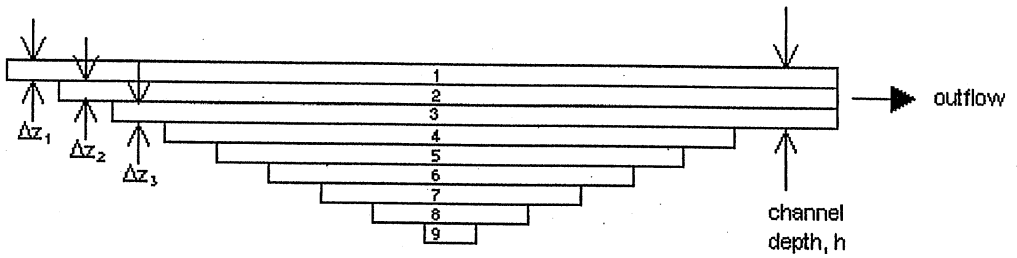

Figure 3.9. Surface outflow as simulated by MINLAKE98.

3.2 Summary of Changes

Below is a summary of the changes made to the Minnesota Lake Model (MINLAKE). Changes are listed by parameters and processes simulated.

Phytoplankton (Chlorophyll *a*)

- Growth is simulated using external nutrient limitation instead of luxury uptake.
- Respiration and nonpreditory mortality are treated separately.
- A minimum temperature for algae growth can be set by the model user. (Previously a default value of 0°C was used).
- Light limitation and inhibition coefficients are set by the user for each specific algae class. (An empirical equation dependent upon the temperature of the water is removed.)

Phosphorus

- Consumption of phosphorus by algae is directly related to the growth of the algae. (Previously luxury uptake was used.)
- Phosphorus in dead algae is released to the water through detrital decay. (Previously phosphorus was released directly to the water.)
- The rate at which phosphorus is released from the sediment is dependent upon the dissolved oxygen concentration in the overlying water.

Nitrogen

- Ammonia and nitrate consumption by algae is directly related to growth instead of using luxury uptake.

- The ammonia in the dead algae is released to the water through detrital decay instead releasing ammonia directly to the water.
- The nitrification rate is made dependent upon the DO concentration, at low DO.

Silica

- Respiration and mortality of algae do not contribute to the silica available in the water.

Dissolved oxygen

- The nitrification rate is made dependent upon the DO concentration, when DO is low.

Runoff

- Snowmelt runoff has been added.

Outflow

- The layers contributing to the outflow from the lake and the volume of water removed from these layers has been simplified to include only the layers down to the bed of the outflow channel.

A continuation of Table 2.1 which listed the developers of the various versions of the lake models, the time period of the simulation and the parameters simulated is presented in Table 3.9.

Table 3.9. The processes simulated in MINLAKE98.

	Time Period	Physical Parameters	Chemical Parameters	Biological Parameters
West, 1998	Year-round, lake specific	temperature, sediment heat flux[1], inflow, outflow, runoff, snowmelt	dissolved oxygen, phosphorus, nitrogen, silica, BOD	chlorophyll[2], zooplankton

[1]all layers.
[2]dynamically simulated.

4. MINLAKE98 MODEL CALIBRATION

4.1 Lake Riley

The MINLAKE98 model was calibrated against data from Lake Riley. Lake Riley is located in the Riley Creek watershed approximately 20 miles southwest of Minneapolis in Eden Prairie, MN. It has a surface area of 1.2 km^2 and a tributary watershed of 2.1 km^2. Riley Creek enters on the northeast side of the lake and exits on the southeast side. The lake has a maximum depth of 14 m to 15 m, is approximately round and bowl shaped with two small bays (Figure 4.1).

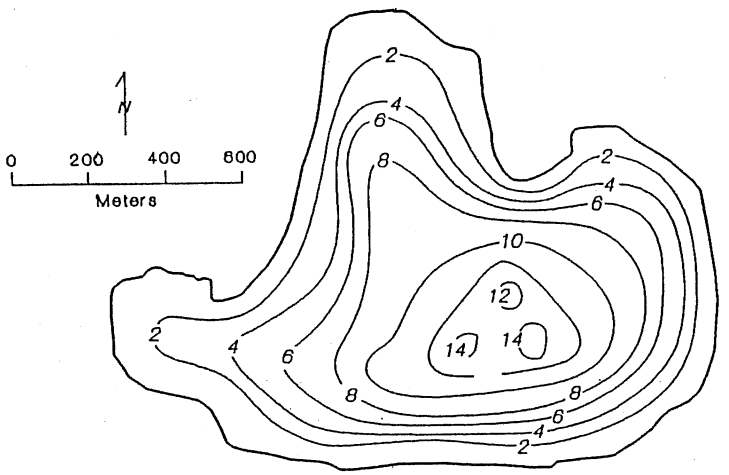

Figure 4.1. Bathymetric map of Lake Riley (after Osgood, 1983).

The processes in Lake Riley were simulated using MINLAKE98. The lake was simulated as a round lake. The following parameters and processes were simulated: temperature, dissolved oxygen, phosphorus, two types of phytoplankton (as chlorophyll *a*) - green and blue-green algae -, detritus (as BOD) and inflow, outflow, and stormwater runoff. The following were not simulated: silica, nitrogen, suspended solids, and dissolved solids. Coefficients for simulating Lake Riley using MINLAKE98 are listed in Appendix D.

4.1.1 Data Base

The lake was extensively monitored in 1982, 1986, 1987, 1990, 1991, and 1993 and periodically monitored in 1980, 1981, and 1985 by the Metropolitan Council (Osgood, 1983). Replicate field measurements were made for 1982, single measurements were made for all other years. The field data were retrieved from the EPA database, STORET.

Inflow rates from Riley Creek for 1982 were retrieved from the USGS web site, and flow rates for 1985 through 1991 were estimated using Elm Creek runoff data (see Appendix B). Inflow temperature and chlorophyll concentration were set to the surface layer temperature and chlorophyll concentrations, respectively; dissolved oxygen was set to the saturated value, available phosphorus to 0.006 mg/L and BOD to 11 mg/L. Suspended and dissolved solids, silica, nitrate+nitrite, and ammonia were set to 0.0 mg/L, as these parameters were not simulated.

4.1.2 Calibration

The model was calibrated using 1982 field data from Lake Riley. MINLAKE98 contains some rate coefficients that need to be adjusted to simulate a specific lake. Calibration was based on both statistical and visual comparison with the field data.

The goodness of fit of the simulated water quality parameters to the field data was evaluated using a linear regression constrained through the origin. The linear regression provides a slope of the regression line, a regression coefficient (r^2), and a standard error of the estimate. A perfect fit would give a slope of 1.0, a regression coefficient of 1.0, and a standard error of 0.0. A slope greater than 1.0 indicates that the model is overpredicting and a slope less than 1.0 indicates that the model is underpredicting.

The regression coefficient and the standard error are related parameters, but provide different information. The regression coefficient in a constrained regression has a range of $-\infty$ to 1.0. Negative values indicate that the standard error of the model prediction (estimate) is greater than the standard deviation of the field data. When the standard deviation of the field data is small, an acceptable simulation may still yield a negative regression coefficient. For this reason, the standard error of the estimate is also calculated. In the case where the regression coefficient is less than zero, the standard error of the estimate is used to evaluate the magnitude of error. The statistical results are calculated only for temperature, dissolved oxygen, total phosphorus, and chlorophyll *a* because field data are available only for these parameters. The statistical results of the calibration are presented in Table 4.1.

The statistical results show that **temperature** is simulated best with a slope of 0.97 and a regression coefficient of 0.90. A comparison of the observed and simulated values versus a 1:1 line (slope = 1.0) is presented in Figure 4.2. Data are available for the open water season only. A comparison of the observed and simulated values versus a 1:1 line shows a good simulation of the extreme values and slightly more variation in the

mid-range values. The model simulates the location of the thermocline during the summer months well but underpredicts its location in the spring and late fall (Figure 4.3).

Dissolved oxygen is simulated with a slope of 1.01 and a regression coefficient of 0.79. A comparison of the observed and simulated values versus the 1:1 line (Figure 4.2) shows that there is a good simulation of the observed data in the middle range of dissolved oxygen concentrations but not as good a simulation at the extremes. The largest errors occur at the surface during the spring and summer (Figure 4.4).

Total phosphorus is simulated with a slope of 1.24 and a regression coefficient of 0.66. A comparison of the observed and simulated values versus a 1:1 line (Figure 4.2) shows that the model is overpredicting the phosphorus concentration on the low end and underpredicting the phosphorus concentration at the higher end. The lower phosphorus concentrations are associated with the epilimnion and the higher concentrations with the hypolimnion. Looking at the profiles of the phosphorus concentration (Figure 4.5), the surface concentrations are simulated well, the mid-depth phosphorus concentrations are overpredicted, and the lower hypolimnion concentrations are underpredicted.

Chlorophyll *a* has the lowest statistical correlation with a slope of 0.49 and a negative regression coefficient. It has a low standard error, indicating a reasonable simulation result despite the negative correlation coefficient (Figure 4.6). Comparison of the observed and simulated values (Figure 4.2) shows that observed values are slightly overpredicted for the low values and underpredicted for the higher values. Figure 4.7 gives a comparison of the simulated surface chlorophyll with the field data. Both green and blue-green algae were simulated. Many factors determine the chlorophyll concentration in each class of algae simulated: available phosphorus, growth rate, mortality rate, and respiration rate of the algae, and zooplankton grazing rate.

Table 4.1. Statistical results from the calibration of the MINLAKE98 model to the 1982 field data for Lake Riley.

	Temperature (°C)	Dissolved Oxygen (mg/L)	Total Phosphorus (mg/L)	Chlorophyll *a* (mg/L)
Standard error	1.48	1.76	0.15	0.009
Maximum error	-5.07	-8.29	-0.83	0.017
Slope of regr. line	0.97	1.01	1.24	0.52
Regr. coefficient	0.93	0.79	0.66	-0.02
No. of data points	213	213	56	14

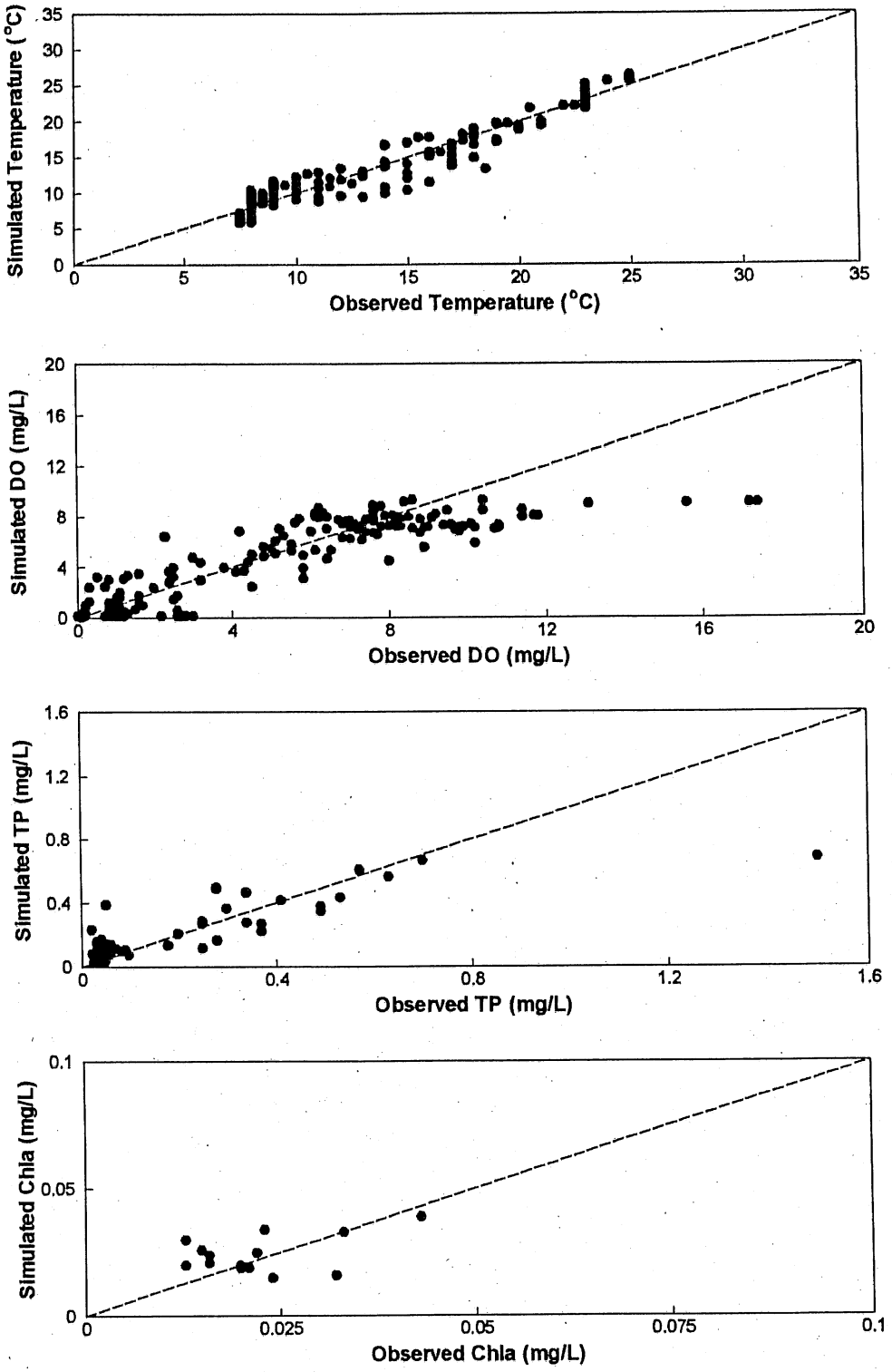

Figure 4.2. Comparison of simulated and observed water quality values for Lake Riley, 1982.

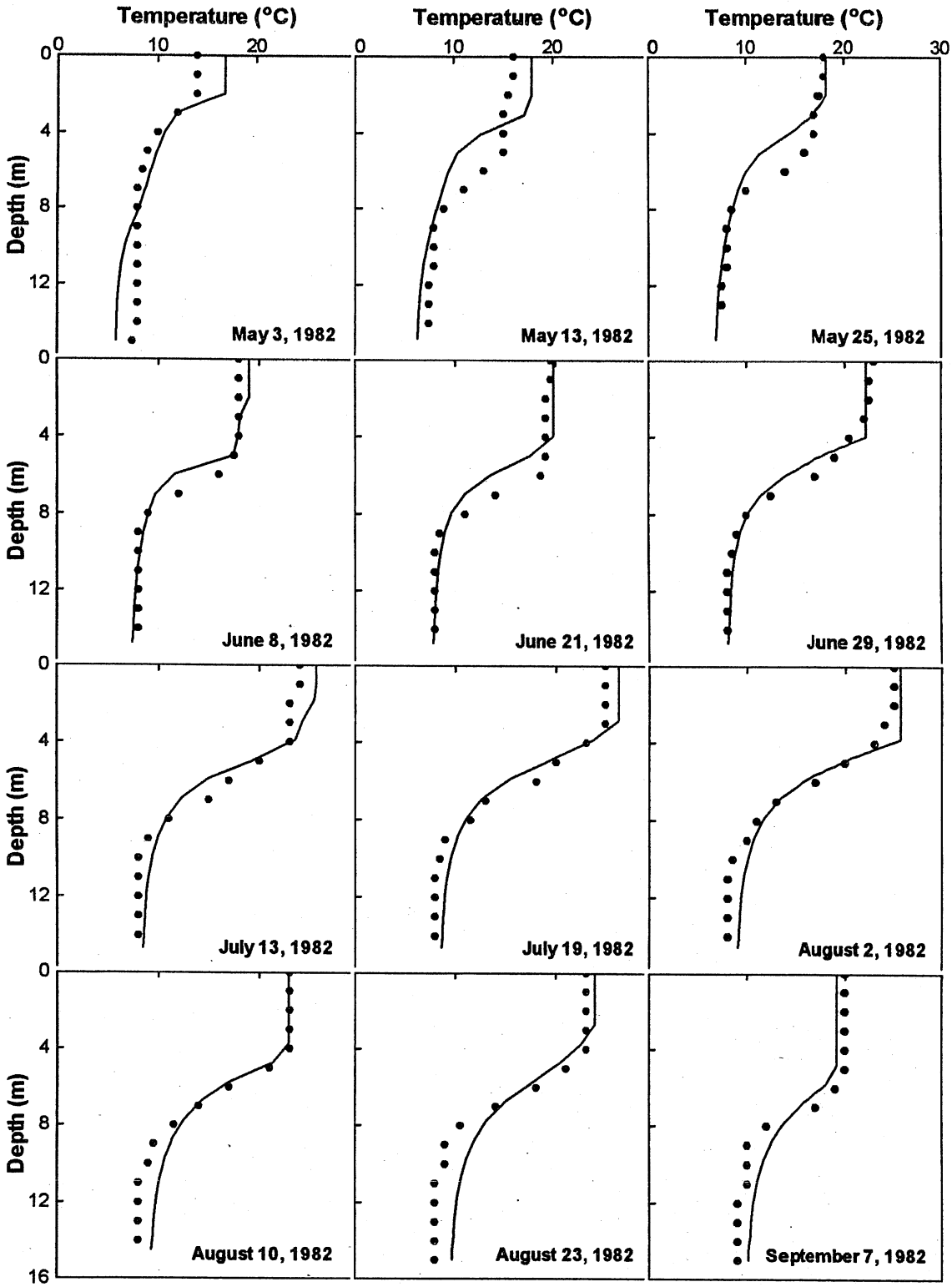

Figure 4.3. Simulated (line) and observed (dot) water temperature profiles for Lake Riley, 1982.

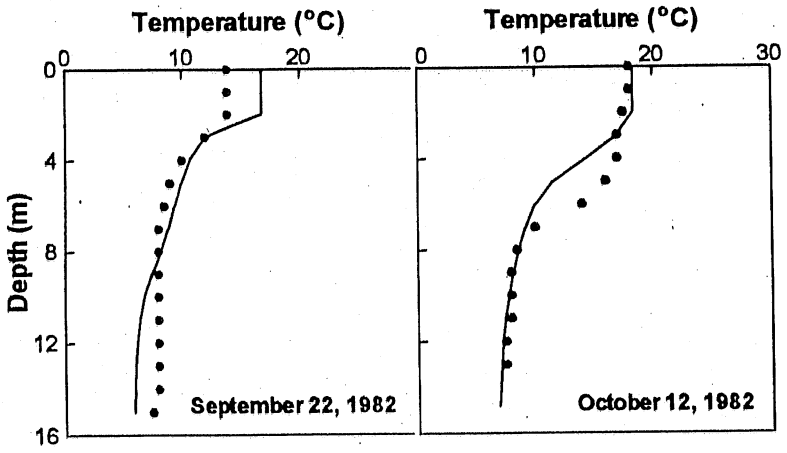

Figure 4.3 (continued). Simulated (line) and observed (dot) water temperature profiles for Lake Riley, 1982.

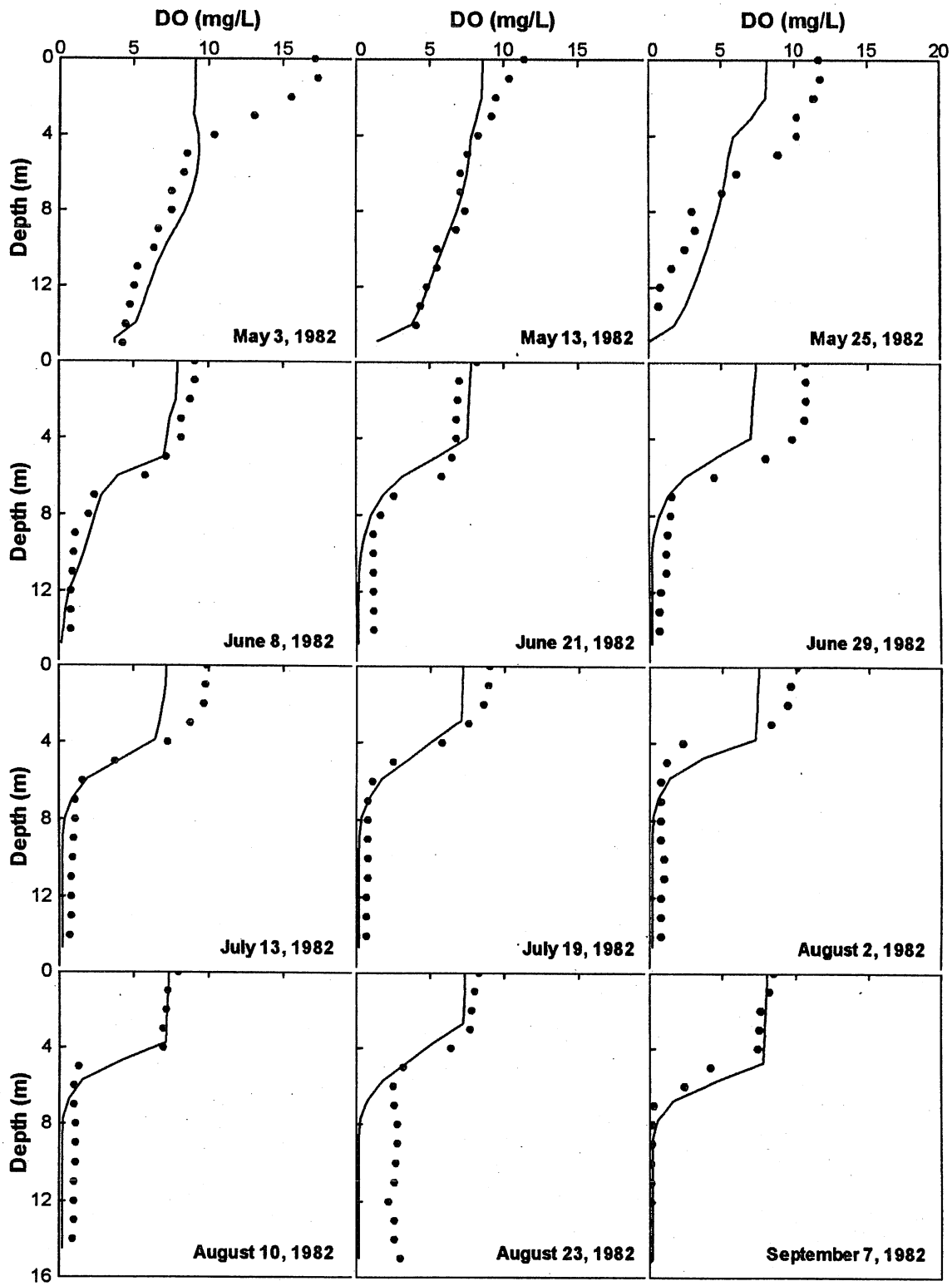

Figure 4.4. Simulated (line) and observed (dot) dissolved oxygen profiles for Lake Riley, 1982.

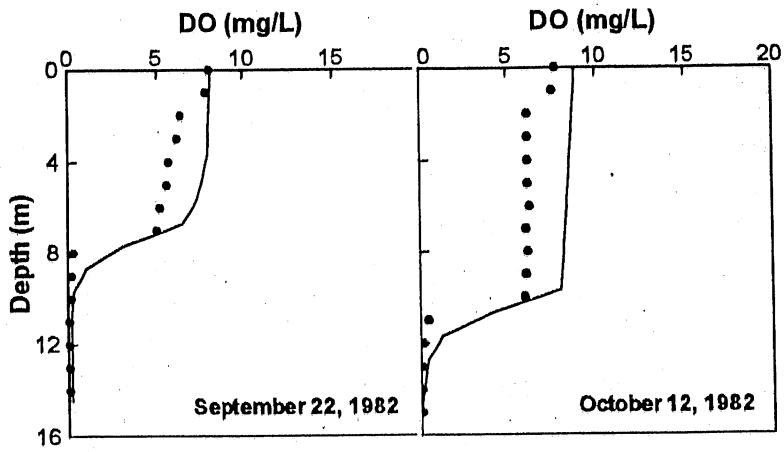

Figure 4.4 (continued). Simulated (line) and observed (dot) dissolved oxygen profiles for Lake Riley, 1982.

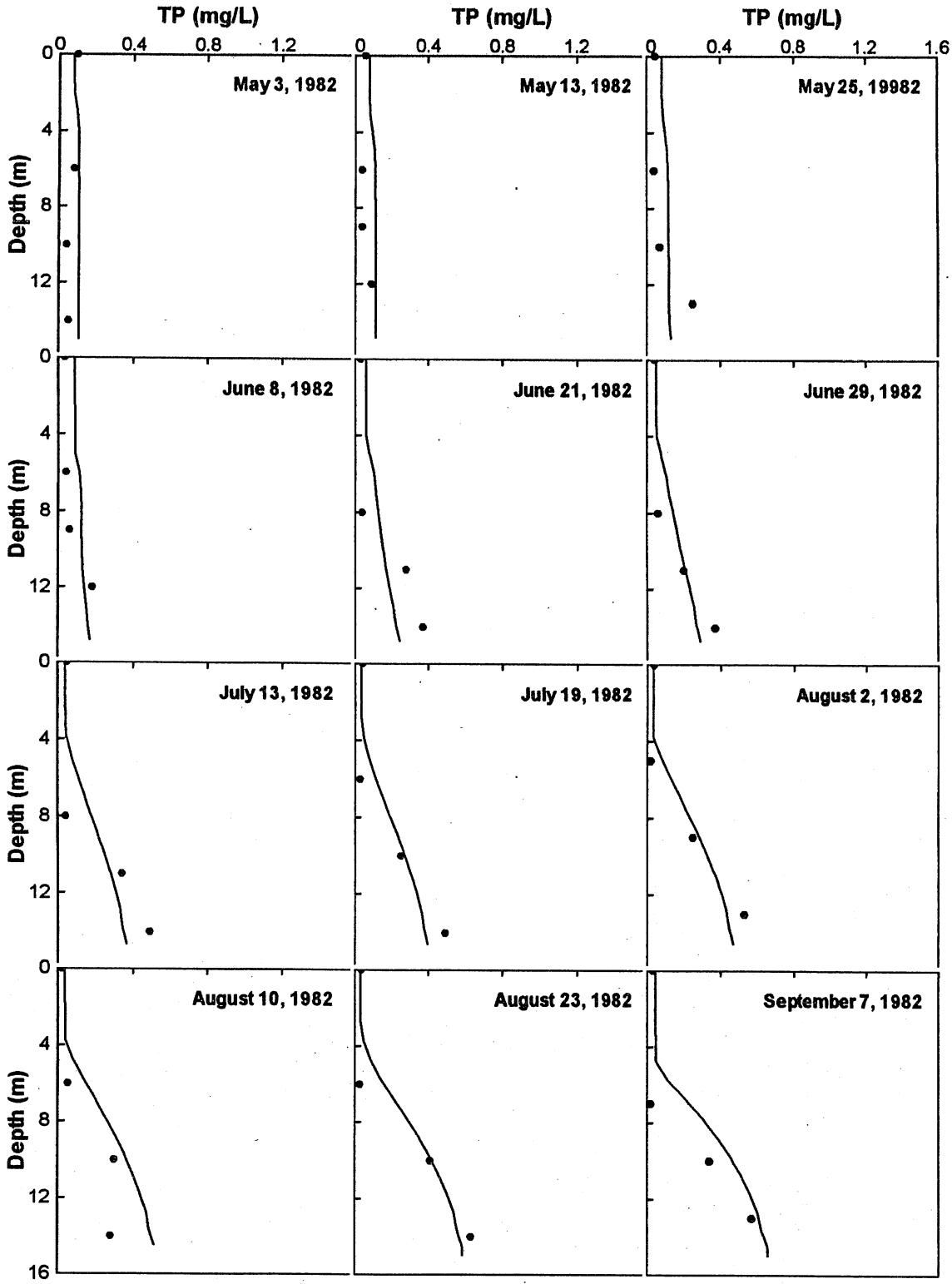

Figure 4.5. Simulated (line) and observed (dot) total phosphorus profiles for Lake Riley, 1982.

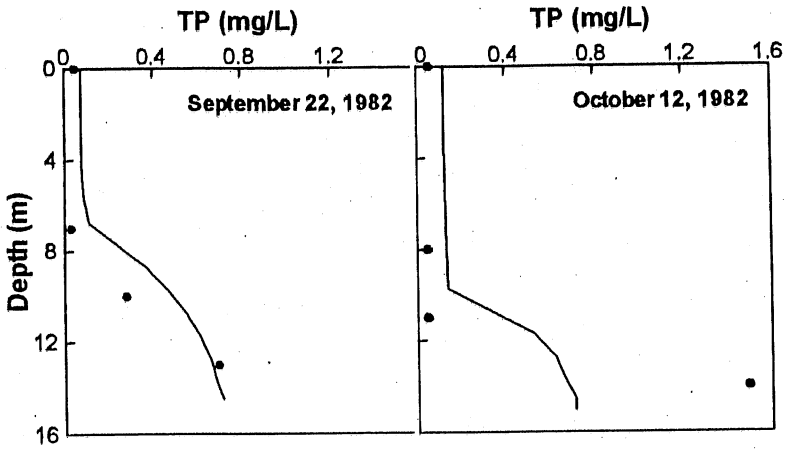

Figure 4.5 (continued). Simulated (line) and observed (dot) total phosphorus profiles for Lake Riley, 1982.

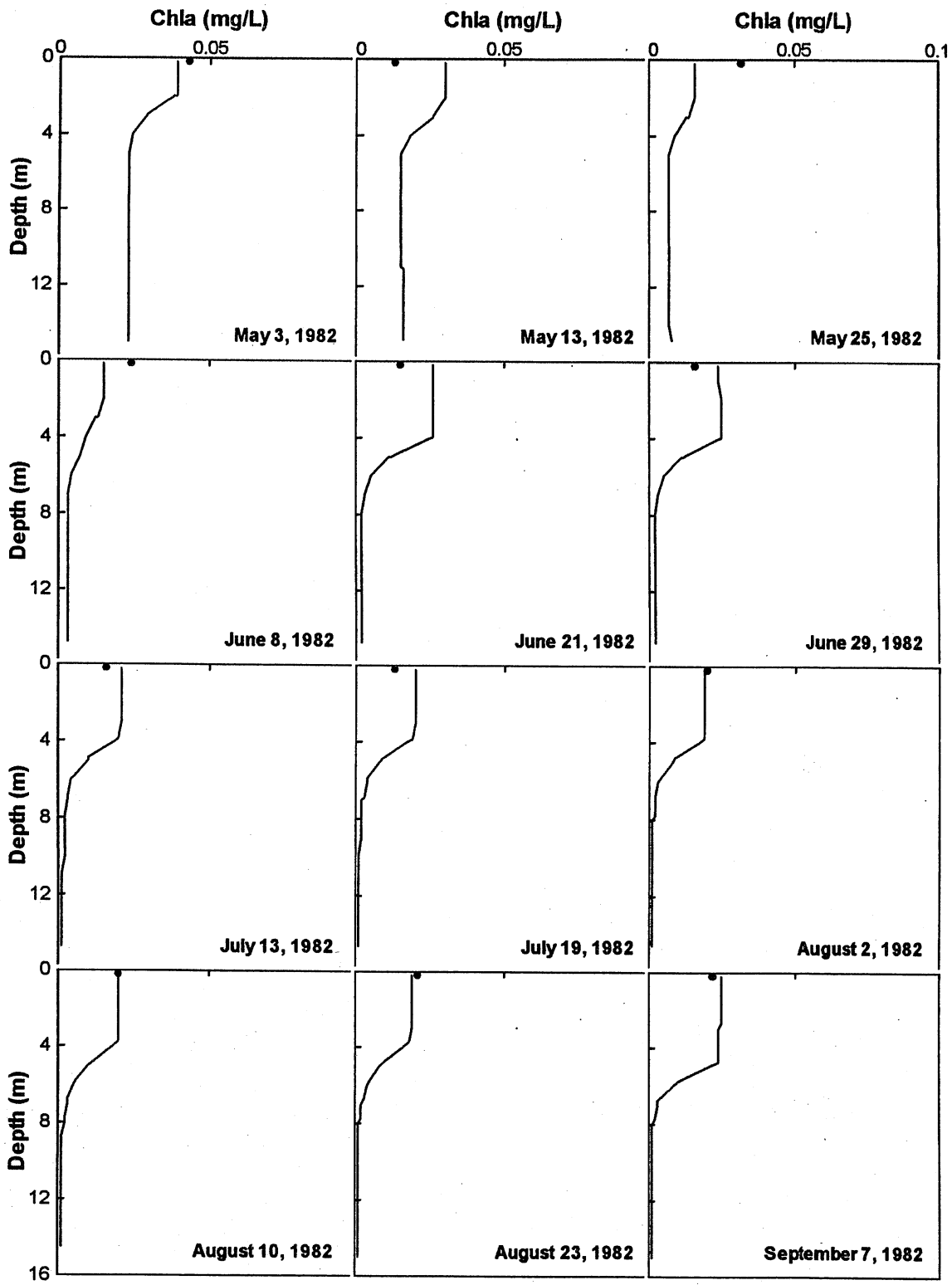

Figure 4.6. Simulated chlorophyll profiles (line) and observed surface values (dot) for Lake Riley, 1982.

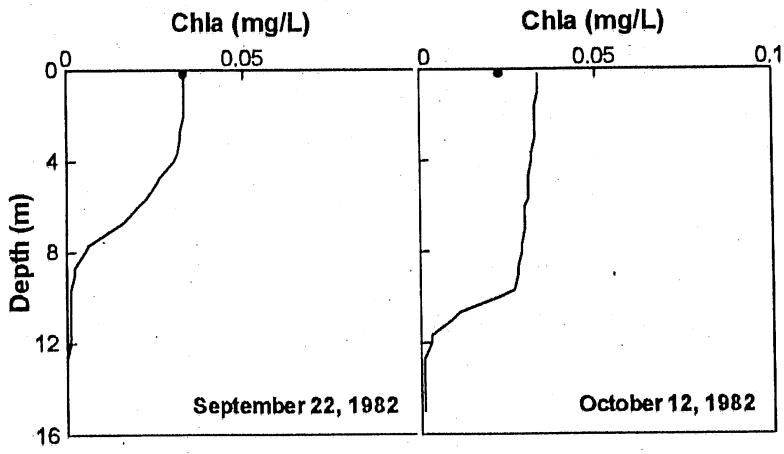

Figure 4.6 (continued). Simulated chlorophyll profiles (line) and observed surface values (dot) for Lake Riley, 1982.

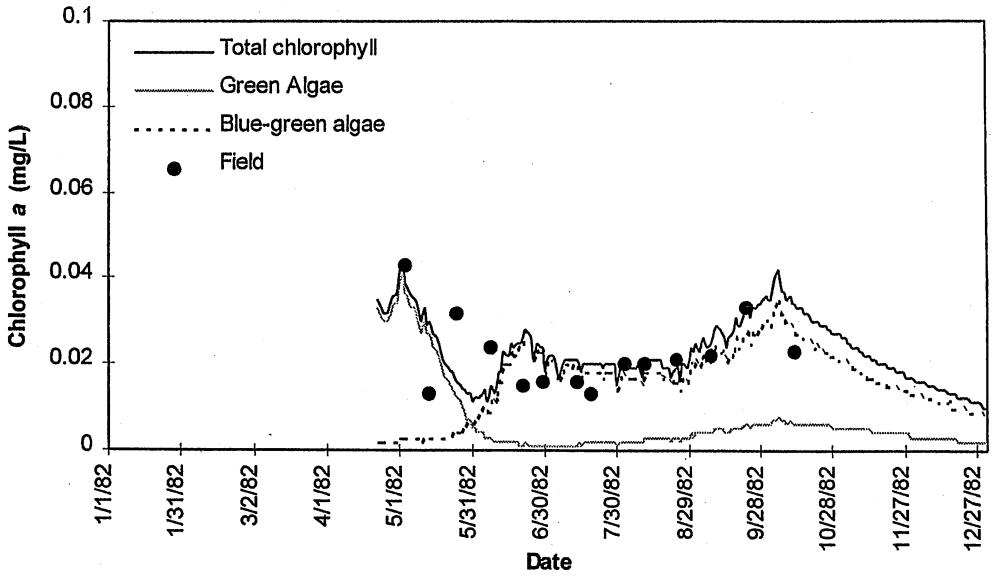

Figure 4.7. Simulated surface chlorophyll *a* (line) after the calibration of the MINLAKE98 model to the 1982 field data (dots) for Lake Riley

4.1.3 Re-calibration

The model was re-calibrated using field data from 1986. The recalibration was made because it appears that the observed seasonal growth pattern of phytoplankton in 1982 differs from the 1985 through 1990 observed values. Either 1982 is an unusual year or an algae changed occurred between 1982 and 1985. (See the discussion of the field data in Appendix B.) Coefficients that were changed for the recalibration are listed in Table B.1 (Appendix B). The statistical results are presented in Table 4.2. Again **temperature** is simulated best with both the slope and regression coefficient close to 1.0. This simulation has an even better correlation coefficient and standard error for temperature than the 1982 simulation. A plot of the observed vs. simulated values (Figure 4.8) shows a good simulation of all of the temperatures except the extremely low temperatures. The simulation gives a good estimate of the location of the thermocline (Figure 4.9). The largest error occurs in the winter under ice cover.

The **dissolved oxygen** is simulated with a slope of 1.02 and a regression coefficient of 0.84. A comparison of the observed and simulated values (Figure 4.8) shows that the model tends to overpredict the lower DO values and underpredict the higher DO values. In the oxygen profiles (Figure 4.10) it can be seen that the largest errors occur at the surface during June and July. This underprediction of DO corresponds to the underprediction of phytoplankton population during that time period (see discussion of chlorophyll below). Even though the surface DO values are underpredicted in the summer months the dissolved oxygen gradient near the thermocline is simulated well.

A comparison of the observed and simulated **total phosphorus** values (Figure 4.8) shows a linear relationship, but consistent underprediction of the phosphorus concentrations for all but the lowest values. This can also be seen in the phosphorus profiles (Figure 4.11) were the simulated concentrations follow the observed trend in the hypolimnion, but are not as elevated after both spring and fall turnover. The underprediction of phosphorus in the hypolimnion in December (winter conditions) may be due to low phosphorus release under ice cover in the model.

Figure 4.12 presents a comparison of the simulated surface **chlorophyll *a*** with field data for 1986. Several of the field data points show chlorophyll concentrations more than twice the values in 1982. Both the statistical results (Table 4.2) and the visual results (Figure 4.12) show a large error in the simulation of chlorophyll *a*. The visual results of the total phosphorus (Figure 4.11) show good agreement especially with the surface water. The simulated phytoplankton appear to be phosphorus limited while the observed phytoplankton is not. This indicates that there was a change in the algae population to one that requires less phosphorus for growth. Following this premus a another simulation of phytoplankton requiring 80% less phosphorus was run for 1986. Although the less phosphorus limited phytoplankton run produced a bloom of equivalent magnitude to the observed bloom, the simulated bloom was still over a month late. The reason for this poor simulation is not clear. It is possible that the model does not simulate important processes that were effective in 1986 but not in 1982. The data show an algae peak in the middle of the summer and not in the fall, where it was observed after fall overturn in 1982 (Figure 4.7). (See Appendix B for further discussion of the field data.)

Table 4.2. Statistical results from the re-calibration of the MINLAKE98 model to the 1986 field data for Lake Riley.

	Temperature (°C)	Dissolved Oxygen (mg/L)	Total Phosphorus (mg/L)	Chlorophyll *a* (mg/L)
Standard error	0.93	1.59	0.13	0.031
Maximum error	-2.78	7.25	-0.62	-0.086
Slope of regr. line	0.96	1.02	1.28	0.26
Regr. coefficient	0.96	0.85	0.79	-0.73
No. of data points	219	219	71	15

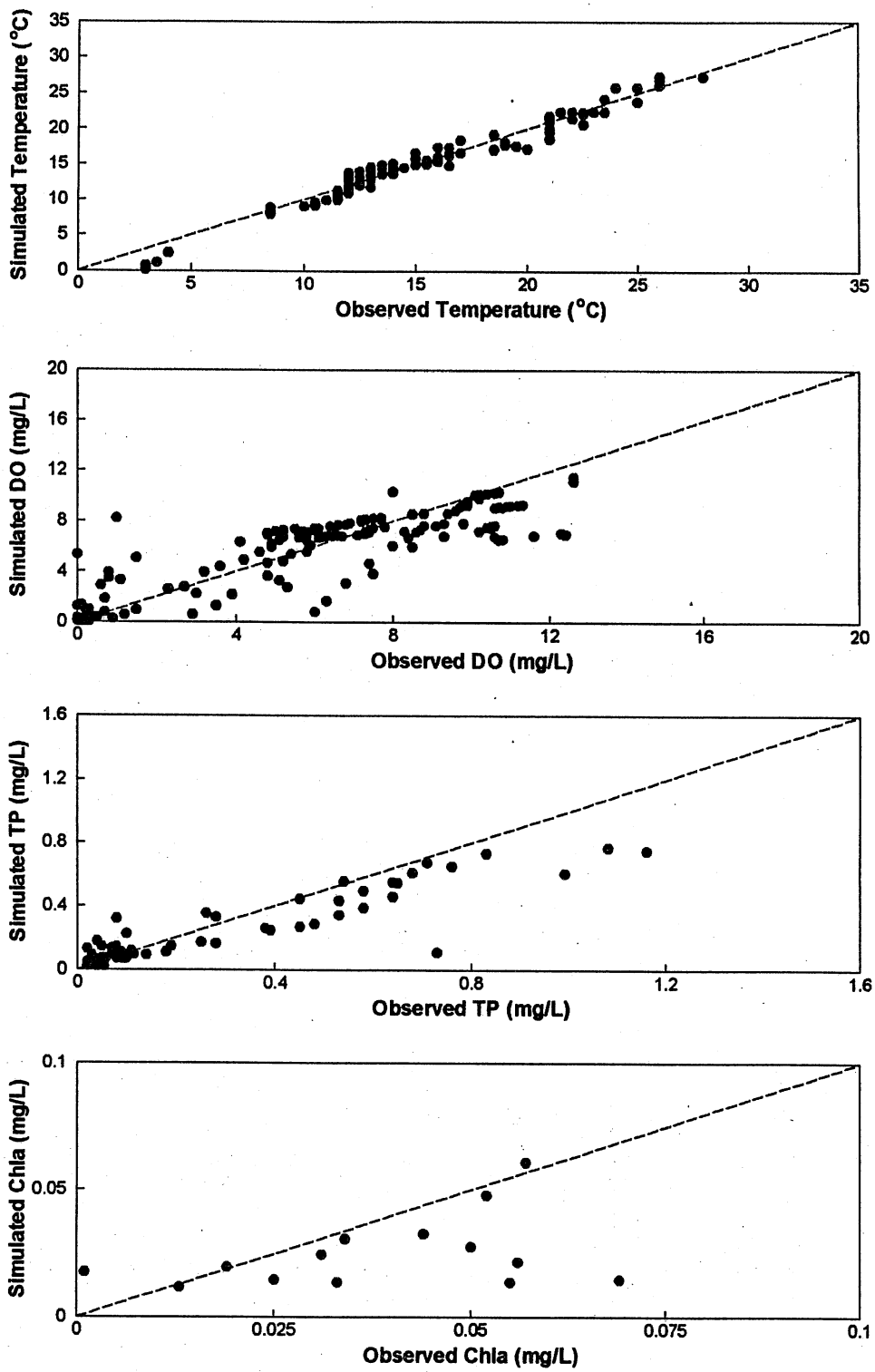

Figure 4.8. Comparison of simulated and observed water quality values for Lake Riley, 1986.

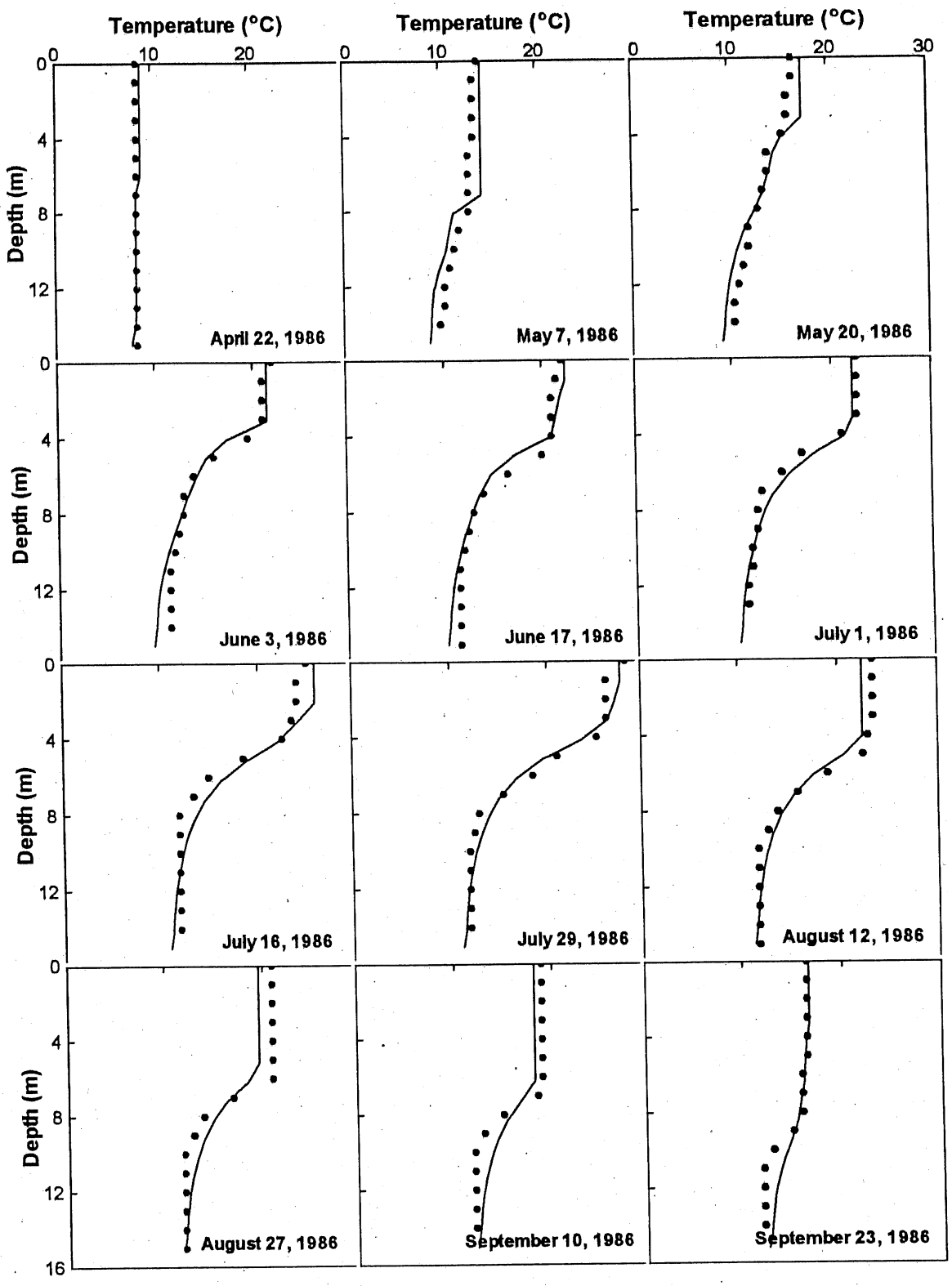

Figure 4.9. Simulated (line) and observed (dot) water temperature profiles for Lake Riley, 1986.

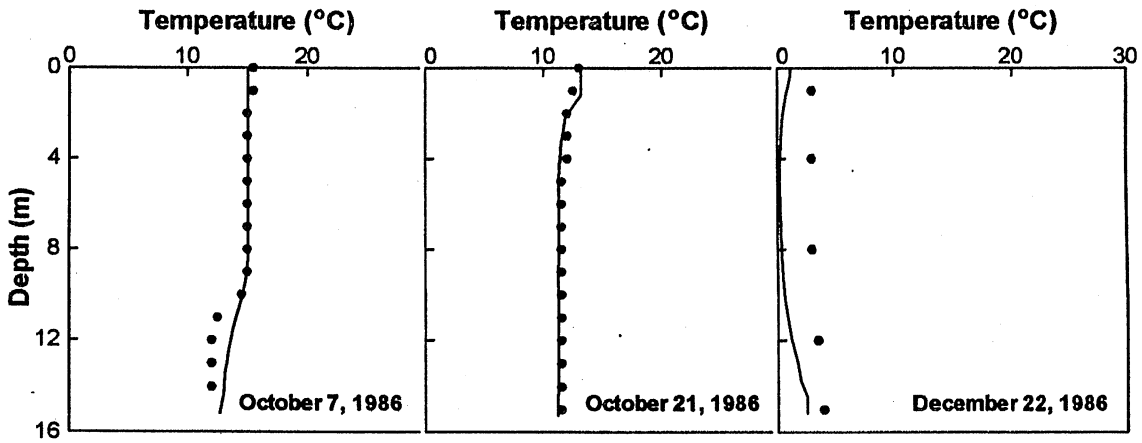

Figure 4.9 (continued). Simulated (line) and observed (dot) water temperature profiles for Lake Riley, 1986.

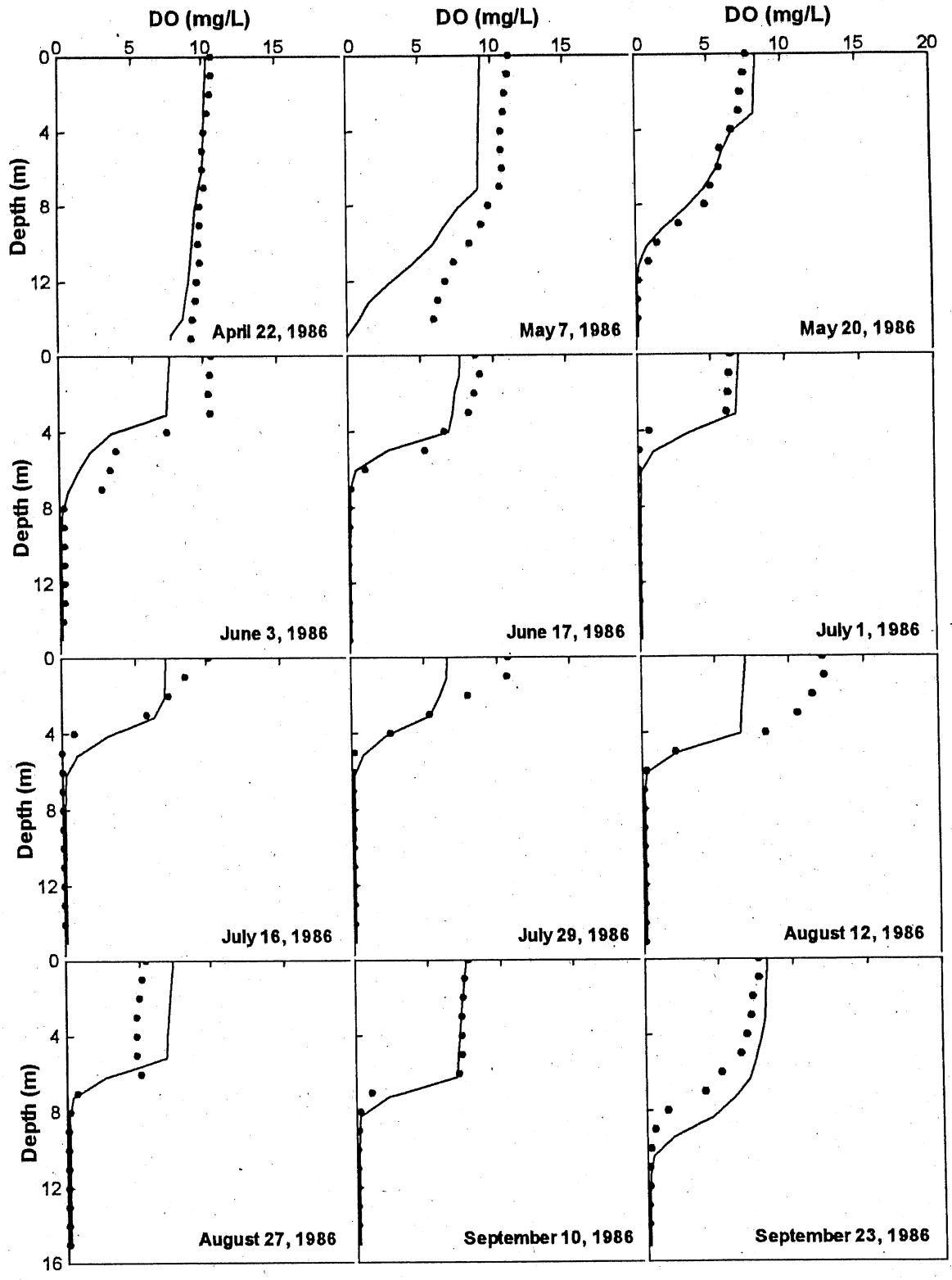

Figure 4.10. Simulated (line) and observed (dot) dissolved oxygen profiles for Lake Riley, 1986.

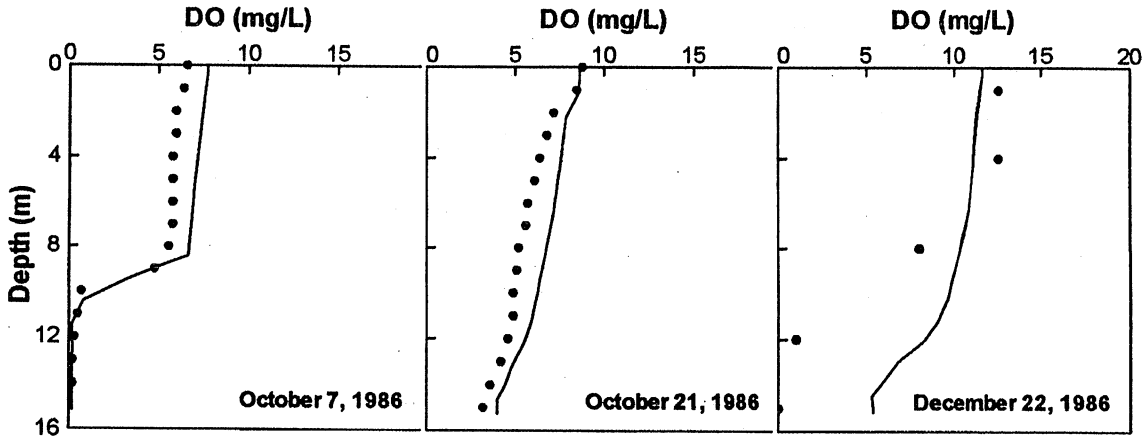

Figure 4.10 (continued). Simulated (line) and observed (dot) dissolved oxygen profiles for Lake Riley, 1986.

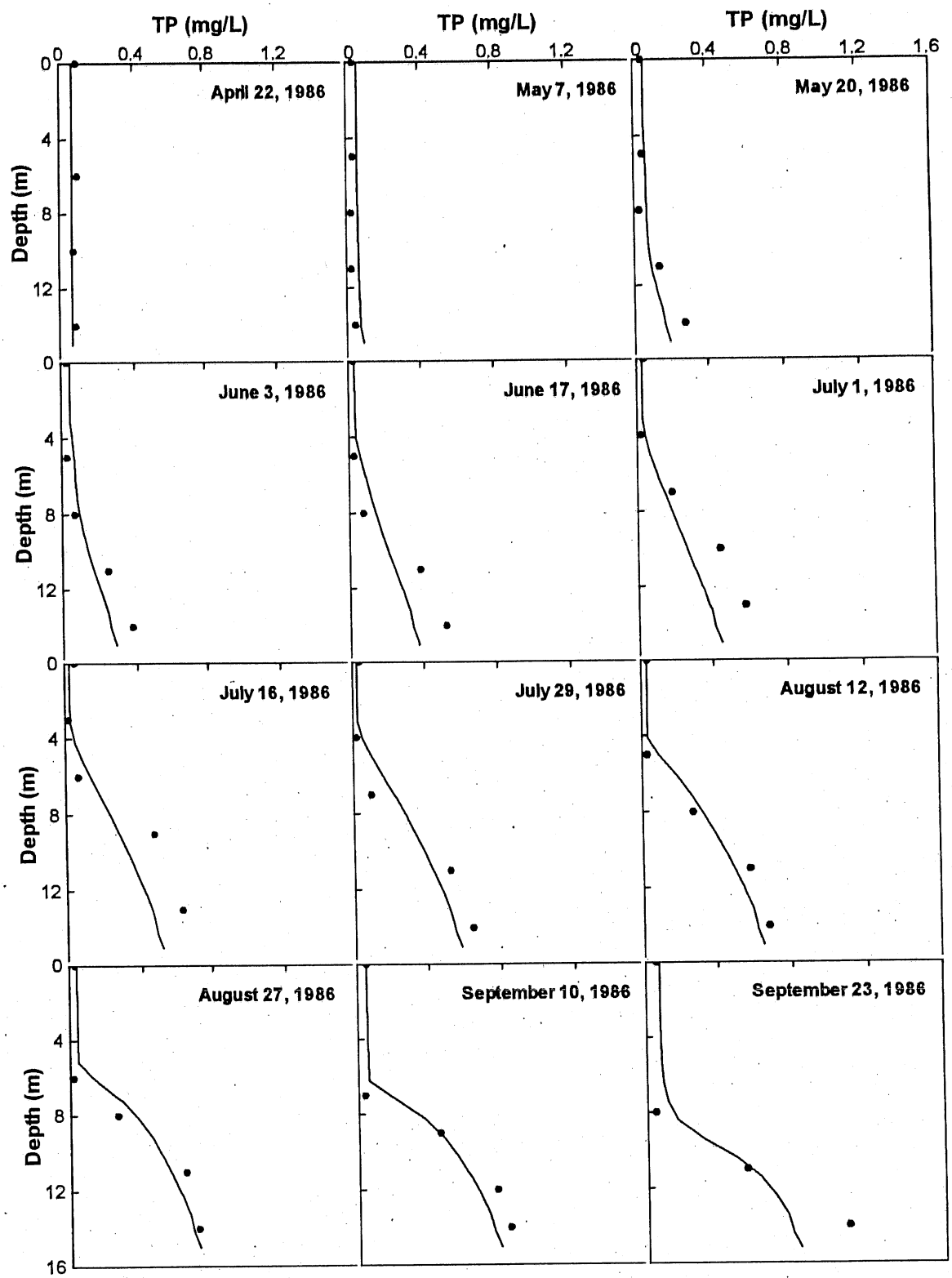

Figure 4.11. Simulated (line) and observed (dot) total phosphorus profiles for Lake Riley, 1986.

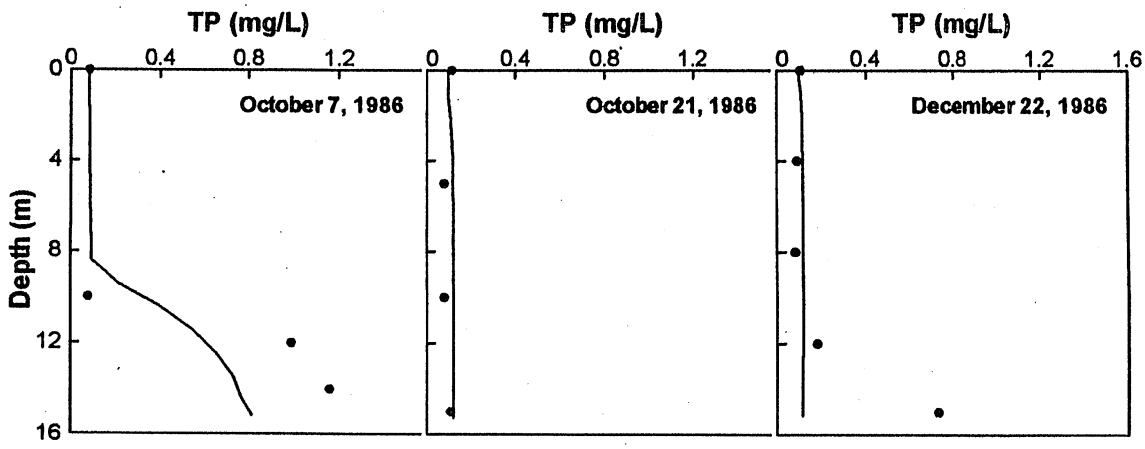

Figure 4.11 (continued). Simulated (line) and observed (dot) total phosphorus profiles for Lake Riley, 1986.

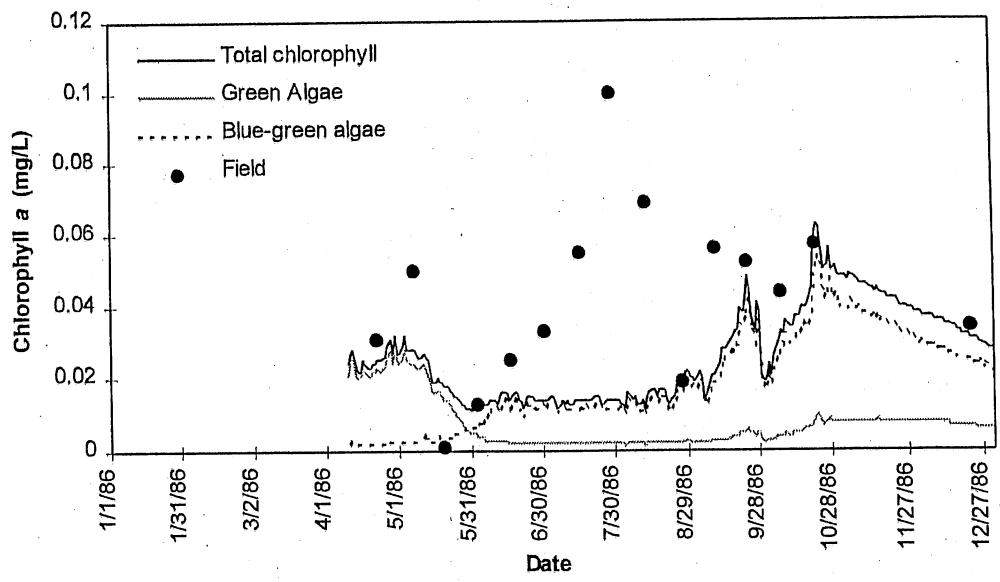

Figure 4.12. Simulated surface chlorophyll *a* (line) and field data (dots) for Lake Riley 1986.

4.1.4 Multiple Year Simulation

MINLAKE98 was also applied in a multiple year-round sequential simulation (1985-1990) of Lake Riley. Coefficients used in the 1986 simulation were kept unchanged. The statistical results are presented in Table 4.3. **Temperature** is simulated best with slope and regression coefficient of 0.98 and 0.91, respectively. Simulated temperatures and field values at four depths (surface, 4 m, 8 m, and 12 m) for 1985 to 1990 are presented in Figure 4.13.

The **dissolved oxygen** simulation has a slope of 1.06 and a regression coefficient of 0.79 (Table 4.3). Simulated dissolved oxygen and field values at four depths (surface, 4 m, 8 m, and 12 m) for 1985 to 1990 are presented in Figure 4.14. The dissolved oxygen appears to be simulated well in the hypolimnion (8 and 12 meters); it generally follows the trends in the surface layer but there is much scatter in 1986. This may be due to the time of data collection. There can be strong diurnal variations in surface DO concentrations because of daytime photosynthesis and possible supersaturation.

The **total phosphorus** simulation has a slope of 0.98 and a regression coefficient of 0.71 (Table 4.3). Simulated total phosphorus and field values at four depths (surface, 4 m, 8 m, and 12 m) for 1985 to 1990 are presented in Figure 4.15. The concentration of phosphorus is simulated best in the epilimnion and the metalimnion. The magnitude of concentration is simulated correctly in the lower hypolimnion but off in the upper hypolimnion.

Simulated **chlorophyll *a*** and field values at the lake surface, and simulated results at 4 m, 8 m, and 12 m below the surface are presented in Figure 4.16. The field data (available for the surface only) show large variations in concentration and do not appear to be simulated well. A discussion of the chlorophyll field data is given in Appendix C.

The plots of the simulated temperature, dissolved oxygen, total phosphorus, and chlorophyll *a* concentration do not reveal any trends over a 5+ year

Table 4.3. Statistical results from the validation of the MINLAKE98 model for the 1985-1990 field data for Lake Riley.

	Temperature (°C)	Dissolved Oxygen (mg/L)	Total Phosphorus (mg/L)	Chlorophyll *a* (mg/L)
Standard error	1.73	1.88	0.15	0.031
Maximum error	8.25	-10.25	0.64	-0.102
Slope of regr. line	0.98	1.06	0.98	0.07
Regr. coefficient	0.91	0.79	0.71	-0.87
No. of data points	849	763	220	51

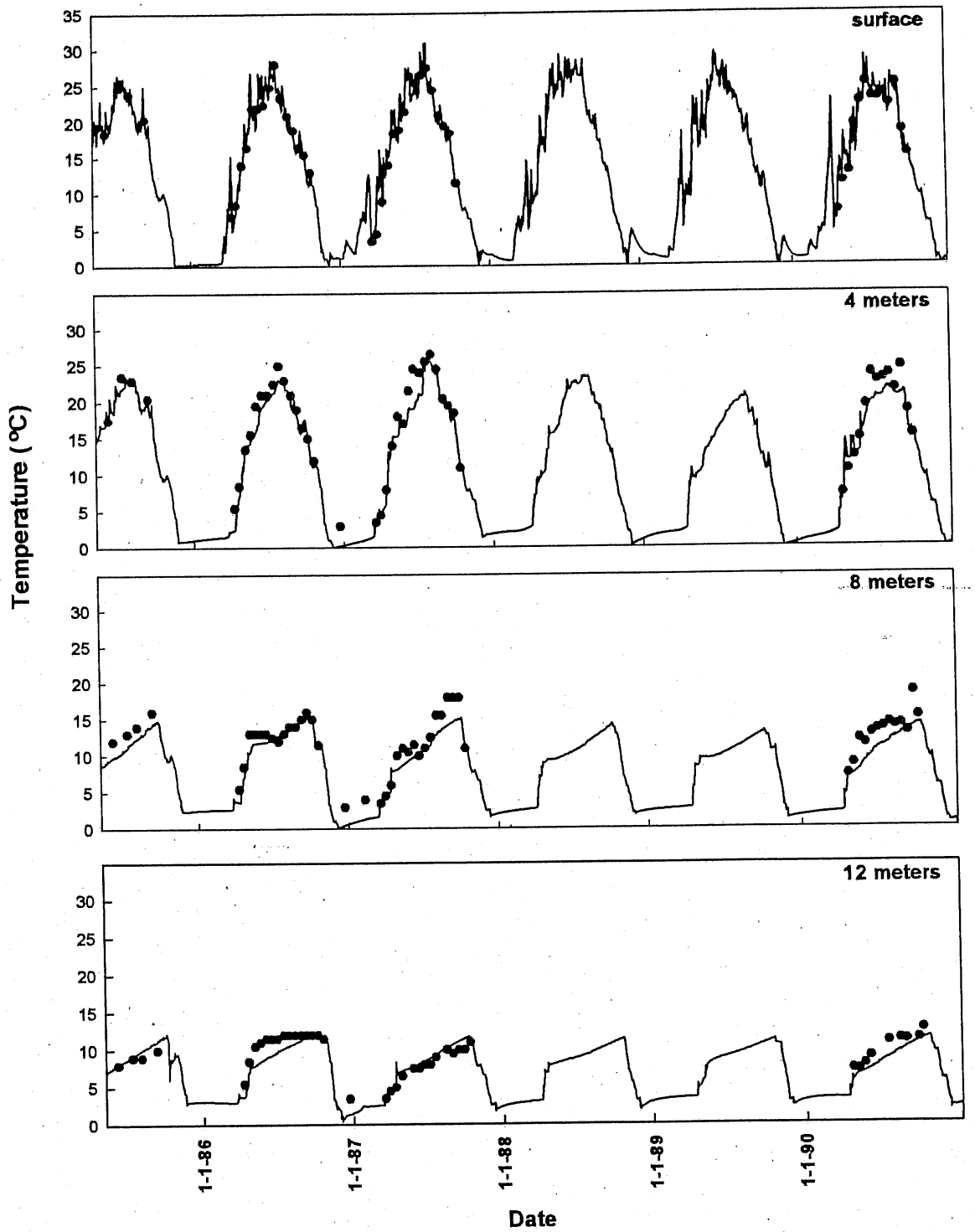

Figure 4.13. Simulated (solid line) and observed (dots) water temperatures at (a) surface, (b) 4 m, (c) 8 m, and (d) 12 m below the surface for Lake Riley, April 1985 to December 1990.

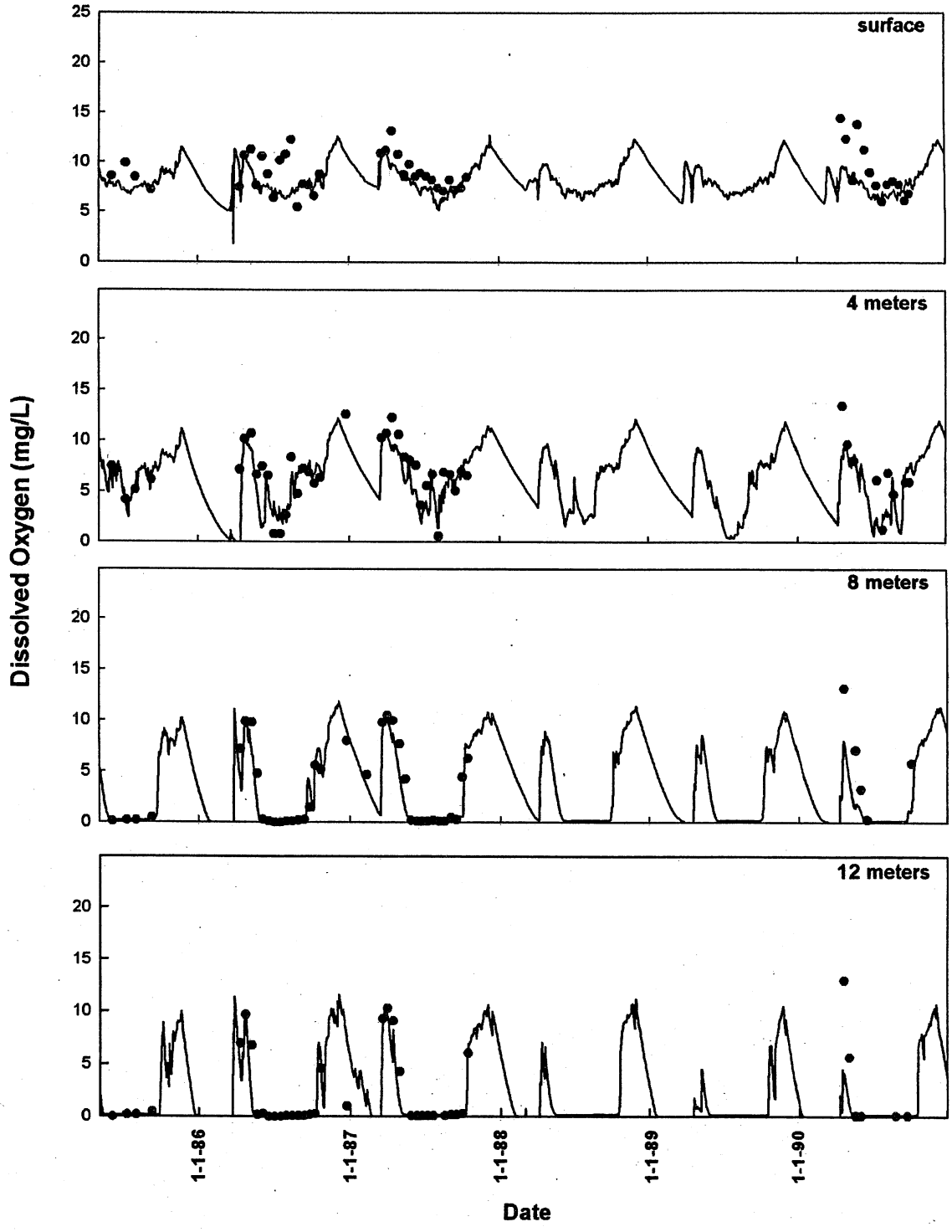

Figure 4.14. Simulated (solid line) and observed (dots) dissolved oxygen concentrations at (a) surface, (b) 4 m, (c) 8 m, and (d) 12 m below the surface for Lake Riley, April 1985 to December 1990.

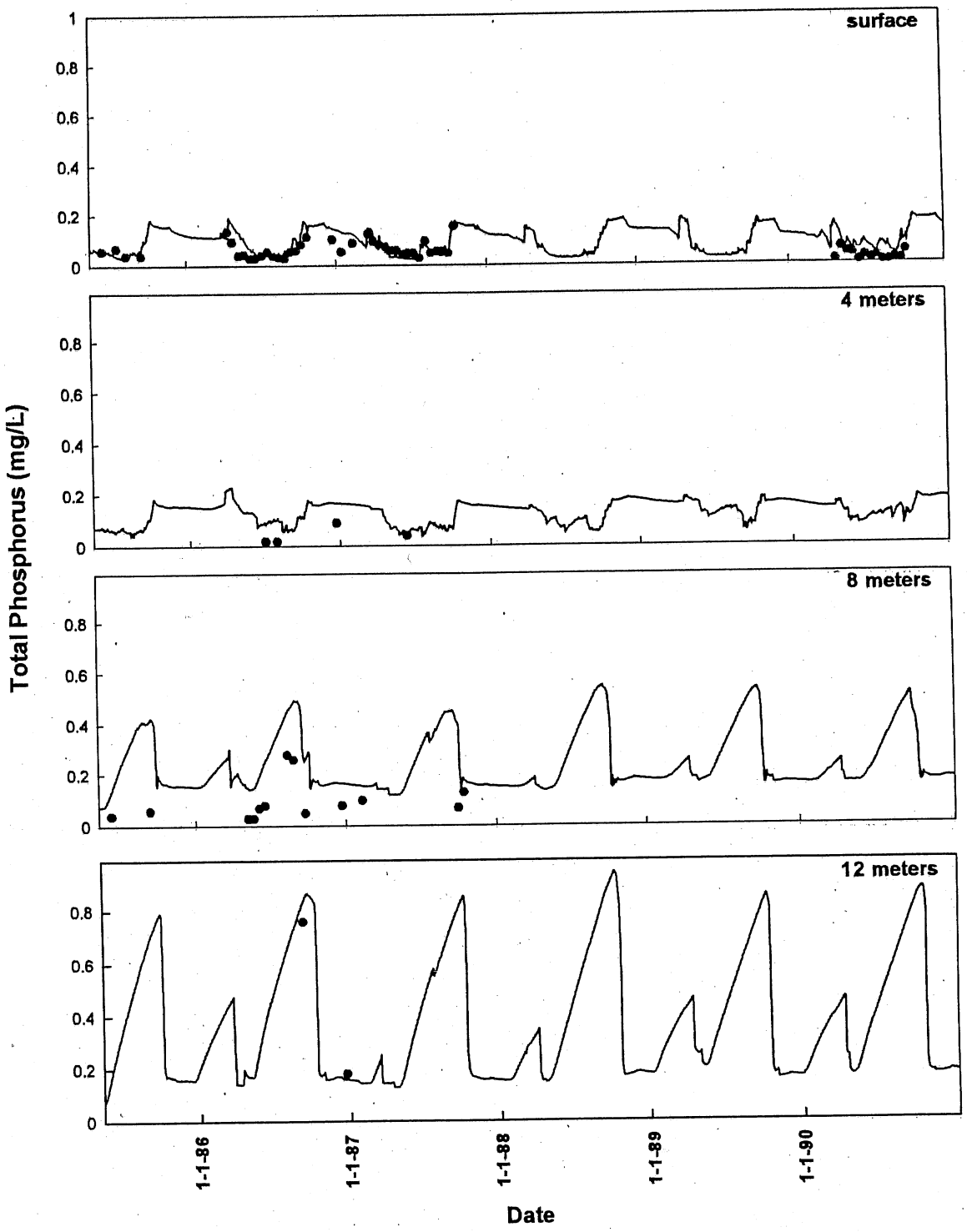

Figure 4.15. Simulated (solid line) and observed (dots) total phosphorus concentrations at (a) surface, (b) 4 m, (c) 8 m, and (d) 12 m below the surface for Lake Riley, April 1985 to December 1990.

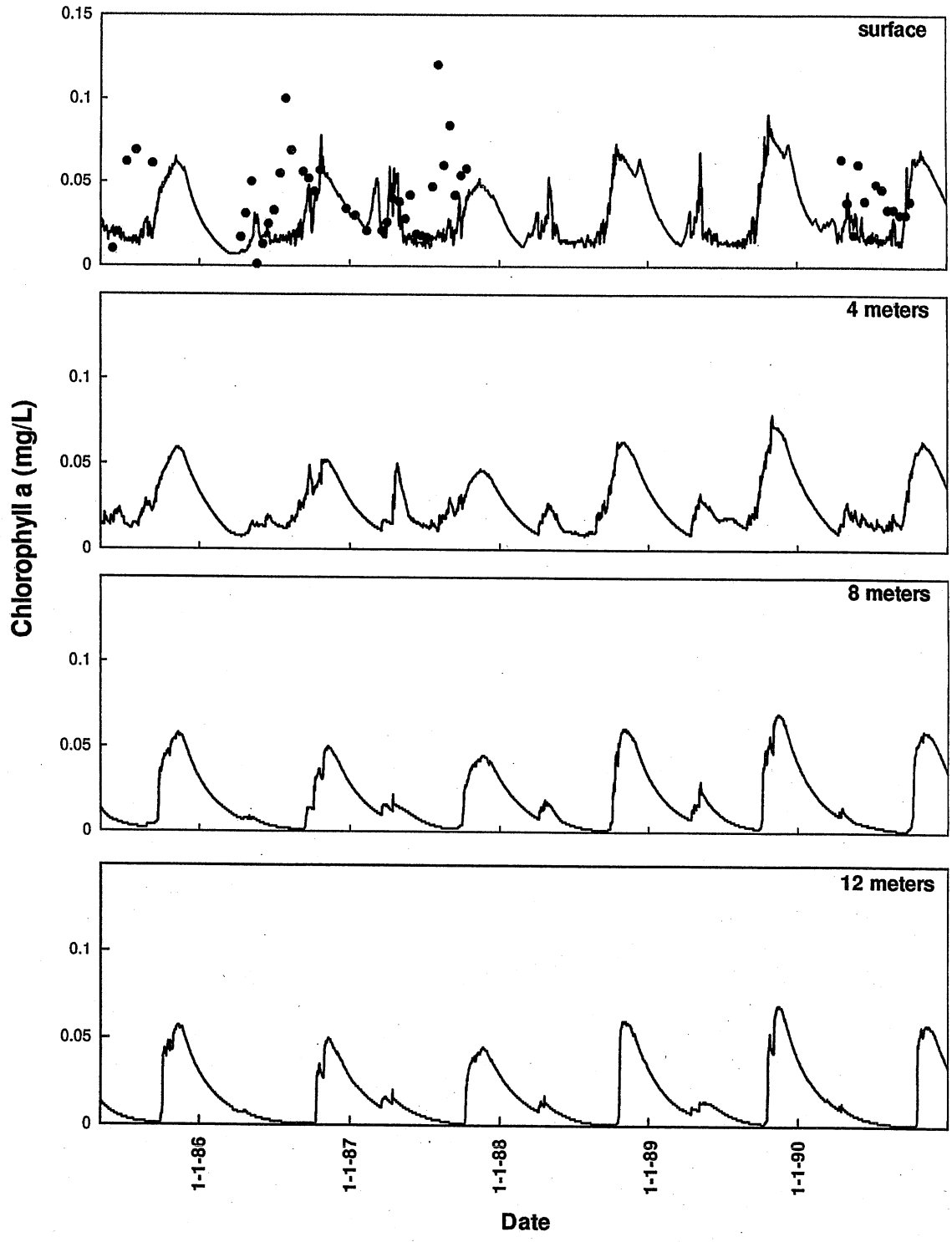

Figure 4.16. Simulated (solid line) and observed (dots) chlorophyll *a* concentrations at (a) surface, (b) 4 m, (c) 8 m, and (d) 12 m below the surface for Lake Riley, April 1985 to December 1990.

4.2 Lake Elmo

The MINLAKE98 model was also applied to Lake Elmo. Lake Elmo is located approximately 10 miles east of St. Paul in Washington County, MN. It has an oval shape, a surface area of 1.23 km^2, a maximum length of 2.5 km, and mean width of 0.49 km, a mean depth of 13.4 m, and a maximum depth of 41.8 m (Figure 4.17). There is a large regional park west of the lake. The lake is oriented away from the prevailing wind direction which, along with its depth, allows for stable seasonal stratification. There are four inlets, one significant, two small inlets and one ephemeral. Major land uses include 35% cropland, 30% grassland and 12% residential. There are no point discharges, industrial or domestic, to the lake since 1978 (Osgood, 1983).

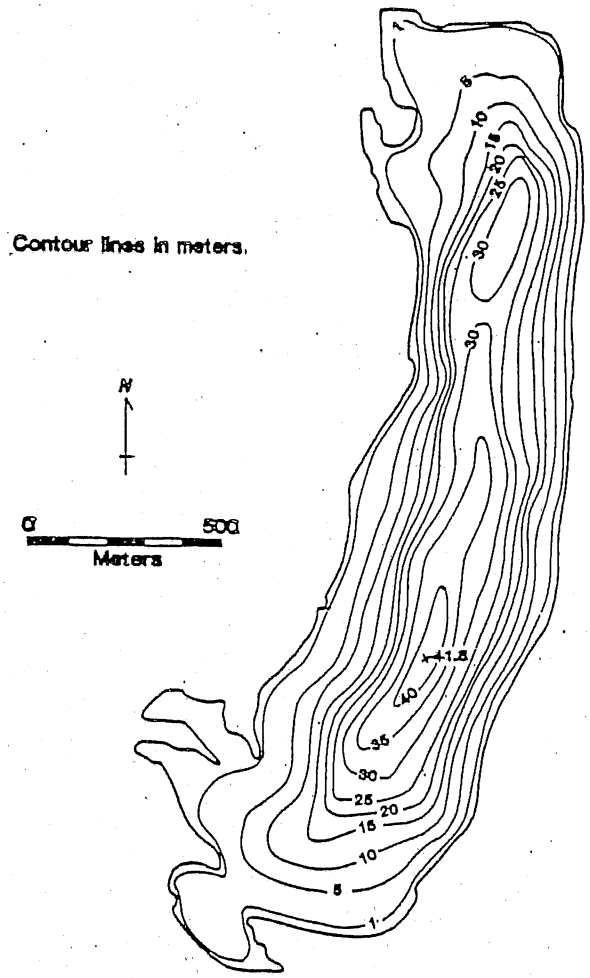

Figure 4.17. Bathymetric map of Lake Elmo (after Osgood, 1983).

4.2.1 Data Base

The lake was extensively monitored in 1982, 1988, 1991, and 1994 and periodically monitored in 1980, 1981, 1984, and 1987 by the Metropolitan Council (Osgood, 1983). Replicate field measurements were made for 1982, single measurements were made for all other years. The field data were retrieved by from the EPA database, STORET.

Lake Elmo was simulated with inflow from stormwater runoff and groundwater. Outflow was simulated as surface outflow (with a flow rate equivalent to the sum of the groundwater inflow and the stormwater runoff). Two classes of algae were simulated: green and blue-green. Algae growth was simulated accounting for phosphorus and light limitation. Computation of the stormwater runoff by the SCS method is presented in Appendix C. A constant year-round groundwater inflow was simulated by the addition of 6500 m^3 of water daily (75 L/s or 5 mm/d) at 8.5 m depth with a temperature of 10°C and a dissolved oxygen concentration of 0.0 mg/L. Coefficients for simulating Lake Elmo using MINLAKE98 are listed in Appendix D.

4.2.2 Calibration

The model was calibrated using 1988 field data retrieved from the EPA STORET database. MINLAKE98 contains some rate coefficients that need to be adjusted to simulate a specific lake. Calibration was based on both statistical and visual comparison with the field data. The statistical results of the calibration are presented in Table 4.4.

The goodness of fit of the simulated water quality parameters to the field data was evaluated using a linear regression constrained through the origin, the same as for Lake Riley.

The statistical results show that **temperature** is simulated best with a slope of 1.03 and a regression coefficient of 0.97. A comparison of the observed and simulated values is presented in Figure 4.18. Field data are available for the open water season only. The plotted points are close to the 1:1 line indicating a good simulation of the observed data. The location of the chemocline is simulated well especially for the summer months (Figure 4.19). Water temperatures in the upper hypolimnion are consistently overpredicted and those in the epilimnion are underpredicted in the fall.

Dissolved oxygen is also simulated well with a slope of 1.03 and a regression coefficient of 0.93. A comparison of the observed and simulated values is presented in Figure 4.18. The location of the dissolved oxygen pycnocline is simulated well (Figure 4.20). The inclusion of groundwater intrusion with a temperature of 10°C and a dissolved oxygen concentration of 0.0 mg/L improves the simulation of the dissolved oxygen profile. The exact volume, temperature, depth, and DO concentration of the groundwater intrusion is not known; a constant intrusion rate during the year was simulated. The volume of groundwater inflow was calibrated to best simulate both DO and temperature. It appears that the volume of groundwater intrusion is insufficient to simulate the DO

depression at approximately 9 m during July and August. Dispite some difficulties in simulating the complex DO profile the standard error is low, 0.89 mg/L DO.

Total phosphorus is simulated with a slope of 0.81 and a regression coefficient of 0.48. A comparison of the observed and simulated values (Figure 4.18) shows that the model in general is overpredicting the phosphorus concentration where it is low. The lower phosphorus concentrations are found in the epilimnion and the higher concentrations in the hypolimnion (Figure 4.21). The largest errors occur in the metalimnion and upper hypolimnion.

Simulated **chlorophyll *a*** values have the lowest statistical correlation with field observations. Both the slope and the regression coefficient are negative. Comparison of the observed and simulated values (Figure 4.18) shows that observed values are slightly overpredicted for the lower values and underpredicted for the higher values. Lake Elmo has approximately one fourth of the chlorophyll concentration of Lake Riley. Figure 4.22 gives a comparison of the simulated surface chlorophyll with the field data. Both green and blue-green algae were simulated. The blue-green algae population is simulated well and the green algae population is generally overpredicted in the spring.

Table 4.4. Statistical results from the calibration of the MINLAKE98 model to the 1988 field data for Lake Elmo.

	Temperature (°C)	Dissolved Oxygen (mg/L)	Total Phosphorus (mg/L)	Chlorophyll *a* (mg/L)
Standard error	1.23	0.89	0.02	0.003
Maximum error	-4,54	-2.79	0.06	0.005
Slope of regr. line	1.03	1.03	0.81	-0.03
Regr. coefficient	0.97	0.93	0.48	-0.89
No. of data points	350	253	66	14

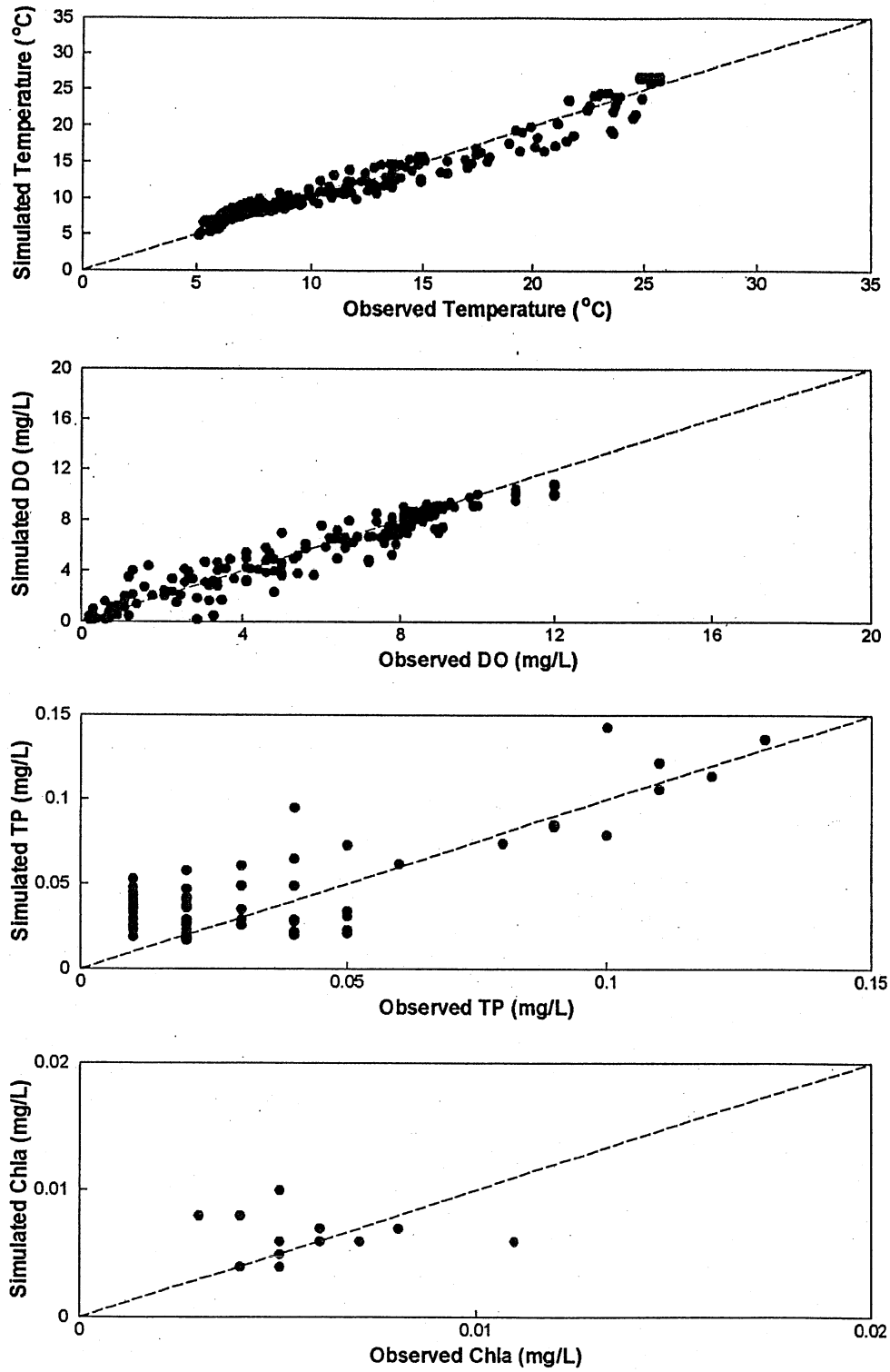

Figure 4.18. Comparison of simulated and observed water quality values for Lake Elmo, 1988.

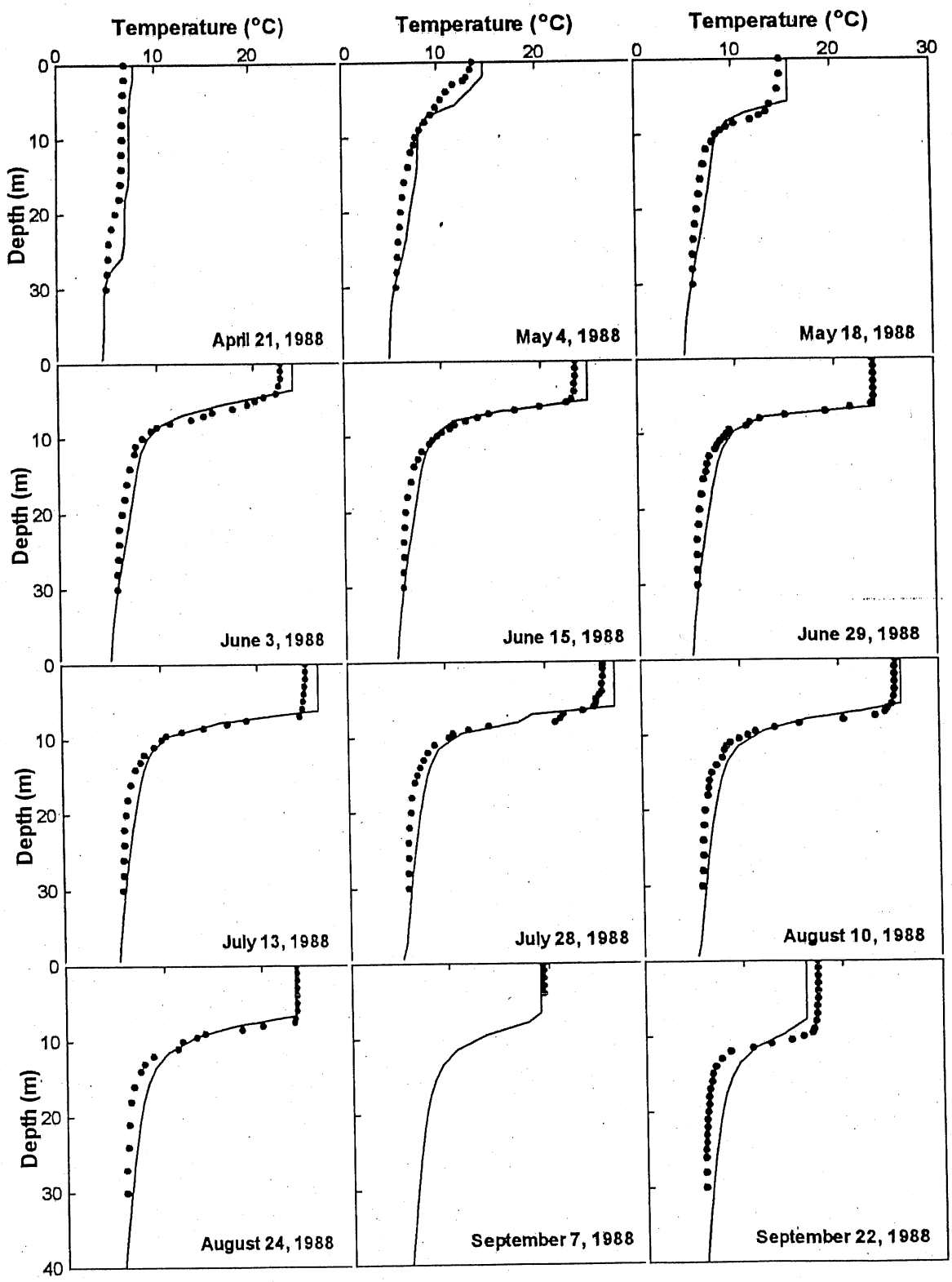

Figure 4.19. Simulated (line) and measured (dot) water temperature profiles for Lake Elmo, 1988.

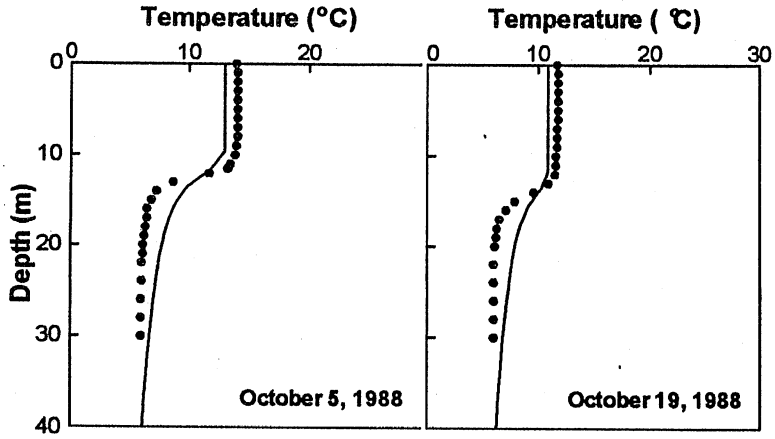

Figure 4.19 (continued). Simulated (line) and measured (dot) water temperature profiles for Lake Elmo, 1988.

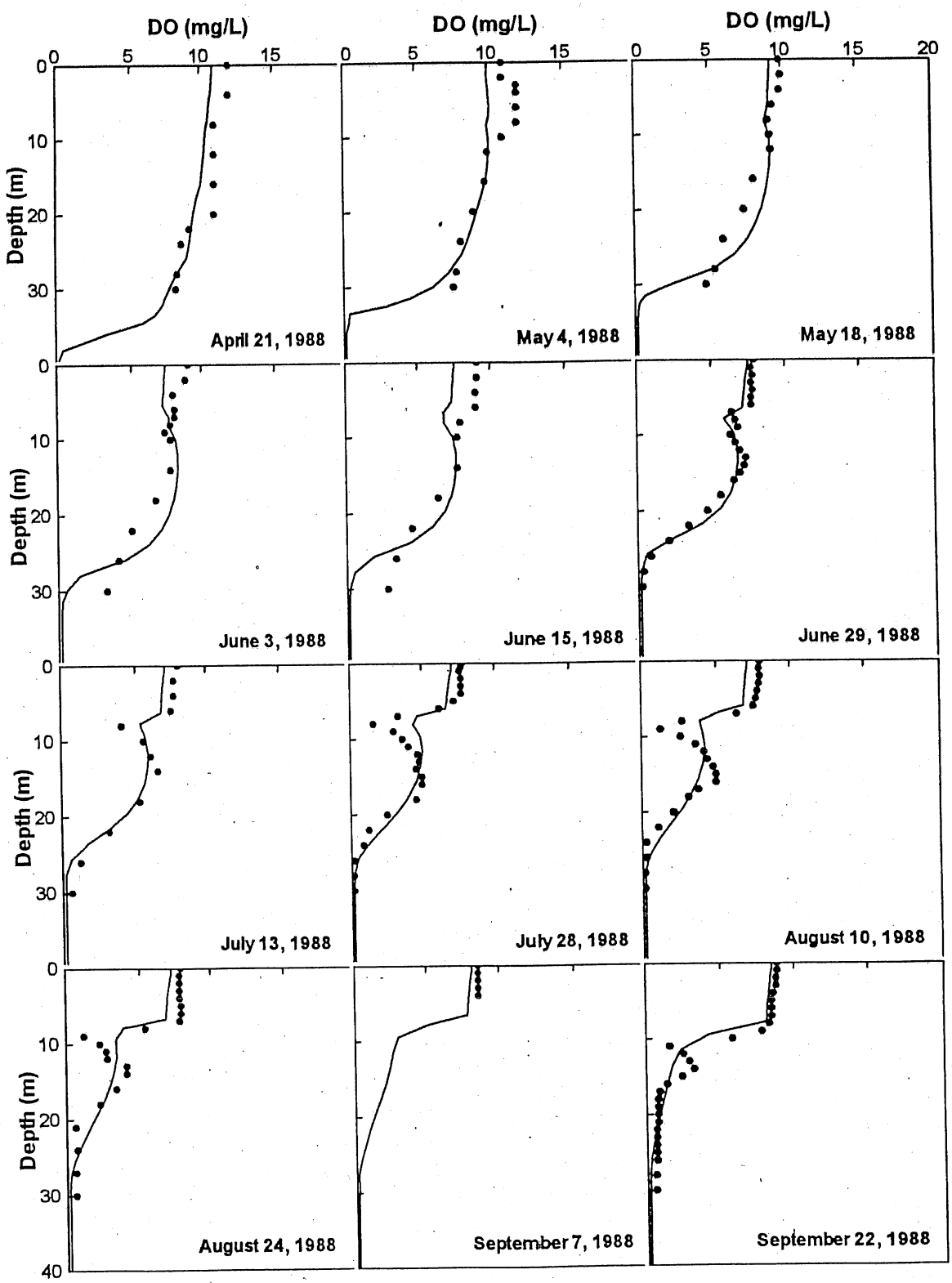

Figure 4.20. Simulated (line) and measured (dot) dissolved oxygen profiles for Lake Elmo, 1988.

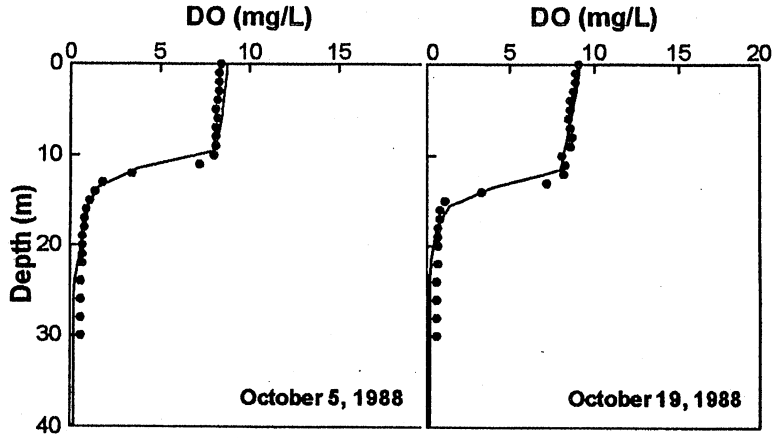

Figure 4.20 (continued). Simulated (line) and measured (dot) dissolved oxygen profiles for Lake Elmo, 1988.

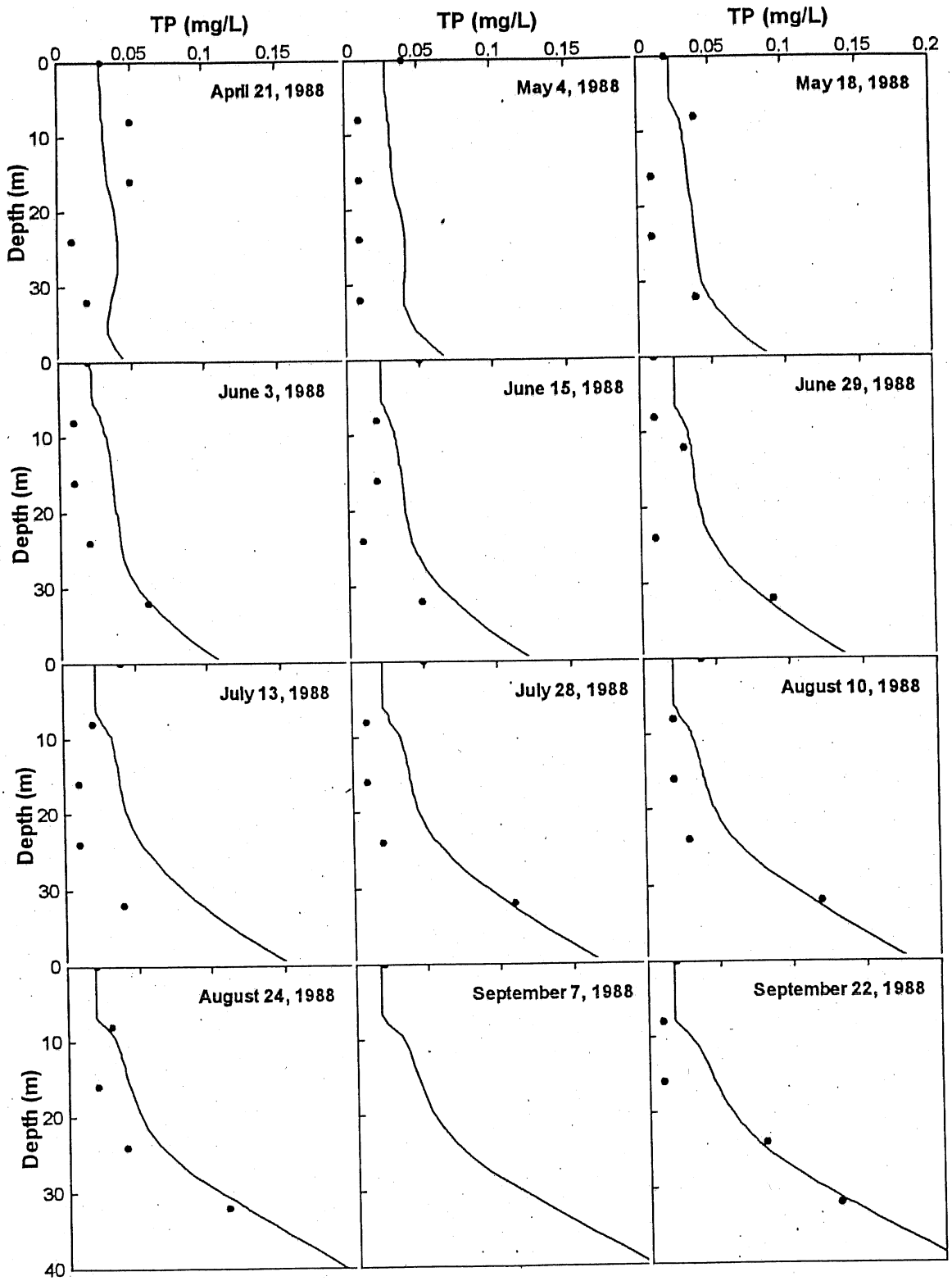

Figure 4.21. Simulated (line) and measured (dot) total phosphorus profiles for Lake Elmo, 1988.

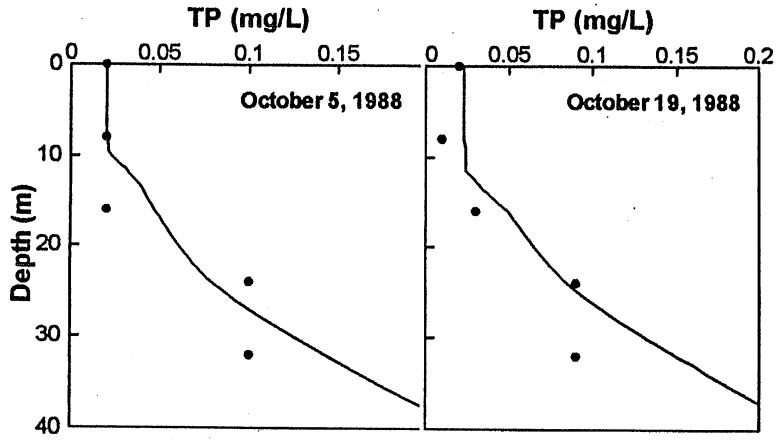

Figure 4.21 (continued). Simulated (line) and measured (dot) total phosphorus profiles for Lake Elmo, 1988.

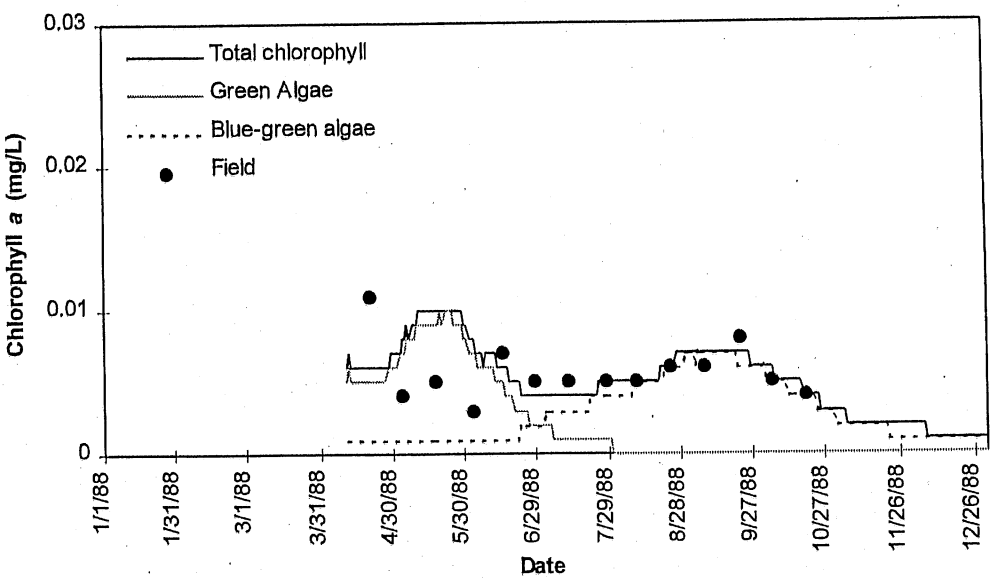

Figure 4.22. Simulated surface chlorophyll *a* (lines) after the calibration of the MINLAKE98 model to the 1988 field data (dots) for Lake Elmo.

4.2.3 Validation

The model was validated against data from 1982 assuming that the morphometric and hydrologic lake conditions were the same as for 1988. All coefficients used in the 1982 simulation were kept unchanged. The statistical results are presented in Table 4.5. **Temperature** is simulated well with a slope of 0.95 and a regression coefficient of 0.96. The extreme temperatures are simulated the best while the mid-range temperatures are consistently underpredicted as seen in Figure 4.23. Most of the mid-range temperatures occur near the thermocline. Unlike the 1988 simulation, the thermocline is simulated with a steeper gradient than was observed (Figure 4.24). However, similar to the 1988 simulation, the hypolimnion temperatures are slightly overpredicted.

The **dissolved oxygen** concentrations are not simulated as well for 1982 as for 1988; the standard error is almost twice as large. A comparison of the observed and simulated values (Figure 4.23) shows that the model generally underestimates the dissolved oxygen concentration, especially for the lower DO values. The dissolved oxygen profiles (Figure 4.25) also show the underprediction.

The simulated **total phosphorus** values are consistently overpredicted as seen in a comparison of the observed and simulated values (Figure 4.23). This can also be seen in the phosphorus profiles (Figure 4.26). The overprediction of phosphorus is consistent with the underprediction of dissolved oxygen, as more phosphorus is released from the sediment at lower DO concentrations. The observed release of phosphorus from the sediment appears to be lower for 1982 than for 1988.

Figure 4.27 presents a comparison of the simulated **surface chlorophyll** with field data for 1982. The chlorophyll concentrations are approximately twice as high for 1982 as for 1988. Both the statistical results (Table 4.5) and visual results (Figure 4.27) show a good simulation of the phytoplankton population for both the green and blue-green algae.

Table 4.5. Statistical results from the validation of the MINLAKE98 model for the 1982 field data for Lake Elmo.

	Temperature (°C)	**Dissolved Oxygen (mg/L)**	**Total Phosphorus (mg/L)**	**Chlorophyll *a* (mg/L)**
Standard error	1.45	1.80	0.03	0.004
Maximum error	-5.42	-6.08	0.07	0.014
Slope of regr. line	0.97	0.95	0.65	0.94
Regr. coefficient	0.95	0.73	-0.37	0.31
No. of data points	421	421	77	18

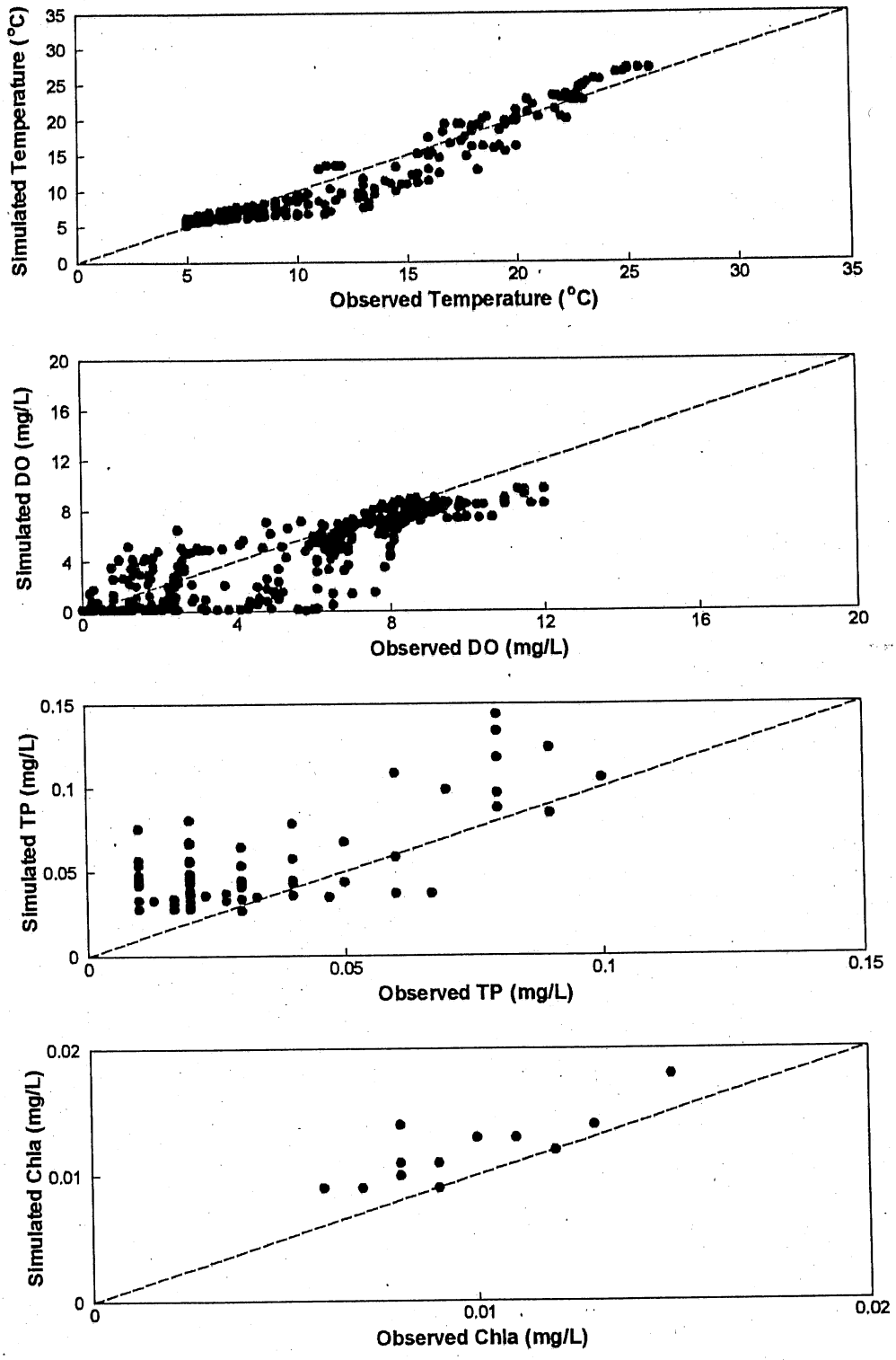

Figure 4.23. Comparison of the simulated and observed water quality values line for Lake Elmo, 1982.

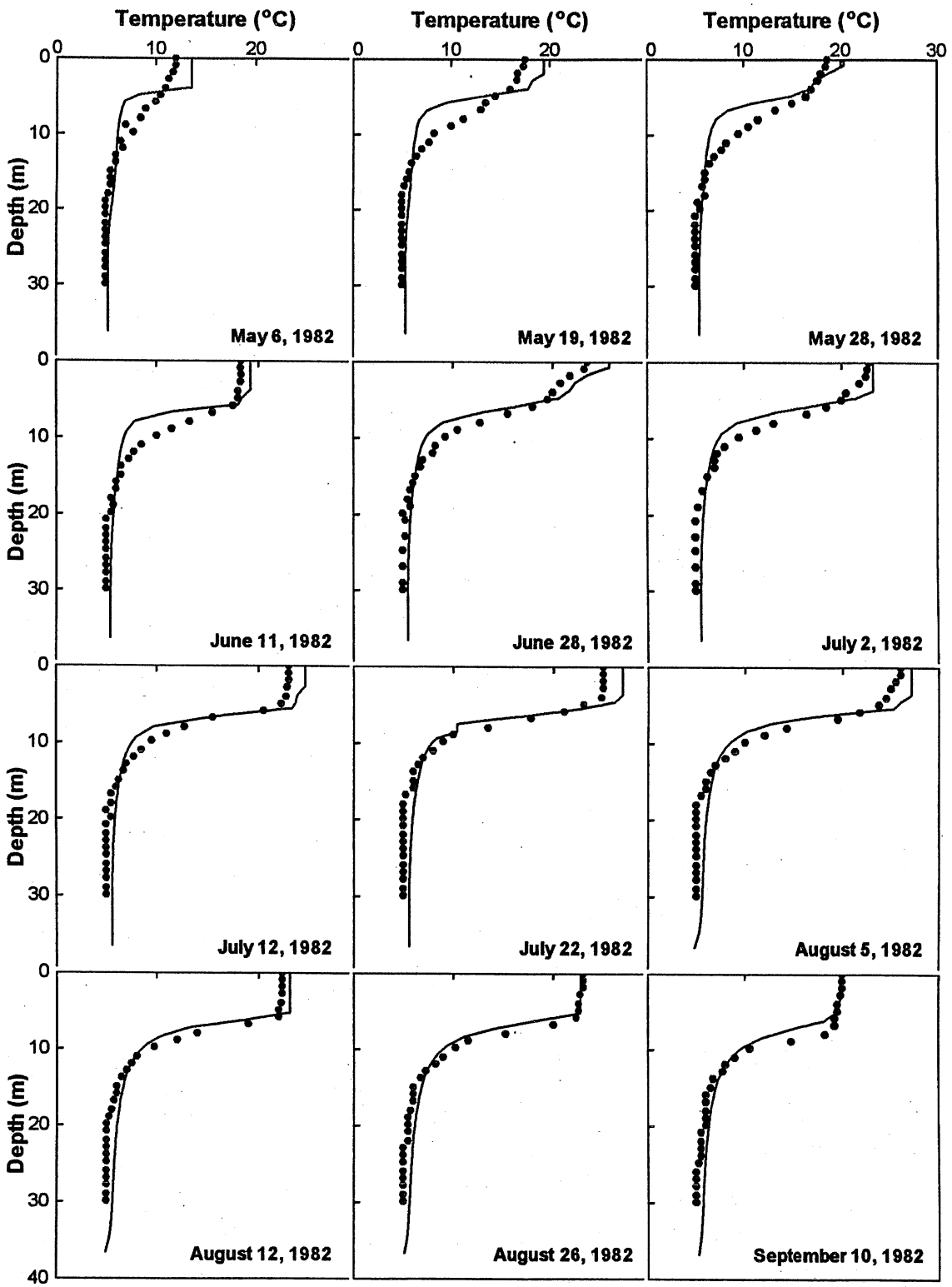

Figure 4.24. Simulated (line) and observed (dot) water temperature profiles for Lake Elmo, 1982.

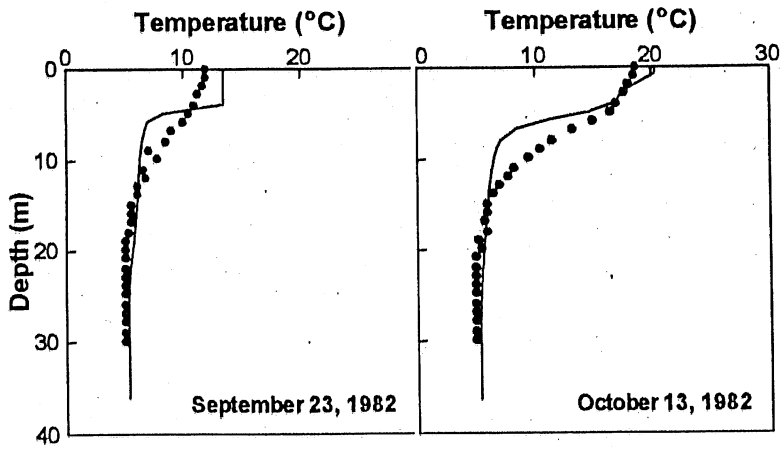

Figure 4.24 (continued). Simulated (line) and observed (dot) water temperature profiles for Lake Elmo, 1982.

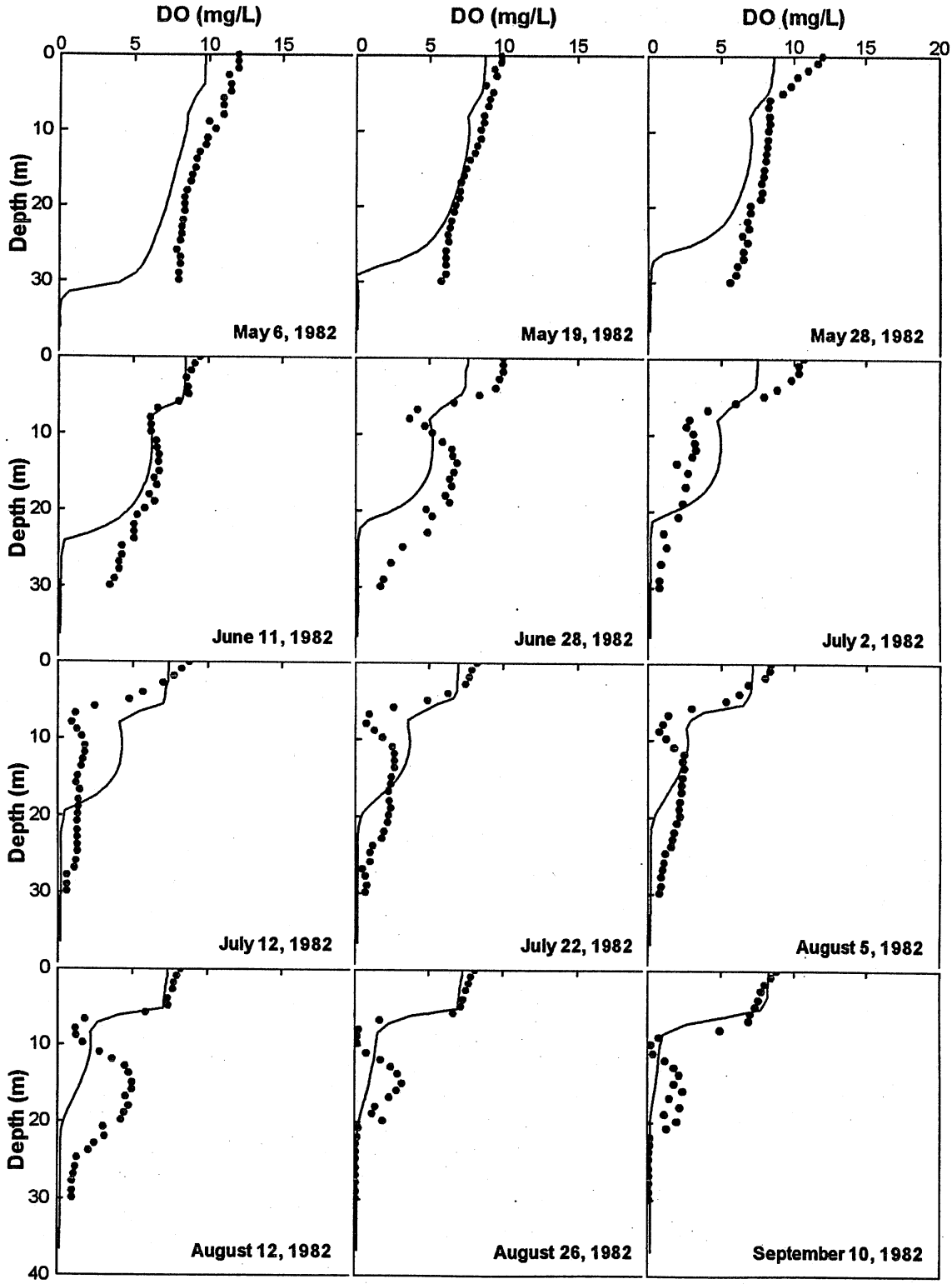

Figure 4.25. Simulated (line) and observed (dot) dissolved oxygen profiles for Lake Elmo, 1982.

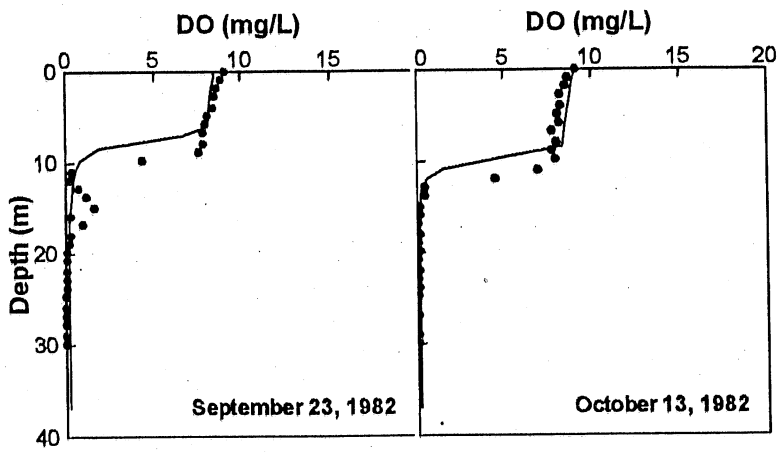

Figure 4.25 (continued). Simulated (line) and observed (dot) dissolved oxygen profiles for Lake Elmo, 1982.

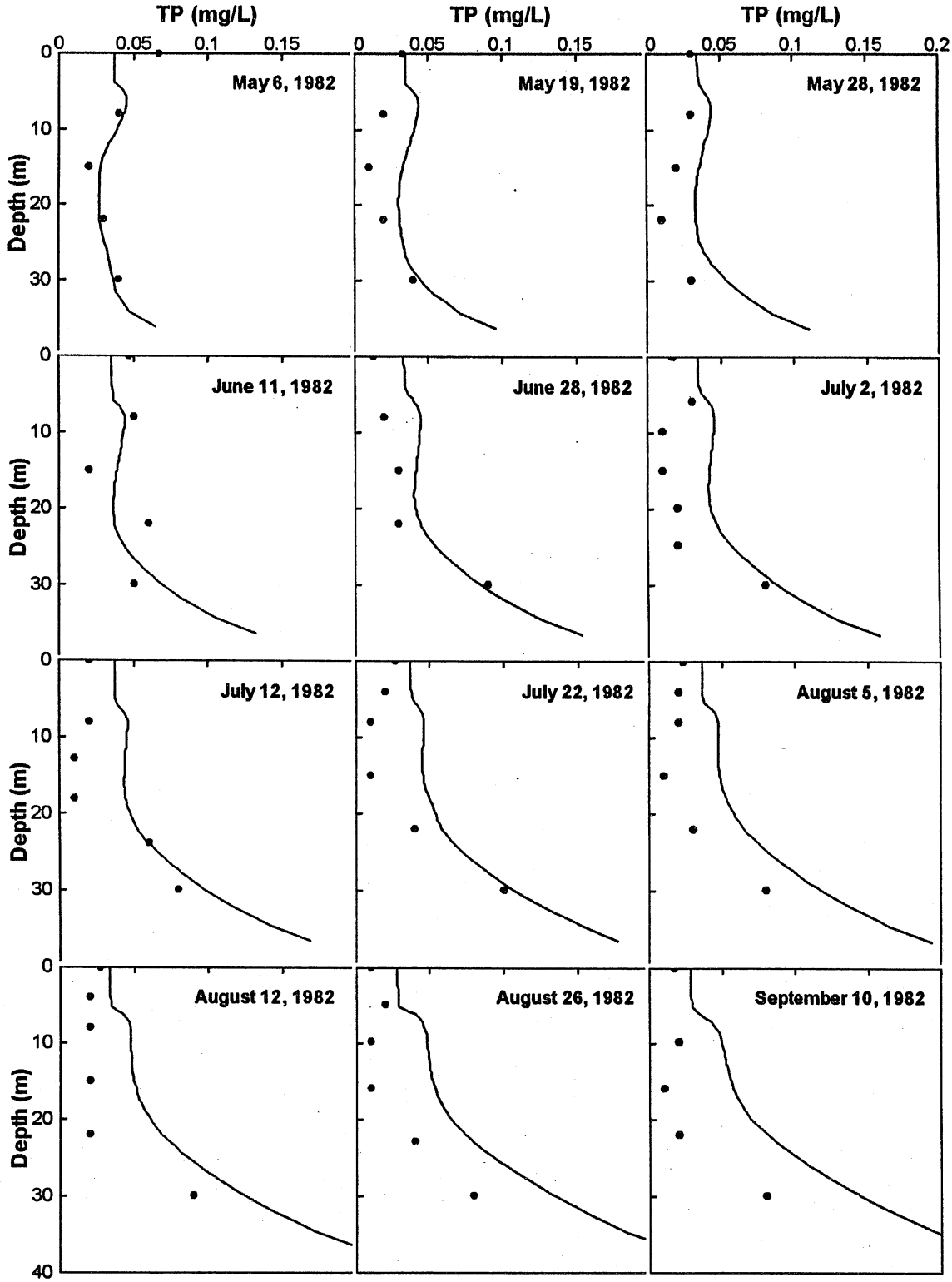

Figure 4.26. Simulated (line) and observed (dot) total phosphorus profiles for Lake Elmo, 1982.

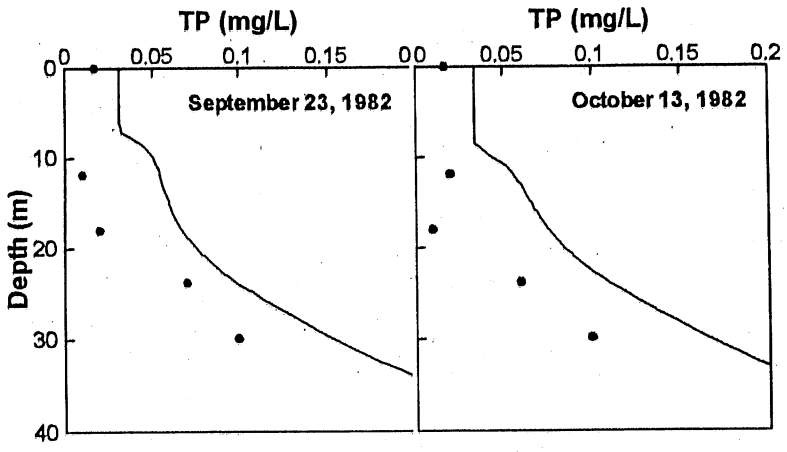

Figure 4.26 (continued). Simulated (line) and observed (dot) total phosphorus profiles for Lake Elmo, 1982.

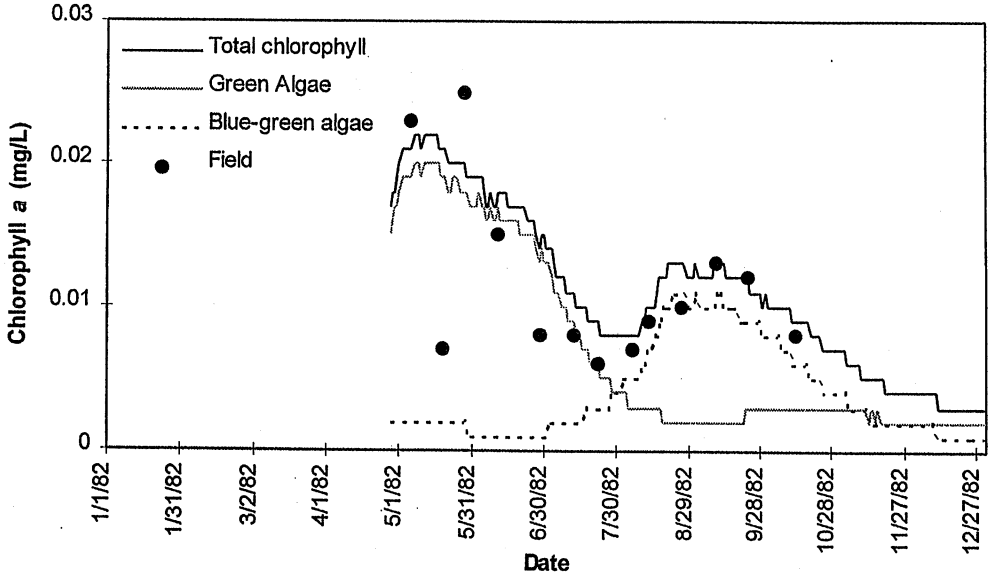

Figure 4.27. Simulated surface chlorophyll *a* (lines) and field data (dots) for Lake Elmo, 1982.

4.2.4 Multiple Year Simulation

MINLAKE98 was also applied in a multiple year simulation (1984-1991) of Lake Elmo. Coefficients used in the 1988 simulation were kept unchanged. **Temperature** is simulated with slope and regression coefficient of 1.00 and 0.95, respectively. The statistical results, presented in Table 4.6, show a good correlation and a slightly higher standard deviation than the 1988 simulation. Simulated and observed temperature values at four depths (surface, 8 m, 16 m, and 30 m) for 1984 to 1991 are presented in Figure 4.28.

The **dissolved oxygen** simulation has a slope of 1.09 and a regression coefficient of 0.79 (Table 4.6). Simulated dissolved oxygen and observed values at four depths (surface, 8 m, 16 m, and 30 m) for 1984 to 1991 are presented in Figure 4.29. Overall the simulated dissolved oxygen appears to have good agreement with the observed values except for the highest and some of the lowest values.

The **total phosphorus** simulation has a slope of 1.28 and a regression coefficient of 0.43 (Table 4.6). Simulated total phosphorus and observed values at four depths (surface, 8 m, 16 m, and 32 m) for 1984 to 1991 are presented in Figure 4.30. The surface concentration in 1984 is simulated well but the peaks during 1988 and 1991 are not. The simulated increase of phosphorus at 32 meters (the lowest depth measured) is simulated late and peaks at a slightly lower concentration than observed. It appears that a larger phosphorus flux from the sediment is required to simulate the observed values over a longer period of time then for the single years of 1982 and 1988. This may indicate that some process that occurs during the winter months is not being properly simulated.

Simulated **chlorophyll *a*** and observed values at the lake surface, and simulated results at 8 m, 16 m, and 30 m below the surface are presented in Figure 4.31 (field data are available for the surface only). The values observed during spring do not appear to be simulated well (i.e. the simulation of the green algae population does not have a significant bloom each spring except for the initial year). The simulation of the blue-green algae population is underpredicted for 1984 and 1988 and predicted well for 1991. The underprediction during 1988 is probably due to the low predicted phosphorus during that year. The only observed values of chlorophyll *a* for the winter period are during 1988. Several of these chlorophyll *a* values are higher than the concentrations during the spring and fall blooms. Without other data it is not clear if the 1988 winter concentrations are typical values.

Table 4.6. Statistical results from the validation of the MINLAKE98 model to the 1984-1991 field data for Lake Elmo.

	Temperature (°C)	Dissolved Oxygen (mg/L)	Total Phosphorus (mg/L)	Chlorophyll *a* (mg/L)
Standard error	1.47	1.55	0.02	0.004
Maximum error	7.36	5.50	-0.08	-0.011
Slope of regr. line	1.00	1.09	1.28	0.29
Regr. coefficients	0.95	0.79	0.43	-1.48
No. of data points	804	587	166	34

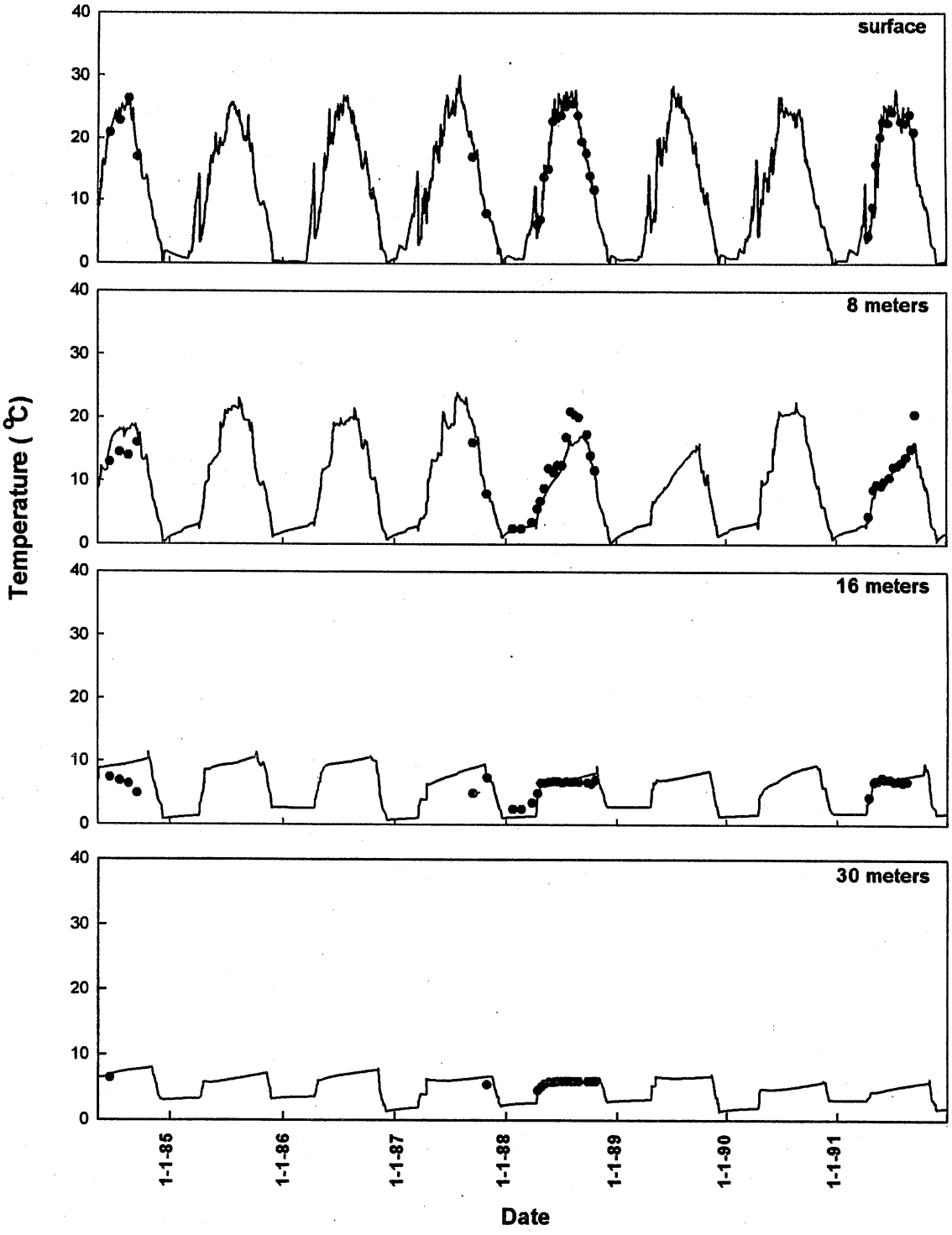

Figure 4.28. Simulated (solid line) and observed (dots) water temperatures at (a) surface, (b) 8 m, (c) 16 m, and (d) 30 m below the surface for Lake Elmo, April 1984 to December 1991.

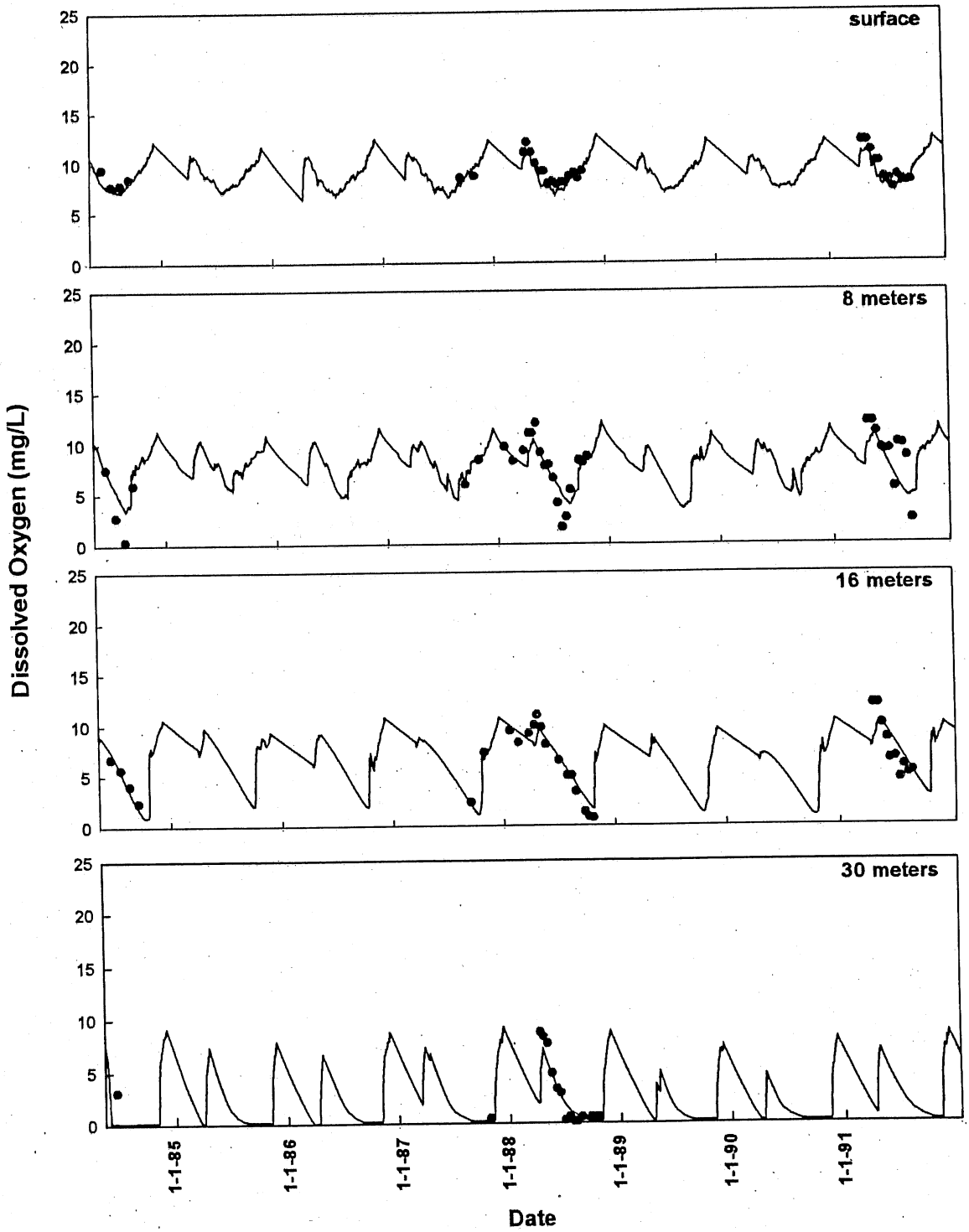

Figure 4.29. Simulated (solid line) and observed (dots) dissolved oxygen concentrations at (a) surface, (b) 8 m, (c) 16 m, and (d) 30 m below the surface for Lake Elmo, April 1984 to December 1991.

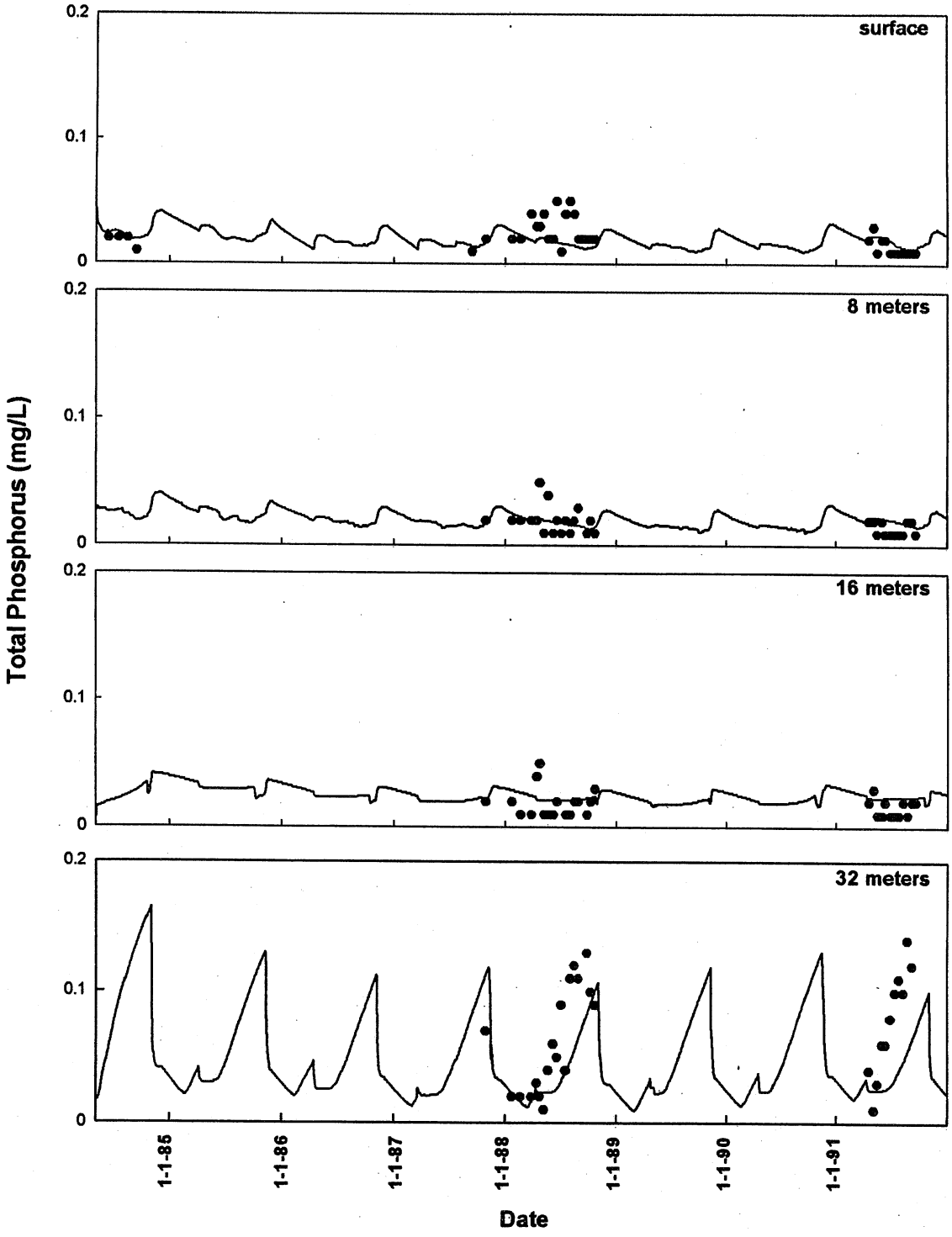

Figure 4.30. Simulated (solid line) and observed (dots) total phosphorus concentrations at (a) surface, (b) 8 m, (c) 16 m, and (d) 32 m below the surface for Lake Elmo, April 1984 to December 1991.

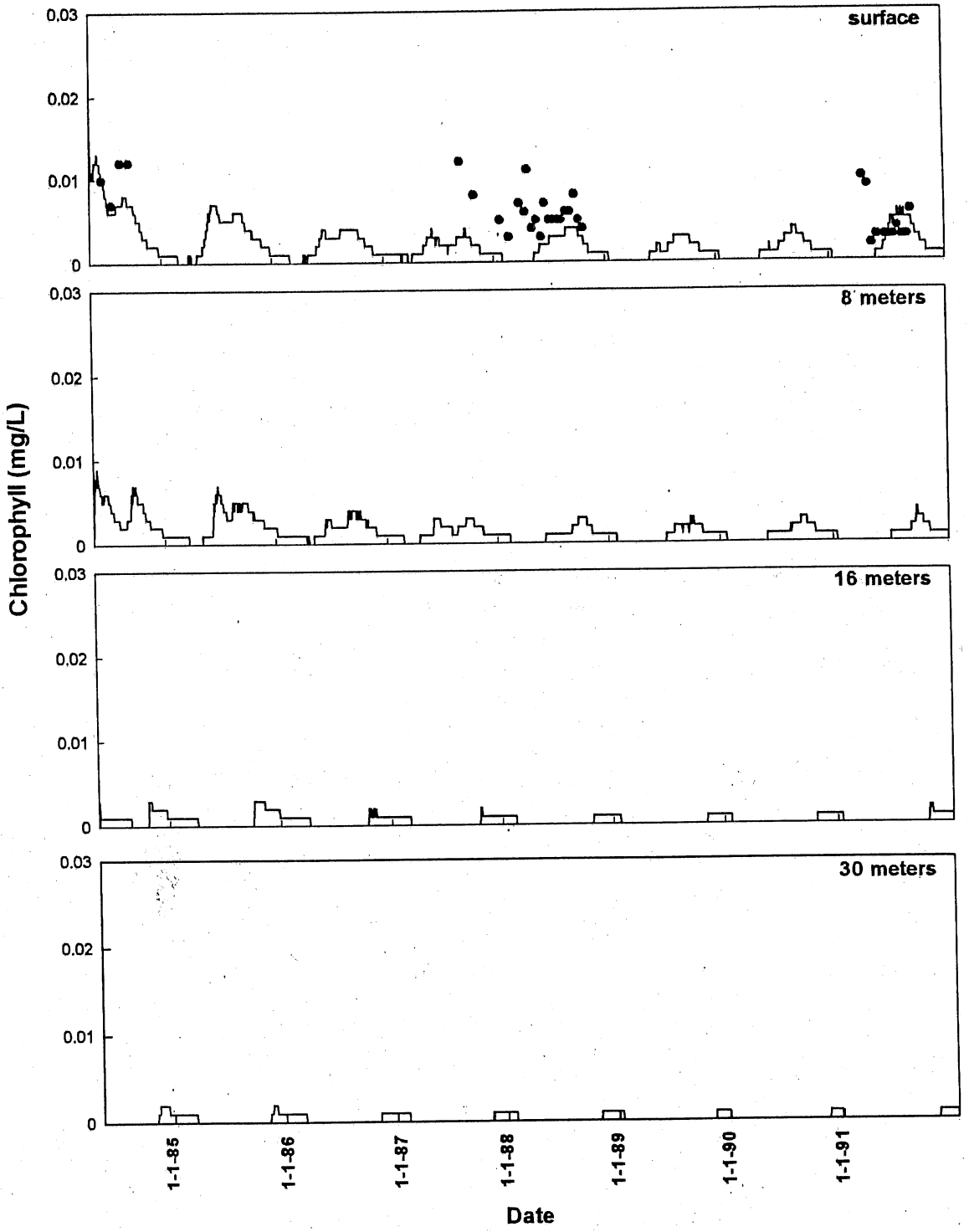

Figure 4.31. Simulated (solid line) and observed (dots) chlorophyll *a* concentrations at (a) surface, (b) 8 m, (c) 16 m, and (d) 30 m below the surface for Lake Elmo, April 1984 to December 1991.

5. DISCUSSION OF THE RESULTS

A deterministic, one-dimensional year-round lake water quality model MINLAKE98 was developed from a previous model by Riley with the inclusion of algorithms developed by Gu, Hondzo, Fang, and Stefan. The MINLAKE98 model incorporates the simulation of phytoplankton, nutrients (phosphorus, nitrate+nitrite, ammonia, silica), biochemical oxygen demand, and zooplankton from Riley's model, with modification, into the year-round temperature and dissolved oxygen model. MINLAKE98 was used to simulate physical, chemical, and biological processes in two Minnesota lakes, Lake Riley and Lake Elmo. Phytoplankton growth was simulated in both lakes using phosphorus and light limitation.

(1) The Need for Lake Inflow Simulation

Lake Elmo was initially simulated without any inflows or outflows. Stormwater and snowmelt runoff were added when simulations showed that the internal phosphorus loading was insufficient to account for the phosphorus concentrations in the surface water after spring or fall turnover. A review of the dissolved oxygen profiles shows a depression at approximately 8 to 9 m in depth corresponding to approximately 10°C in the temperature profile. With additional information on the water budget for Lake Elmo groundwater inflow was added to the simulation. The addition of groundwater inflow at 8.5 m was able to account for most of the DO depression. Clearly the inclusion of inflows (stormwater, snowmelt, and groundwater) is important in simulating the dynamics of Lake Elmo.

Lake Riley was initially simulated and calibrated as a closed basin (no inflows or outflows). A closed basin approach simulated the processes in Lake Riley well for 1982. However, the resulting calibrated MINLAKE98 model did not simulate the lake processes well for other years (1986 and 1985-1990), especially chlorophyll and phosphorus concentrations. From the weather data it appears that 1982 was a particularly dry year compared to the other years simulated. Inflow and stormwater runoff were added to the simulation to correct the low simulated phosphorus and chlorophyll concentrations during the summer months. In addition, MINLAKE98 was re-calibrated with 1986 data (a year with a more typical precipitation record). Although inflow and stormwater runoff where added to the model this did not significantly improve either the simulation of the phosphorus concentration or the summer phytoplankton blooms observed in later years. These results indicate that inflows and stormwater runoff as modeled do not play a significant role in accurately simulating Lake Riley and therefore the simulation of them is not required.

(2) Correct Modeling of Phytoplankton Growth

Simulating phytoplankton growth is very complex. There are many varieties of phytoplankton as well as localized phytoplankton adaptions (i.e. an algae class can become conditioned to the temperature of a region and therefore the same algae class can have a different optimum, maximum, or minimum temperature requirement in two different regions). MINLAKE98 uses many coefficients for simulating phytoplankton growth. The simulation of phytoplankton growth is more sensitive to some of the coefficients than others, however, many of the coefficients can offset each other to a degree, and calibration of the model may result in different sets of optimum coefficient values.

MINLAKE98 is able to simulate the average weekly phytoplankton population but not able to capture growth spikes (population which grow and decline dramatically in a few days). After calibration MINLAKE98 was able to simulate phytoplankton growth in Lake Elmo for individual years but not as well for multiple-year series. Simulation of phytoplankton growth in Lake Riley was successful for 1982 but not for later years. MINLAKE98's ability to simulate phytoplankton growth for individual years for Lake Elmo and 1982 for Lake Riley indicates that several processes are being modeled correctly. MINLAKE98's inability to simulate a summer phytoplankton bloom in Lake Riley indicates that some process which is occurring after 1982 is not being simulated or is not correctly simulated. It is clear after reviewing both the simulations and the field data that some changes occurred in Lake Riley between 1982 and 1986.

Calibration of MINLAKE98 for both lakes was performed on less than a one-year period (openwater season - April through December). The simulation start during April was used because in most cases there is no ice cover and the water column is well mixed. The calibration is somewhat year specific. A longer time period covering two open water seasons and two ice cover seasons (with corresponding field data) should provide better simulations of multiple-year series. Year-specific calibration appears to have occurred for Lake Riley were the lake dynamics in 1982 and 1986 are significantly different. In the case of Lake Elmo the calibration of MINLAKE98 provided good simulations of individual years but not as good for multi-year series. In Lake Elmo the biological and chemical processes during the openwater season were accurately modeled but some processes during the icecover season were not simulated well.

(3) Data Needs

The need for additional information usually becomes apparent when the model is set up for simulating a specific lake or when simulated results are compared with observed data. In the first case when information is not available, many assumptions must be made which will tend to generalize the model instead of modeling specifics in an individual lake. In the second case where there is insufficient or no observed data it can be difficult to calibrate a model or know if a simulation is accurate. By simulating individual lakes using MINLAKE98 it became apparent that additional information on inputs to and outputs from a lake, as well as icecover data are needed.

The addition of inflows and outflows can be important to the nutrient load and oxygen supply of a lake. This was the case for Lake Elmo. Including the intrusion of groundwater was important in simulating the depression in the dissolved oxygen profile. Like Lake Elmo, several other lakes near Lake Elmo receive a portion of their water budget from groundwater. Generally very little data concerning the flowrate of groundwater intrusion rates or recharge rates of aquifers from lakes have been collected. Sometimes actual numbers are not known but are incorporated with other inflow e.g. precipitation. For Lake Elmo 80% of the water budget is from precipitation and groundwater inputs. Even less is known about the nutrient content of the groundwater.

Stormwater runoff and snowmelt runoff can be major contributors to the loading of phosphorus, ammonia, nitrate+nitrite, and BOD. The lack of data requires the development of a watershed runoff-washoff model with the same time scale resolution as the MINLAKE98 model. A simplified SCS model for stormwater inflow and degree-day model for snowmelt are incorporated into MINLAKE98. These models have simplified nutrient washoff functions. Neither method provides a process oriented approach to nutrient washoff, which makes it difficult to incorporate the effects of nonpoint source management practices into the washoff models.

MINLAKE98 was used to simulate lake processes in a lake over multiple years. For both lakes simulated, a multi-year series includes periods of ice cover. To avoid year-specific calibrations, MINLAKE98 should be calibrated for a minimum of a two-year period. Calibration of the ice cover period is difficult because of limited winter data availablility. Lake Riley had data during the winter months for only one year of the 5+ year simulation period. Lake Elmo also had only one year of data for the 6+ year simulation.

Due to the lack of data many assumptions had to be made concerning the amount and quality of the inflows and outflows entering or leaving a lake as well as the biological and chemical rates occurring during the icecover periods. Many of the processes (phytoplankton mortality and respiration, detrital decay, nitrification, zooplankton grazing and respiration, and sediment oxygen demand) have temperature adjustments coefficients which are valid for a moderate temperature range of 10°C to 40°C. In MINLAKE98 these temperature adjustment coefficients were used phytoplankton mortality and zooplankton grazing for the entire year-round simulation. The rates for sediment oxygen demand, phytoplankton respiration, nitrification, and detrital decay during icecover were specified as constants. The sediment oxygen demand rates were adjusted to the rates specified in Table 3.6 dependent upon the eutrophic state of the lake. The phytoplankton respiration was assumed to be negligible and the detrital decay was assumed to be low. Nitrification was assumed to cease under icecover. Water under icecover generally ranges between 0°C and 4°C, no adjusts were made for water temperatures between 4°C and 10°C.

6. CONCLUSIONS

MINLAKE98 was developed to simulate some of the physical, biological, and chemical processes occurring in lakes and impoundments under different climate scenarios. To test the model, the vertical profiles of water temperature, dissolved oxygen, phosphorus, and phytoplankton were simulated for Lake Riley and Lake Elmo in Minnesota. Temperature and dissolved oxygen were simulated with mean standard errors of 1.4°C and 1.5 mg/L, respectively. Making the phosphorus release from the sediment dependent upon dissolved oxygen concentration improved the simulation of the phosphorus concentration. The phosphorus concentration was simulated with a mean relative standard error of 15%.

MINLAKE98 simulates phytoplankton (as chlorophyll) well only part of the time (i.e. well for individual years of Lake Elmo and 1982 for Lake Riley, but not for multiple year simulations). The poor simulations of phytoplankton did not significantly degrade the simulation of temperature and dissolved oxygen. Even though the phytoplankton results are somewhat sketchy for Lakes Elmo and Riley, it is worthwhile to test MNLAKE98 on other lakes. In addition, more data are required to calibrate the model for the winter ice-cover period.

The effect of watershed input on lake trophic level was found to be important. The inclusion of groundwater inflow into the simulation of dissolved oxygen was necessary for Lake Elmo.

REFERENCES

Allen, P.B. and J.W. Naney. 1991. Hydrology of the Little Washita River Watershed, Oklahoma: Data and Analyses. National Agricultural Water Quality Laboratory, Durant, Oklahoma.

APHA (American Public Health Association). 1985. *Standard Methods for the Examination of Water and Waste Water*, 16th ed., Washington, D.C. , 974pp.

Baity, H.G. 1938. Some Factors Affecting the Aerobic Decomposition of Sewage Sludge Deposits. *Sewage Works J.* 10(2):539-568.

Barica, J. And J.A. Mathias. 1979. Oxygen Depletion and Winterkill Risk in Small Prairie Lakes under Extended Ice Cover. *J. Fish. Res. Board Can.* 36:980-986.

Chapra, S.C. 1997. *Surface Water-Quality Modeling*. McGraw-Hill, Inc. St. Louis. p. 614.

Chapra, S.C. 1977. Total Phosphorus Model for the Great Lakes. *J. Environ. Engr. Div.* ASCE. 103(EE2):147-161.

Chow, V.T., D.R. Maidment, and L.W. Mays. 1988. *Applied Hydrology*. McGraw-Hill, Inc., St. Louis. Chapter 5.

EPA. 1985. Rates, Constants, and Kinetics Formulations in Surface Water Quality Modeling (Second Edition). EPA/600/3-85/040. pp.455.

Fair, G.M., J.C. Geyer, and D.A. Okun. 1968. *Water and Wastewater Engineering.* John Wiley and Sons, New York.

Fang, X. and H.G. Stefan. 1996. Long-Term Lake Water Temperature and Ice Cover Simulations/Measurements. *Cold Regions Science and Technology*. 24:289-304.

Fang, X. and H.G. Stefan. 1994a. Temperature and Dissolved Oxygen Simulations for a Lake with Ice Cover. Project Report No. 356, St. Anthony Falls Hydraulic Laboratory, Univerisity of Minnesota, Minneapolis, MN 55414.

Fang, X. And H.G. Stefan. 1994b. Modeling of Dissolved Oxygen Stratification Dynamics in Minnesota Lakes under Different Climate Scenarios. Project Report No. 339, St. Anthony Falls Hydraulic Laboratory, University of Minnesota, Minneapolis, MN 55414.

Ford, D.E. and H.G. Stefan. 1980. Thermal Predictions using Integral Energy Model. *Journal of the Hydraulics Division,* ASCE. 106(HY1):39-55.

Gu, R. and H.G. Stefan. 1990. Year-Round Temperature Simulation of Cold Climate Lakes. *Cold Regions Science and Technology.* 18:147-160.

Hanratty, M.P. and H.G. Stefan. 1997. Simulating the Effect of Climate Change on Three Rural Watersheds. Submitted to Water Resources Research.

Harms, T.E. and D.S. Chanasyk. 1998. Runoff Response from Two Reclaimed Watersheds. *Journal of the American Water Resources Association.* 34(2):289-299.

Heiskary, S.A. and C.B. Wilson. 1988. Minnesota Lake Water Quality Assessment Report. Minnesota Pollution Control Agency. St. Paul, MN. p. 19.

Hoffmann, K.A. and S.T. Chiang. 1993. *Computational Fluid Dynamics for Engineers - Volume 1.* Education Engineering Systems, Wichita, Kansas. Chapter 9.

Hondzo, M. and H.G. Stefan. 1991. Three Case Studies of Lake Temperature and Stratification Response to Warmer Climate. *Water Resources Research.* 27(8):1837-1846.

Horne, A.J. and C.R. Goldman. 1994. *Limnology.* McGraw-Hill, St. Louis. Chapters 9 & 10.

Hutchinson, G.E. 1957. *A Treatise on Limnology: Volume 1 - Geography, Physics, and Chemistry.* John Wiley & Sons, Inc. New York. p. 792.

Ishikawa, M., and H. Nishimura. 1989. Mathematical Model of Phosphate Release Rate from Sediments Considering the Effect of Dissolved Oxygen in Overlying Water. *Wat. Res.* 23(11): 1357-1366.

Lam, D.C.L., W.M. Schertzer, and A.S. Fraser. 1984. Modeling the Effects of Sediment Oxygen Demand in Lake Erie Water Quality Conditions Under the Influence of Pollution Control and Weather Variations.

Larsen, D.P., D.W. Schults, and K.W. Malueg. 1981. Summer Internal Phosphorus Supplies in Shagawa Lake, Minnesota. *Limnol. Oceanogr.* 26(4):740-753.

Maidment, D.R. 1993. *Handbook of Hydrology.* McGraw-Hill, New York. Chapter 7.

Marshall, C.T. and R.H. Peters. 1989. General Patterns in the Seasonal Development of Chlorophyll *a* for Temperate Lakes. *Limnol. Oceanogr.* 34(5):856-867.

Osgood, R.A. 1983. Diagnostic-Feasibility Study of Seven Metropolitan Area Lakes - Part Two: Lake Elmo. Metropolitan Council of the Twin Cities Area. Publication 10-83-093B. pp. 34.

Osgood, R.A. 1984. A 1984 Study of the Water Quality of 43 Metropolitan Area Lakes. Metropolitan Council of the Twin Cities Area. Publication 10-84-172. p.12.

Perkins, W.W., E.B. Welch, J. Frodge, and T. Hubbard. 1997. A Zero Degree of Freedom Total Phosphorus Model; 2. Application to Lake Sammamish, Washington. *Journal of Lake and Reservoir Management.* 13(2):131-141.

Pivovarov, A.A. 1972. *Thermal Condition in Freezing Lakes and Rivers.* Wiley, New York, New York.

Riley, M.J. and H.G. Stefan. 1988. MINLAKE: a dynamic lake water quality simulation model. *Ecol. Modelling.* 43:155-182.

Stefan, H.G. and S. Dhamotharan, F.R. Schiebe, A.Y. Fu, and J.J. Cardoni. 1989. Dynamic Simulation of Turbidity and Its Correction in Lake Chicot, Arkansas. Chapter 6 in Water Quality Modeling. Vol. IV Decision Support Techniques for Lakes and Reservoirs (B. Henderson-Sallers, editor), CRC Press, Baton Ronge, LA, pp. 189-245.

Thomann, R.V. and J.A. Mueller. 1987. *Principles of Surface Water Quality Modeling and Control.* Harper Collins Publishers. 644 pp.

U.S. Army Corps of Enineers. 1982. CE-QUAL-R1: A Numerical One-Dimensional Model of Reservoir Water Quality - User's Manual. Instruction Report E-81-2. Waterways Experiment Station, Vicksburg, Miss. 515 pp.

Walter, R.A., G.F. Cary, and D.F. Winter. 1978. Temperature Computation for Temperate Lakes. *Applied Mathematical Modeling.* 2:41-48.

Wanninkhof, R., J. Ledwell, and J. Crusius. 1990. Gas Transfer Velocities on Lakes Measured with Sulfur Hexafluoride. *In* **Air-Water Mass Transfer** edited by S.C. Wilhelms and J.S. Gulliver, American Society of Civil Engineers, Reston, VA, pp. 441-458.

APPENDIX A. WHOLE LAKE MASS BALANCE DIAGRAMS FOR MINLAKE98.

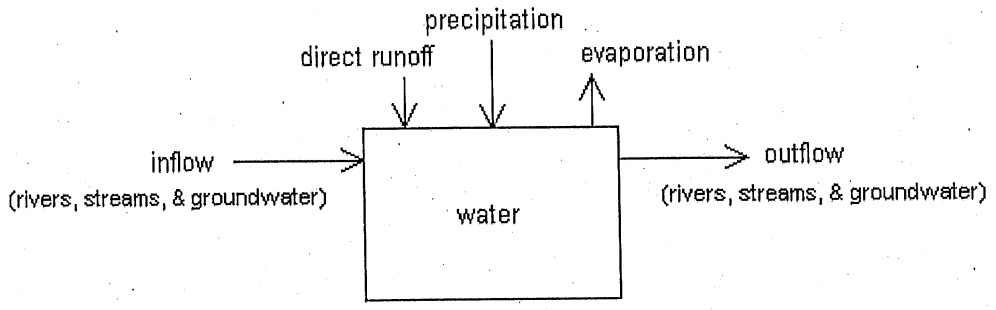

Figure A.1. Water Mass Balance.

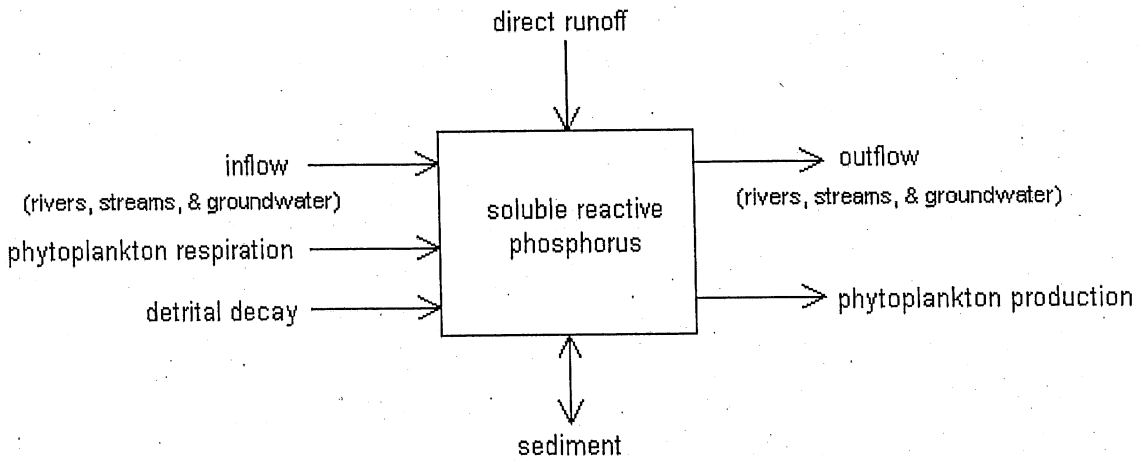

Figure A.2. Phosphorus Mass Balance.

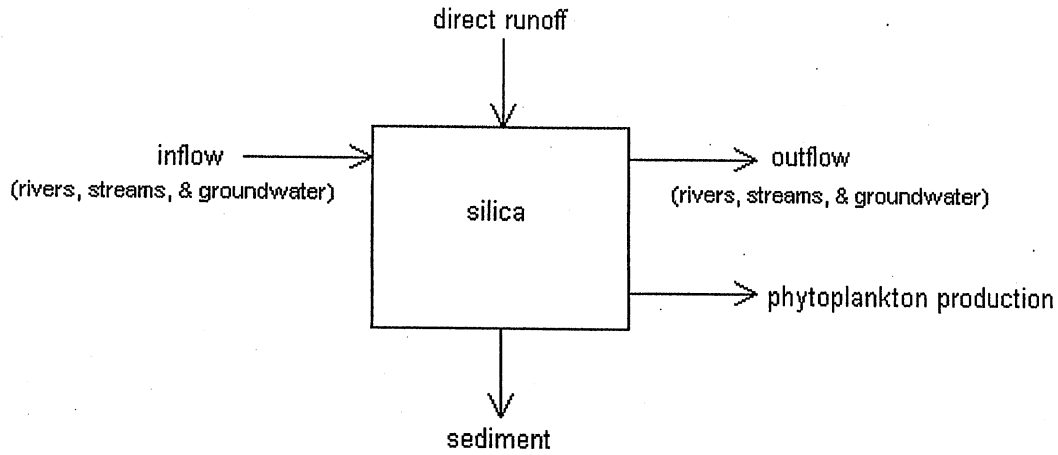

Figure A.3. Silica Mass Balance.

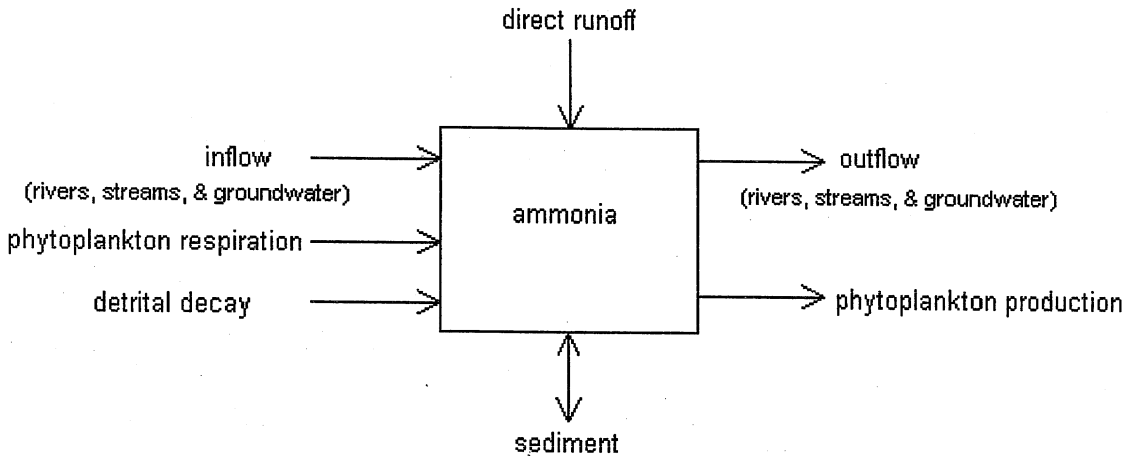

Figure A.4. Ammonia Mass Balance.

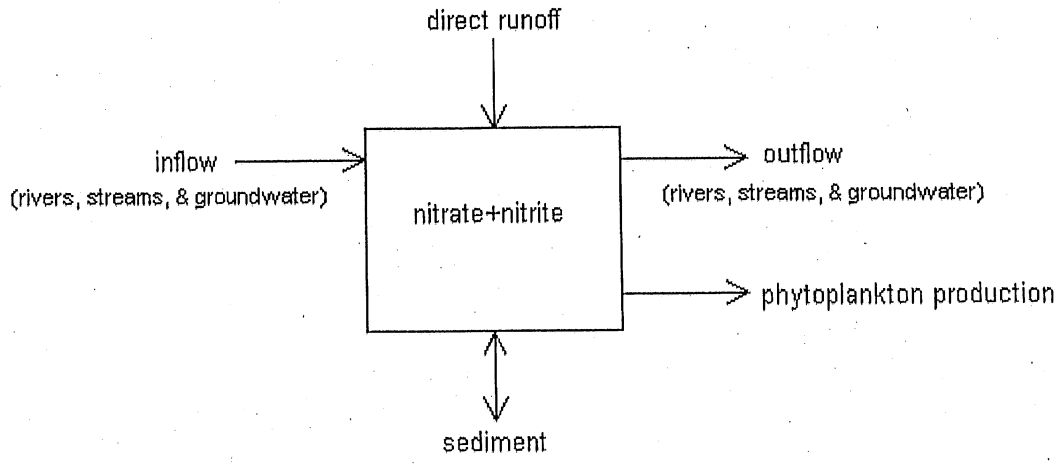

Figure A.5. Nitrate+Nitrite Mass Balance.

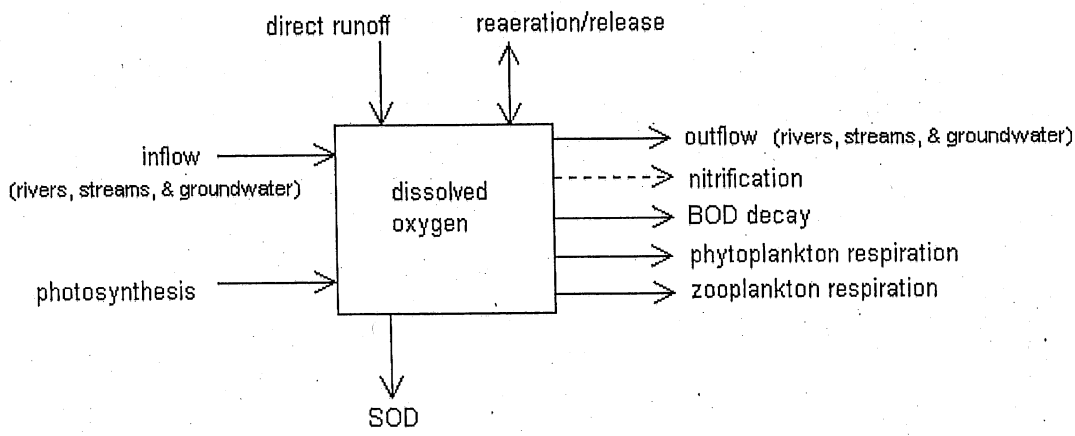

Figure A.6. Dissolved Oxygen Mass Balance.

APPENDIX B. EXTERNAL PHOSPHORUS SOURCES FOR LAKE RILEY

Inflow

Lake Riley was originally simulated as a closed basin with no inflow or outflow. MINLAKE98 was able to simulate the phytoplankton population Lake Riley for 1982, but not for 1986. The simulated phytoplankton is phosphorus limited during the summer months. It appeared that there is a source of phosphorus that was not being simulated. Therefore inflow and outflow were added to the simulation. The flow rate for Riley Creek was estimated from Elm Creek as follows.

The flow rate at the Lake Riley Inlet near Shakoppe, MN was measured at USGS gaging station number 445023093305201 from March 25, 1982 to September 30, 1982. The nearest USGS gaging station with flow rates for 1982 through 1990 in either Carver, Hennepin, and Scott Counties is at Elm Creek near Champlin, MN (USGS gaging station number 05287890). Data were retrieved from the USGS web page at http://waterdata.usgs.gov/nwis-w/MN/. Even though Elm Creek is a larger creek than Riley Creek the flow rate over time follows the same pattern for 1982 (Figure B.1).

The flow rates in Elm Creek differed for 1982 and 1986. The flow rate during the summer months is lower in 1982 than in 1986 (Figure B.2). This corresponds to the no flow conditions during the summer of 1982 for Riley Creek (Figure B.1).

A comparison of the flow rates from 4/1/82 through 9/30/82 shows that the flow rate in Riley Creek is approximately 5% of that in Elm Creek. Using this information, the flow rate for Riley Creek was estimated using 5% of the flow rate from Elm Creek during the periods when there are no gaged flow rate data for Riley Creek. Flow rates for Riley Creek were estimated for the following periods: 10/1/82 - 12/31/82 and 1/1/85 - 12/31/91.

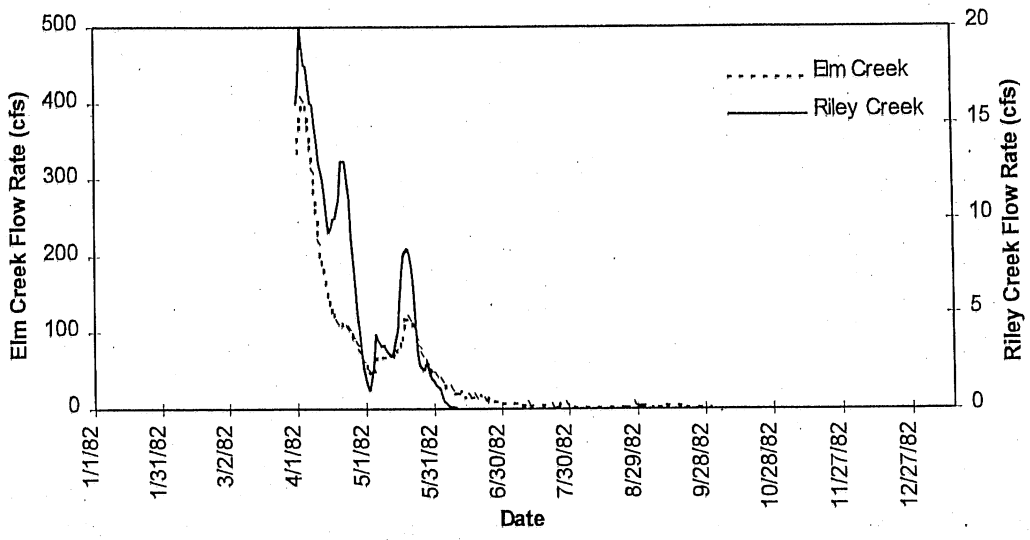

Figure B.1. Flow rate in Elm Creek, MN and Riley Creek, MN for 1982.

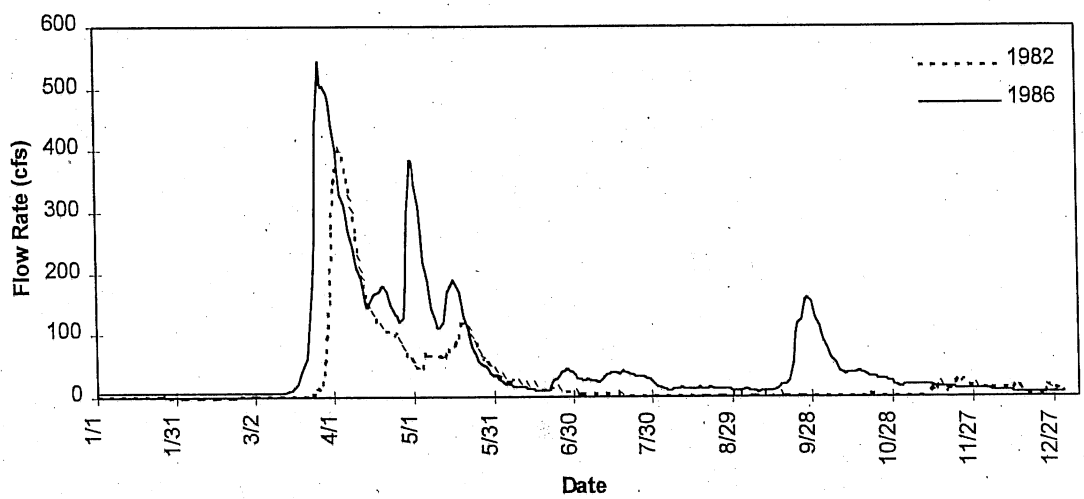

Figure B.2. Flow rate in Elm Creek, MN for 1982 and 1986.

Phosphorus Sources

The flow rate for the summer of 1982 (no flow) and the estimated flow rate for the summer of 1986 (maximum estimated flow rate of 2 cfs) vary only slightly. As the phosphorus concentration in the inflow water was not measured the phosphorus concentration was used to calibrate the phytoplankton growth (phosphorus limited) in the model. However, no concentration of available phosphorus in the inflow produced a

large enough phytoplankton population to match the field values without producing erroneously large blooms in the spring or fall. The majority of the inflow occurs between late March and the middle of May, with very little during the summer months (see Figure B.2). As the simulated phytoplankton is phosphorus limited during the summer an inflow with a source of phosphorus that is not immediately available but available through decay (e.g. detritus - BOD) was simulated. Again no amount of BOD in the inflow allowed for simulation of the phytoplankton population in the summer without erroneously high phytoplankton population during spring and fall. Clearly the inflow is not the source of phosphorus which is limiting the simulated summer phytoplankton growth.

Another possible source of phosphorus to the lake is stormwater runoff. The volumes of runoff entering Lake Riley in 1982 and 1986 are presented in Figure B.3. The precipitation for 1986 was greater than in 1982 but even then the volume of runoff was still small compared to the volume of the lake. No data are available for concentrations of available phosphorus or BOD in the runoff. Various concentrations of phosphorus and BOD in the runoff were simulated to simulate the phytoplankton growth in the summer. The additional source of phosphorus from the runoff was not sufficient to produce the large observed phytoplankton population.

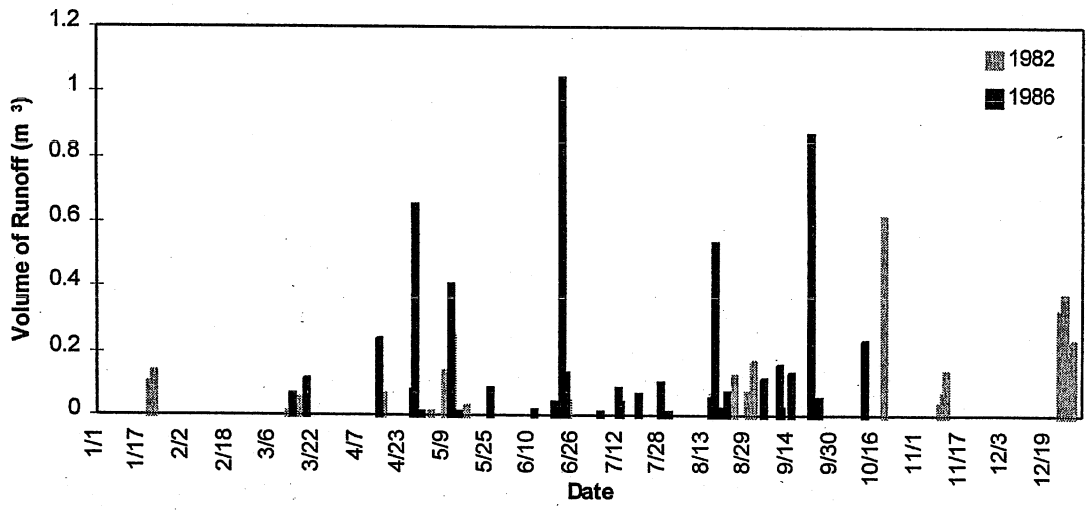

Figure B.3. Runoff into Lake Riley for 1982 and 1986.

External Limitation versus Luxury Uptake

A comparison of simulation results for Lake Riley for 1986 using Riley's MINLAKE and MINLAKE98 show very little difference in predicted phytoplankton population. This demonstrates that the simulation of phytoplankton using external nutrient concentration limitation (MINLAKE98) versus luxury uptake (Riley MINLAKE) is not the cause of the poor simulation.

The simulated phytoplankton is clearly phosphorus limited. Figures B.4 and B.5 show the simulated surface chlorophyll *a* concentration and the corresponding simulated available phosphorus concentration, respectively.

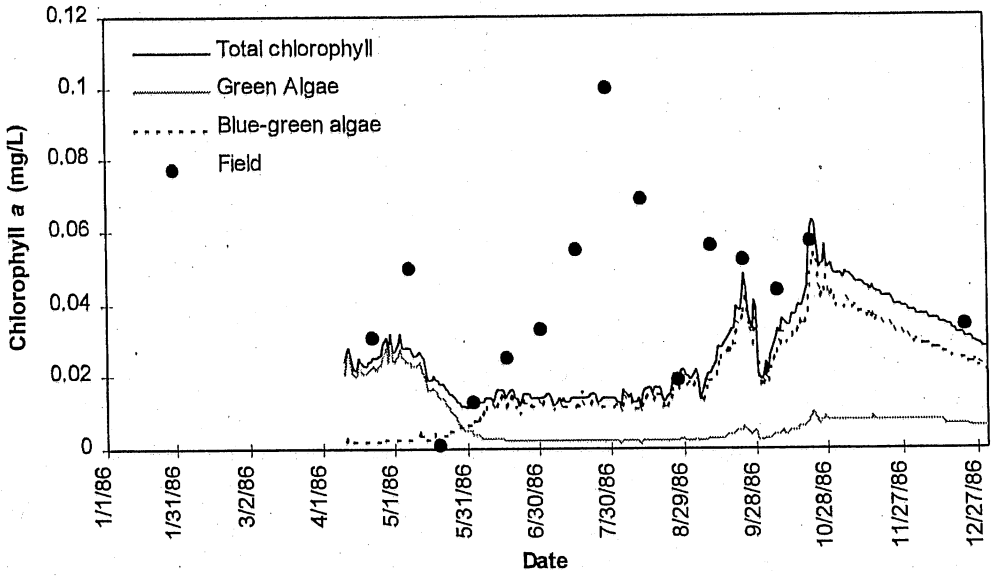

Figure B.4. Simulated surface chlorophyll *a* in Lake Riley for 1986 using MINLAKE98.

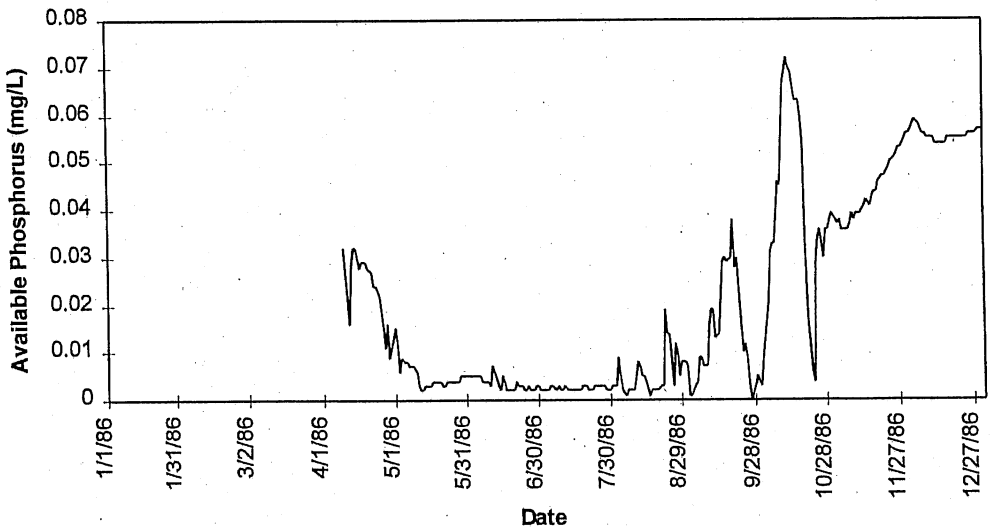

Figure B.5. Simulated available surface phosphorus in Lake Riley for 1986 using MINLAKE98.

Field Data

To determine whether MINLAKE98 is not simulating a process in Lake Riley that accounts for the phytoplankton bloom in the middle of the summer, a comparison of the **field data** available for 1982 and 1986 was made to determine what is different between the two years. A comparison of the observed surface temperature (Figure B.6), the observed surface total phosphorus (Figure B.7), and the observed solar radiation (Figure B.8) for 1982 and 1986 show little difference between the two years. The surface chlorophyll *a* concentrations for the two years (Figure B.9) are, however, very different. The chlorophyll *a* concentration in 1982 has a spring bloom and a fall bloom with lower chlorophyll *a* concentrations in the summer. As the total phosphorus concentration is simular for both years it appears that the phytoplankton producing the bloom in the summer of 1986 are not as phosporus depended as the phytoplankton in 1982. The mean phytoplankton concentration in 1986 is twice as high as that in 1982. In addition, the second bloom of the year occurs in the summer in 1986 and in the fall in 1982. Simplified seasonal patterns of chlorophyll for eutrophic and oligotrophic lakes is presented in Figure B.10 (Fang, 1994 from Marshall and Peters, 1989) showing that the second bloom occurs earlier for eutrophic lakes than oligotrophic lakes. Marshall and Peters (1989) found that blooms in eutrophic lakes are more pronounced especially in the late summer/early fall. From the higher mean chlorophyll *a* concentration and the change in the seasonal pattern it is clear that Lake Riley became even more eutrophic between 1982 and 1986.

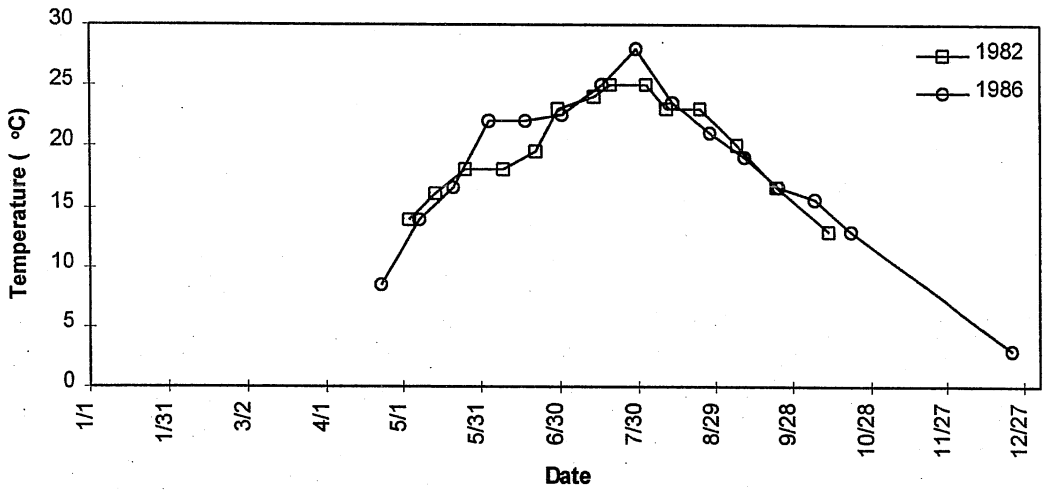

Figure B.6. Observed surface water temperature for Lake Riley.

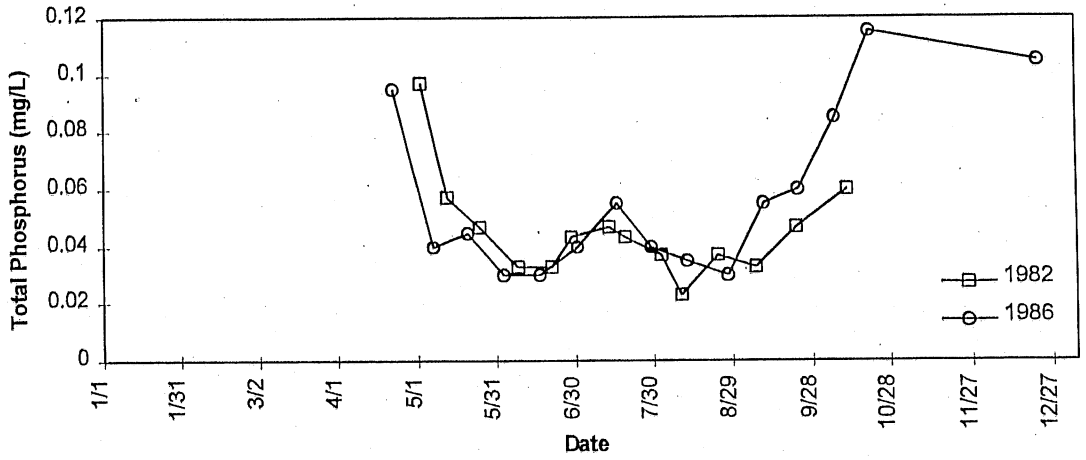

Figure B.7. Observed total phosphorus concentration in the surface water of Lake Riley.

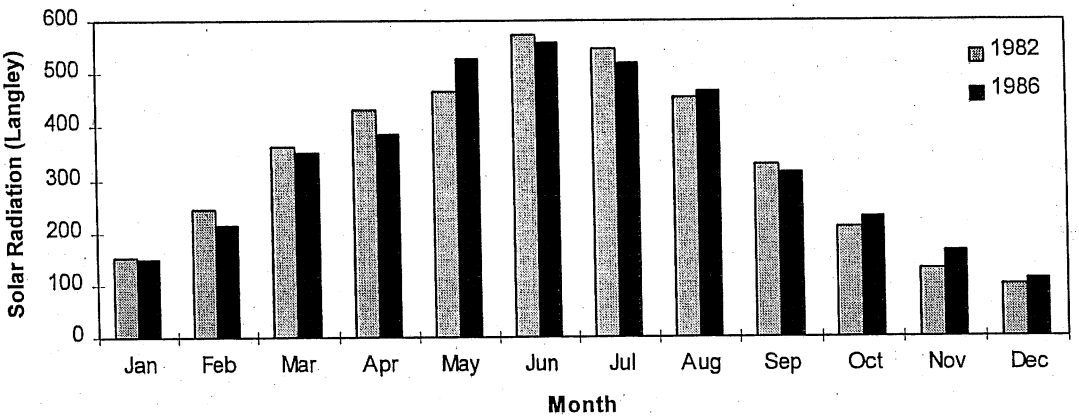

Figure B.8. Mean monthly observed solar radiation in Minneapolis/St. Paul, MN.

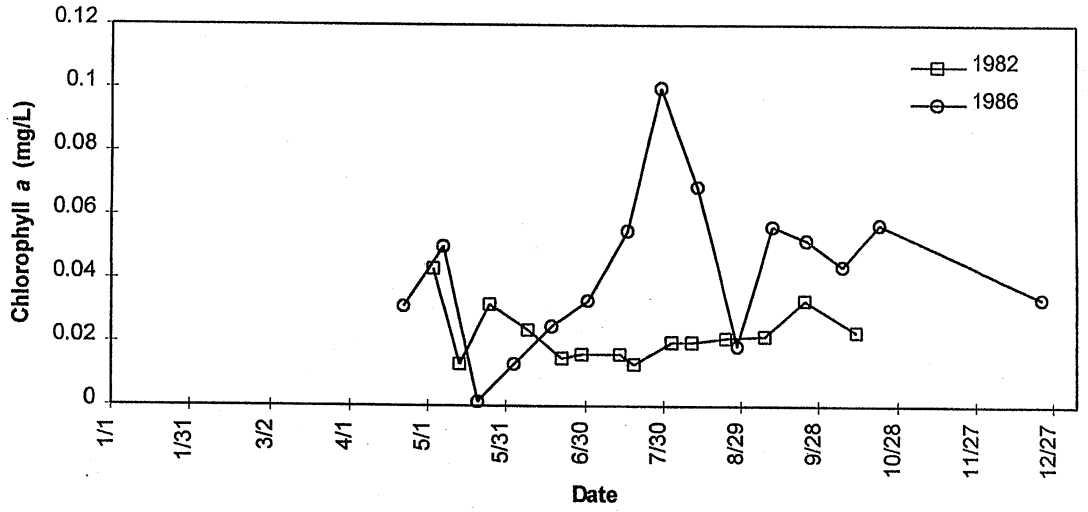

Figure B.9. Observed surface chlorophyll *a* concentrations in Lake Riley for 1982 and 1986.

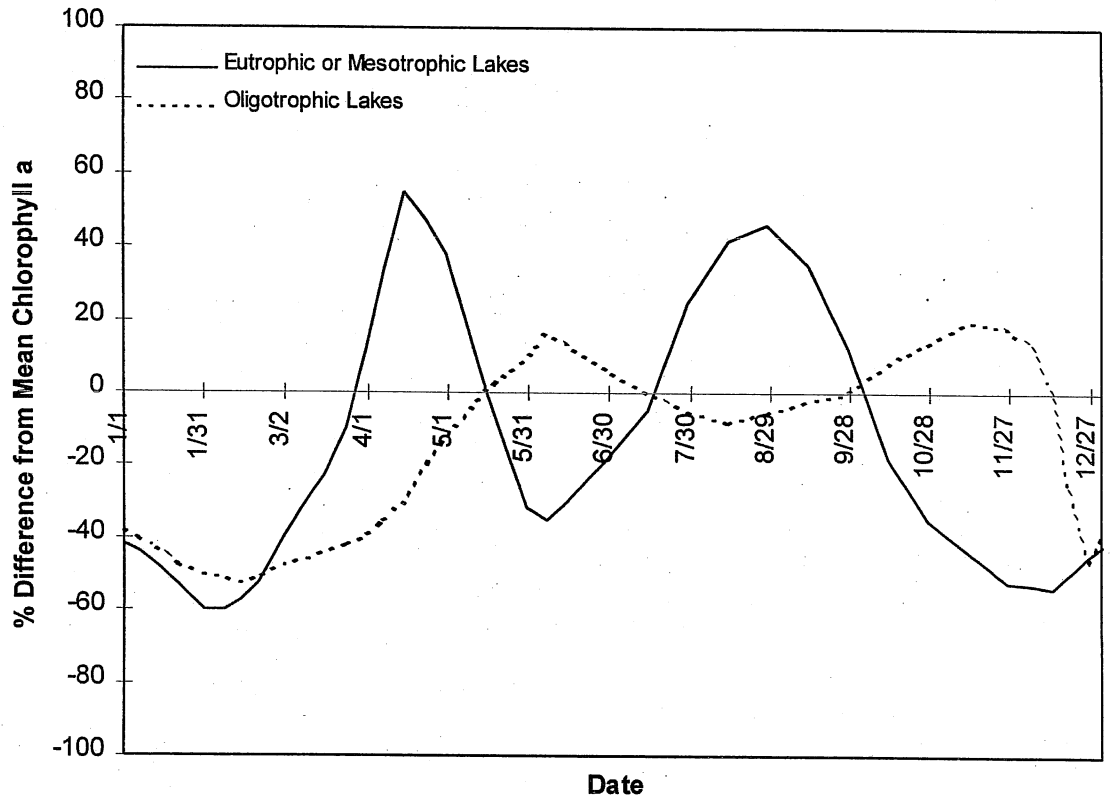

Figure B.10. Simplified seasonal patterns of chlorophyll *a* for eutrophic and oligotrophic lakes (Fang, 1994).

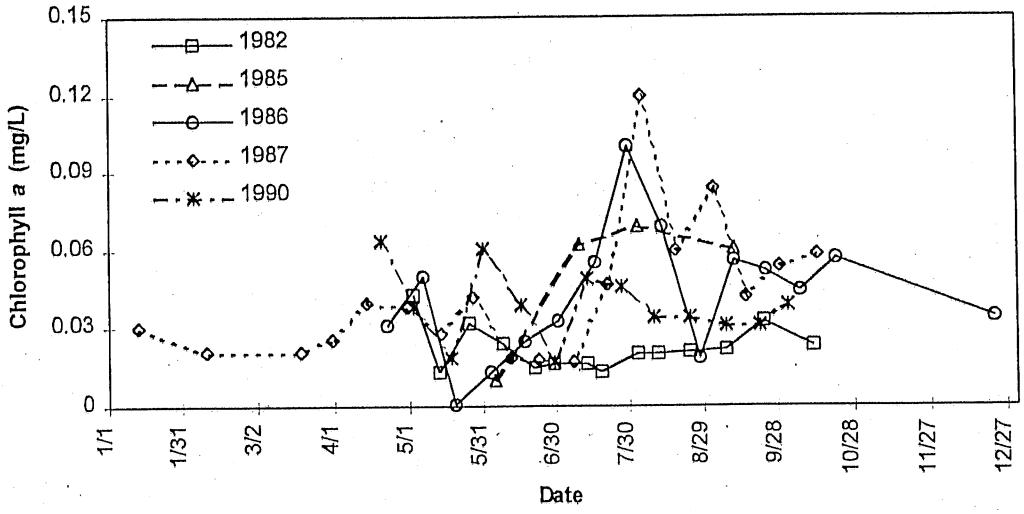

Figure B.11. Observed surface chlorophyll *a* concentrations in Lake Riley.

Table B.1. Coefficients for 1982 and 1986 calibrations of Lake Riley.

Coefficient	Abbreviation	1982 value	1986 value
Wind sheltering, summer	WSTR	0.9	0.4
Wind function, spring and fall	WCFSF	0.8	0.7
Wind sheltering, spring and fall	WSSF	0.2	0.3
Sediment oxygen depletion rate	SB20	0.5	2.0
Mortality rate for 2nd algal group	XKM(2)	0.03	0.02
Temperature minimum for 1st algal group	TMIN(1)	10.0	2.0
Temperature minimum for 2nd algal group	TMIN(2)	11.0	6.0
Initial zooplankton population	ZP	2600	1300

APPENDIX C. COMPUTATION OF SCS CURVE NUMBER AND FLOW INTO LAKE ELMO

Assumptions: Soil Type B

Antecedent Moisture Condition II

Land Use	Percent Area[1]	Curve Number[2]	Weighted
low-density residential	3.0	69	207.0
medium-density residential	8.2	73	14.6
multi-family	1.0	85	85.0
wetlands	6.2	78	483.6
parks	0.2	61	12.2
commercial, industrial	1.3	90	117.0
crops	35.0	76	2660.0
pastureland	0.6	70	42.0
grassland	29.7	58	1722.6
woodland	8.7	60	522.0
miscellaneous	6.1	62	378.2
Total	100		6244.2
Weighted Curve Number		62.4	

[1]Land use is from Osgood, 1983.

[2]Curve Numbers and equations for direct runoff from a storm by the SCS method are from Chow, V.T., *et al.*, 1988.

$$S = \frac{1000}{CN} - 10 = \frac{1000}{62.4} - 10 = 6.03 \; inches$$

$$Q = \frac{[P - 0.2S]^2}{P + 0.8S} = \frac{[P - (0.2)(6.03)]^2}{P + (0.8)(6.03)} = \frac{(P - 1.21)^2}{P + 4.82}$$

where:

P = precipitation in inches/day

Q = runoff in inches/day

APPENDIX D. COEFFICIENTS FOR SIMULATING LAKE RILEY AND LAKE ELMO USING MINLAKE98

Table D.1. Table of phytoplankton coefficients for simulations of Lake Riley and Lake Elmo using MINLAKE98.

	Units	Lake Riley 1982	Lake Riley 1986	Lake Elmo
Algae 1				
Maximum growth rate	1/d	1.4	1.4	0.6
Half-saturation P	mg/L	0.02	0.02	0.03
Optimum temperature	°C	27	27	20
Maximum temperature	°C	40	42	25
Minimum temperature	°C	10	2	2
Settling velocity	m/d	0.02	0.02	0.02
Respiration rate	1/d	0.04	0.04	0.03
Non-predatory mortality rate	1/d	0.03	0.03	0.03
Zooplankton grazing gate	mg chla/ indiv d	0.0015	0.0015	0.00001
Light limitation	$\mu E/m^2$ s	100	100	100
Light inhibition	$\mu E/m^2$ s	700	700	700
Algae 2				
Maximum growth rate	1/d	1.5	1.5	0.8
Half-saturation P	mg/L	0.03	0.02	0.03
Optimum temperature	°C	25	25	24
Maximum temperature	°C	32	32	30
Minimum temperature	°C	11	6	12
Settling velocity	m/d	0.001	0.001	0.02
Respiration rate	1/d	0.05	0.05	0.03
Non-predatory mortality rate	1/d	0.03	0.03	0.03
Zooplankton grazing rate	mg chla/ indiv d	0.0001	0.0001	0
Light limitation	$\mu E/m^2$ s	400	400	400
Light inhibition	$\mu E/m^2$ s	1000	1000	1000

indiv = individual, 0.003 mg/ individual

Table D.2. Table of zooplankton coefficients for simulations of Lake Riley and Lake Elmo using MINLAKE98.

	Units	Lake Riley 1982	Lake Riley 1986	Lake Elmo
Zooplankton population	$\#/m^3$	2600	1300	20976
Min. Zooplankton population for predation	$\#/m^3$	100	100	10
Minimum seasonal zooplankton predation rate	1/d	0.05	0.05	0.05
Maximum seasonal zooplankton predation rate	1/d	0.7	0.7	0.7
Minimum predation rate	1/d	0.05	0.05	0.03
Minimum light intensity for zooplankton predation	$kcal/m^2d$	0.0	0.0	0.0
Optimal light level for predation on zooplankton	$\mu E/m^2s$	0.1	0.1	0.1
Minimum predation period	–	140	140	110
Beginning of maximum predation period	–	180	180	140
Zooplankton respiration rate	1/indiv d	0.001	0.001	0.002
Zooplankton reproduction rate	1/d	0.08	0.08	0.02
Temperature coefficient zooplankton respiration	–	1.06	1.06	1.06
Algae 1				
Maximum zooplankton grazing rate	mg chla/ indiv d	0.0015	0.0015	0.00001
Half-saturation coefficient for grazing	mg/L	0.01	0.01	0.0001
Minimum chlorophyll concentration for zooplankton grazing	mg/L	0.001	0.001	0.001
Algae 2				
Maximum zooplankton grazing rate	mg chla/ indiv d	0.0001	0.0001	0.0
Half-saturation coefficient for grazing	mg/L	0.01	0.01	0.0001
Minimum chlorophyll concentration for zooplankton grazing	mg/L	0.002	0.002	0.001

indiv = individual, 0.003 mg/ individual

Table D.3. Table of physical coefficients for simulations of Lake Riley and Lake Elmo using MINLAKE98.

	Units	Lake Riley 1982	Lake Riley 1986	Lake Elmo
Minimum layer thickness	m	0.5	0.2	0.75
Maximum layer thickness	m	1.2	1.2	2.0
Surface radiation absorption coefficient	–	0.4	0.4	0.4
Emissivity of water	–	0.97	0.97	0.97
Light extinction coefficient of water	1/m	0.9	0.9	0.5
Light extinction coefficient of chlorophyll	m^2/g chla	16.0	16.0	30.0
Wind coefficient	–	0.8	0.8	0.8
Wind sheltering coefficient	–	0.9	0.4	2.0
Wind function coefficient spring and fall	–	0.8	0.7	1.0
Wind sheltering coefficient spring and fall	–	0.2	0.3	0.6
Detrital decay rate	1/d	0.07	0.07	0.05
Sediment oxygen depletion rate	g/m^2 d	0.5	2.0	1.7
Sediment phosphorus release rate	g/m^2 d	0.02	0.02	0.007
Settling rate of detritus	m/d	0.04	0.04	0.04
Mass yield ratio of chlorophyll to DO	mg chla/ mg DO	0.0083	0.0083	0.0083
Mass yield ratio of chlorophyll to BOD	mg chla/ mg BOD	0.0083	0.0083	0.0083
Mass yield ration of phosphorus to BOD	mg P/ mg BOD	0.0091	0.0091	0.0091
Average mass of individual zooplankton	mg/ind.	0.003	0.003	0.003
Mass yield of phosophorus to chlorophyll	mg P/ mg chla	1.1	1.1	1.1

indiv = individual

Table D.4. Table of winter coefficients for simulations of Lake Riley and Lake Elmo using MINLAKE98.

	Units	Lake Riley 1982	Lake Riley 1986	Lake Elmo
Snow compaction factor	--	0.25	0.25	0.25
Ice conductivity	W/m °C	2.6	2.6	2.6
Thermal conductivity of snow	kcal/ m °C d	0.27	0.27	0.27
Conductive heat transfer coefficient	kcal/ m °C d	11.35	11.35	11.35
Factor to increase temperature gradient	–	1.0	1.0	1.0
Wind function coefficient with ice cover	–	0.0	0.0	0.0
Wind sheltering coefficient with ice cover	–	0.0	0.0	0.0
Absorption coefficient of ice	–	0.17	0.17	0.17
Reflectivity coefficient of ice	–	0.55	0.55	0.55
Attenuation coefficient of ice	1/m	1.6	1.6	1.6
Absorption coefficient of snow	–	0.34	0.34	0.34
Reflectivity coefficient of snow	–	0.8	0.8	0.8
Attenuation coefficient of snow	1/m	40.0	40.0	40.0
Depth mean temperature at which lake starts to freeze	°C	3.3	3.3	3.3
Air temperature at which lake starts to freeze	°C	-2.0	-2.0	-2.0
Total depth of sediment	m	10.0	10.0	10.0
Number of sediment layers	–	11	11	11
Thermal diffusivity of sediment	m^2/d	0.035	0.035	0.035
Density * heat capacity	kcal/kg °C	550	550	550
Mean sediment temperature	°C	7.0	7.0	7.0
Coefficient for exponential function	–	2.0	2.0	2.0
Initial bottom water temperature	°C	4.5	4.5	4.5